CANADIAN THESES ON MICROFICHE

ISBN

THESES CANADIENNES SUR MICROFICHE

NOTICE

The quality of this microfiche is heavily dependent upon the quality of the original thesis submitted for microfilming Every effort has been made to ensure the highest quality of reproduction possible

If pages are missing, contact the university which granted the degree

Some pages may have indistinct print especially if the original pages were typed with a poor typewriter ribbon or if the university sent us a poor photocopy

Previously copyrighted materials (journal articles, published tests, etc) are not filmed

Reproduction in full or in part of this film is governed by the Canadian Copyright Act, R S C 1970, c C-30 Please read the authorization forms which accompany this thesis

AVIS

La qualité de cette microfiche dépend grandement de la qualité de là thèse soumise au microfilmage Nous avons tout fait pour assurer une qualité supérieure de reproduction

S'il manque des pages, veuillez communiquer avec l'université qui a conféré le grade

La qualité d'impression de certaines pages peut laisser à désirer, surtout si les pages originales ont éte dáctylographiées à l'aide d'un ruban usé ou si l'université nous a fait parvenir une photocopie de mauvaise qualité

Les documents qui font déjà l'objet d'un droit d'auteur (articles de revue, examens publies, etc) ne sont pas microfilmés

La reproduction, même partielle, de ce microfilm est soumise à la Loi canadienne 'sur le droit d'auteur, SRC 1970, c C-30 Veuillez prendre connaissance des formules d'autorisation qui accompagnent cette thèse

THIS DISSERTATION
HAS BEEN MICROFILMED
EXACTLY AS RECEIVED

LA THÈSE A ÉTÉ
MICROFILMÉE TELLE QUE
NOUS L'AVONS REÇUE

Canadä

1,n-RADICAL IONS

PART I.   THE OXIDATION OF 1,1,2,2-TETRAPHENYLCYCLOPROPANE.

PART II. THE ONE-ELECTRON TWO-CENTRE BOND IN 1,3-RADICAL

CATIONS.

SUBSTITUENT EFFECTS ON BENZYL RADICALS

PART III. SUBSTITUENT INTERACTIONS BY ESR SPECTROSCOPY.

by

Danial D. M. Wayner

Department of Chemistry

Submitted in partial fulfillment

of the requirements for the Degree of

Doctor of Philosophy

at Dalhousie University

August, 1984.

TABLE OF CONTENTS

PAGE

PART I - 1,n-RADICAL IONS: PHOTOSENSITIZED (ELECTRON-
TRANSFER) VERSUS ELECTROCHEMICAL OXIDATION
OF 1,1,2,2-TETRAPHENYLCYCLOPROPANE

PART II - 1,n-RADICAL IONS: THE NATURE OF THE ONE-
ELECTRON TWO-CENTRE BOND IN CYCLOPROPANE RADICAL
CATIONS. AN SCF MO APPROACH

v

LIST OF TABLES

LIST OF FIGURES

x

ABSTRACT

In Part I, the photosensitized (electron-transfer) and electrochemical oxidation of 1,1,2,2-tetraphenyl cyclopropane have been studied. The products obtained photochemically are 1,1,3,3-tetraphenylpropene, 1,1,3-triphenylindene tetraphenylallene and 3-methoxy-1,1,3,3-tetraphenylpropene. The product ratios are dramatically dependent upon solvent conditions, particularly sensitizer and solvent. The variations in product ratios are attributed to variations in the redox behaviour of the sensitizer radical anion and upon the basicity and nucleophilicity of the medium. The oxidation products from the electrochemical study are the same as those from the photosensitized (electron-transfer) study. Common intermediates have been identified and a mechanism for formation of the products is proposed.

In Part II, the nature of the one-electron two-centre bond in the radical cations of cyclopropane and 1,2-divinylcyclopropane has been investigated using ab initio self consistent field molecular orbital (SCF MO) calculations. The charge and spin distributions in several conformers of the cyclopropane radical cation have are compared. From the energy difference between the 90,90 conformer and the 90,0 conformer, the activation barriers to cis-trans isomerization of the cyclopropane and the 1,2-divinylcyclopropane radicals are estimated. Similarly, from the energy difference between the 90,90 conformer and the

.0,0 conformer of the cyclopropane radical cation, the barrier to the orbital symmetry allowed opening of the cyclopropane ring is estimated. The implication of these results to experimental data are discussed.

In Part III, the substituent effects on benzyl radical hyperfine coupling constants are investigated. Emphasis is placed on the discussion of hyperconjugation in the delocalization of spin and the interaction of sulphur containing substituents. In general, substituents will interact as β-spin donors or α-acceptors in the para position. Substituents in the meta position give an indication that inductive withdrawl of charge from the σ-framework decreases delocalization into the aryl ring.

LIST OF ABBREVIATIONS

Electrochemical: C – concentration

                        D – diffusion coefficient

                        E – potential

                        ı – current

                        α – transfer coefficient

                        δ – diffusion layer thickness

Esr: G – gauss

                        hfc – hyperfine coupling constant

Infrared spectra: s – strong

                        m – medium

                        w – weak

NMR spectra: s – singlet

                        d – doublet

                        t – triplet

                        q – quartet

                        m – multiplet

All other abbreviations and symbols used are standard
notation.

ACKNOWLEDGEMENTS

The efforts and inspiration of a great many people have contributed to the success of this graduate thesis. I am indebted to my supervisor Dr. D. R. Arnold for his many suggestions, his interest, his encouragement and his never ending enthusiasm during my tenure at Dalhousie University.

I would also like to thank the students and staff I have worked with in the lab, especially Miles Snow and Martin Nicholas for numerous discussions and Brian Millier (electronics) and Jurgen Muller (glass blowing) for their invaluable technical expertise.

I owe a debt of gratitude to many of the Faculty members, particularly Dr. R. J. Boyd for his interest and the contribution of his expertise in the area of theoretical chemistry, and, Dr. L. Ramaley for his advice in the area of electroanalytical chemistry.

Finally, I owe the greatest debt to my wife, Donna, who has had the patience to put up with the last four years. I certainly could not have done it without her.

PART I.   1,n-RADICAL IONS: PHOTOSENSITIZED (ELECTRON-
              TRANSFER) VERSUS ELECTROCHEMICAL OXIDATION OF
              1,1,2,2-TETRAPHENYLCYCLOPROPANE

1.1   INTRODUCTION

1.1.1 ASPECTS OF THE GENERATION OF RADICAL IONS

The chemical and physical properties of ions and
radicals have been studied so extensively that we can
predict, with confidence, the course of a reaction involving
these intermediates. Radical ions, on the other hand, are
not as well understood. In fact, there are an increasing
number of reactions where the existence of radical ions is
now implicated (1). While there is much research
activity into the nature and reactivity of radical ions in
general, much of the focus has been on the formation,
properties and reactivity of radical cations (2).

Radical cations are generated by the removal of one
electron from a neutral molecule. There are many ways to
induce the one-electron oxidation; the most common methods
being concentrated sulphuric acid, metal ion oxidation,
pulse radiolysis, electron impact (mass spectrometry),
anodic oxidation and photoinduced oxidation. Many aromatic
hydrocarbons are oxidized by concentrated sulphuric acid
(Equation 1), and, since these strong acid solutions of the
radical cations are generally stable, this method has been

$$2ArH \pm 3H_2SO_4 \longrightarrow 2ArH^{\bullet +} + 2H_2O + SO_2 + 2HSO_4^- \qquad [1]$$
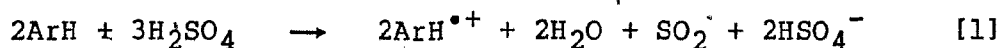
used to characterize radical cations by electron spin resonance (esr) spectroscopy (3). Although Kehrmann, in 1914 (4), concluded that a one-electron oxidation of phenothiazine had occurred, the mechanism by which aromatic hydrocarbons are oxidized in sulphuric acid solutions is still not well established. However, it is believed that a key step is the protonation of the hydrocarbon (Equation 2-4) (3c).

$$ArH + H_2SO_4 \rightleftharpoons ArH_2^+ + HSO_4^- \qquad [2]$$

$$ArH + ArH_2^+ \rightleftharpoons ArH_2^{\bullet} + ArH^{\bullet +} \qquad [3]$$

$$ArH_2^{\bullet} + 2H_2SO_4 \rightleftharpoons ArH^{\bullet +} + 2H_2O + HSO_4^- + SO_2 \qquad [4]$$
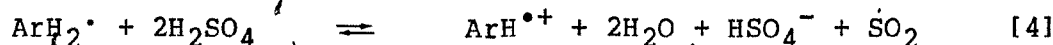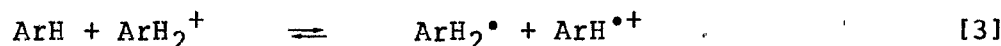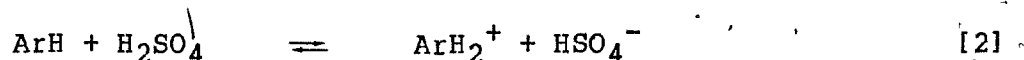
The most convenient methods for the generation of radical ions under mild conditions, however, are the photoinduced electron transfer and the electrochemical approaches. Since the work presented in this thesis has made use of both of these methods, it is useful to briefly describe some of the theoretical and physical aspects associated with the generation of radical ions in these ways.

The interaction of a donor molecule (D) and an acceptor molecule (A) in terms of a ground state charge-transfer model was first described by Mulliken in 1950 (5).

2

According to Mulliken, the interaction of a donor having a high energy filled orbital (ie., low ionization potential) and an acceptor having a low energy unfilled orbital (ie., high electron affinity) can lead to an interaction to form what he called a "charge-transfer complex" (6). In molecular orbital terms, this "ground state charge-transfer (CT) complex" was represented by a wave function of the form

$$\psi_G = a\psi_0(D,A) + b\psi_1(D^+,A^-) \qquad [5]$$

shown in Equation 5, where, $\psi_0(D,A)$ is the "no bond" wave function of the donor and acceptor and $\psi_1(D^+,A^-)$ is the wave function representing the transfer of an electron from D to A. The relative contribution of the two wave functions is indicated by the size of the two coefficients (a and b). The relative size of these coefficients is governed, in the most simplistic approach, by the energy difference between the highest occupied molecular orbital (HOMO) of the donor and the lowest unoccupied molecular orbital (LUMO) of the acceptor.

The appearance of absorption bands (often visible) not present in either the donor molecule or the acceptor molecule is characteristic of the formation of a ground state CT complex (7). The wave function associated with the electronically excited CT complex is shown in Equation 6 (in both Equations 5 and 6 contributions from locally excited

3

$$\psi_E = a^* \psi_1(D^+, A^-) + b^* \psi_0(D, A) \qquad [6]$$

states and higher energy CT states have been neglected for the sake of simplicity). For weak complexes, the contribution of $_1(D^+, A^-)$ in the ground state is small and, $b \ll a$, while normally, in the excited state, $b^* \ll a^*$.

Ground state charge-transfer complexation is not necessary in order to photochemically induce an electron transfer between a donor molecule and an acceptor molecule. The interaction of an electronically excited molecule (either D^* or A^*) with a ground state molecule (either A or D) can also lead to the formation of radical ion pairs (Equation 7,8) (2). The generality of this excited state

$$A + D^* \longrightarrow A^- + D^+ \qquad [7]$$

$$A^* + D \longrightarrow A^- + D^+ \qquad [8]$$
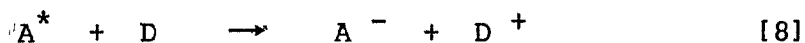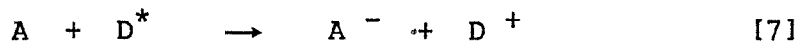
electron-transfer process was recognized by Weller (8). In his now classic work, Weller measured the fluorescence quenching rate constants (k_q) for a series of typical donor-acceptor systems. From the model shown in Scheme I, the fluorescence quenching rate constant is defined by Equation

4

9, where K_{23} is defined by Equation 10. The free-energy change associated with the electron transfer process (from the encounter complex to the radical ion pair), ΔG_{23}, is calculated from the oxidation potential of the donor ($E_{ox}(D/D^{\bullet+})$), the reduction potential of the acceptor ($E_{red}(A^{\bullet-}/A)$), the singlet energy of the excited species (E_{oo}) and the coulombic attraction energy gained by bringing the two radical ions to the encounter distance (α) in a solvent of dielectric constant (ϵ) (Equation 11). The rate constants k_{12} and k_{21} are diffusional rate constants

$$\text{A*} \quad + \quad \text{D} \underset{k_{21}}{\overset{k_{12}}{\rightleftharpoons}} [\text{A}\cdots\text{D}]^* \underset{k_{32}}{\overset{k_{23}}{\rightleftharpoons}} \text{A}^-\cdots\text{D}^{\bullet+}$$

diffusion   electron transfer

$\dfrac{1}{\tau_0}$ $\downarrow$ k_{30} $\downarrow$
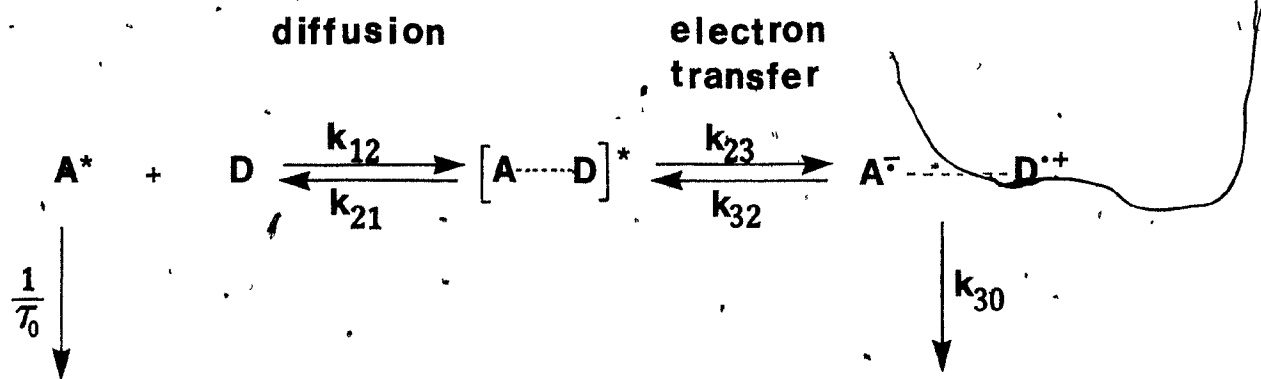
Scheme I

$$k_q = \frac{k_{12}}{1 + k_{21}/k_{23} + k_{21}/(k_{30}K_{23})} \qquad [9]$$

5

$$K_{23} = k_{23}/k_{32} = \exp(-\Delta G_{23}/RT) \qquad [10]$$

$$\Delta G_{23} = 23.06[E_{ox}(D/D^{\bullet+}) - E_{red}(A^{\bullet-}/A) - e^2/\alpha\epsilon] - E_{oo} \qquad [11]$$

and, therefore, can be expressed in terms of the diffusion coefficients for the two interacting molecules (8,9). The rate constants involving electron transfers (k_{23}, k_{32} and k_{30}) are more conveniently expressed in their Arrhenius form (Equation 12). Substitution of these expressions into [9]

$$k_{ij} = k_o \exp(-\Delta G^{\ddagger}_{ij}/RT) \qquad [12]$$

gives a new expression for k_q (Equation 13) which relates k_q to the free-energy change associated with the electron-transfer (ΔG_{23}) and the activation free-energy for electron-transfer ($\Delta G^{\ddagger}_{23}$).

$$k_q = \frac{2.0 \times 10^{10} \ M^{-1} \ s^{-1}}{1 + 0.25[\exp(\Delta G^{\ddagger}_{23}/RT) + \exp(\Delta G_{23}/RT)]} \qquad [13]$$

Weller assumed that the $\Delta G^{\ddagger}_{23}$ was a monotonous function of ΔG_{23} (Equation 14), where, $\Delta G^{\ddagger}_{23}(0)$ is the activation free-energy at $\Delta G_{23} = 0$. (This value has been experimentally determined to be 2.4 kcal mol^{-1}). This model

6

predicts that for exothermic electron-transfer quenching, k_q will be at the diffusion controlled limit.

$$\Delta G^{\ddagger}_{23} = [(\Delta G_{23}/2)^2 + (\Delta G^{\ddagger}_{23}(0))^2]^{1/2} + \Delta G_{23}/2 . \qquad [14]$$

The empirical expression for ΔG_{23} (Equation 11) has become known as the Weller equation and, is used to predict the possibility of electron-transfer quenching of an electronically excited molecule by a quencher molecule. This relationship can be understood by considering the relative energies of the HOMO and LUMO of the interacting molecules (Figure 1). Consider, for example, Figure 1a. The molecule with the lower singlet energy is excited (in this case the donor molecule) and the electron transfer can occur from the singly occupied MO of the donor to the LUMO of the acceptor. The energy required to induce the electron transfer is represented by the energy difference between the HOMO of the donor and the LUMO of the acceptor. The energy available is the singlet energy of the donor. If the singlet energy of the donor is greater than the energy difference between the HOMO and the LUMO then the electron transfer process will be exothermic. Similarly, if the acceptor molecule has the lower singlet energy (Figure 1b), the electron transfer will occur from the HOMO of the donor to the singly occupied (originally the HOMO) molecular
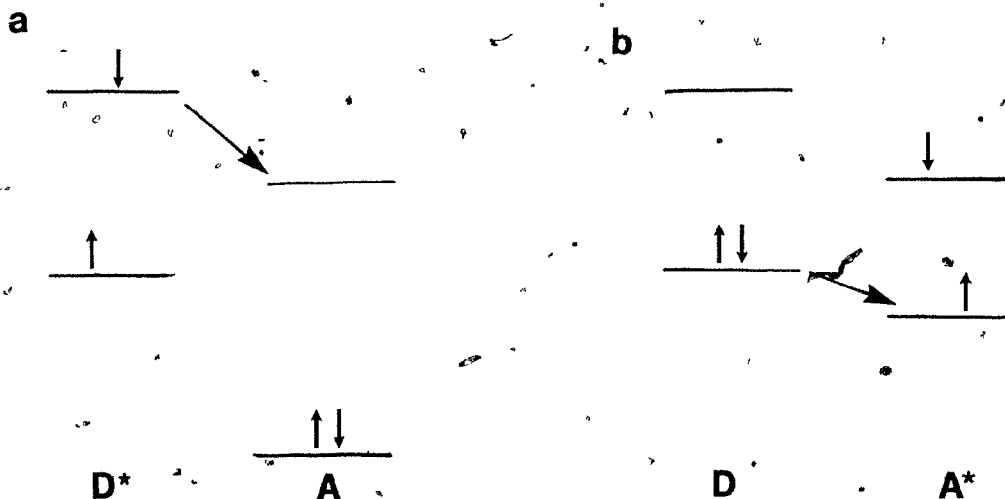
Figure 1. A simplified molecular orbital representation of the photosensitized electron-transfer process.

orbital of the acceptor. Again, the energy difference between the HOMO of the donor and the LUMO of the acceptor' must be less than the singlet energy of the acceptor. The energy difference between the HOMO of the donor and the LUMO of the acceptor is approximately $E_{ox}(D/D^{\cdot+})-E_{red}(A^{\cdot-}/A)$, the first term of the Weller equation (Equation 11).

Marcus (10) has derived an expression for k_q similar to Equation 13. However, in this case, a different expression for $\Delta G^{\ddagger}_{23}$ was used (Equation 15). The expressions in Equations 14 and 15 are in agreement with the experimentally determined values of k_q when ΔG_{23} is greater

$$\Delta G\ddagger_{23} = \Delta G\ddagger_{23}(0) \, [1 + \Delta G_{23}/4 \, \Delta G\ddagger_{23}(0)]^2 \qquad [15]$$

than -15 kcal mol^{-1}. However, the Marcus relation predicts that k_q will decrease as the reaction becomes more exothermic. This is known as the "Marcus inverted region" and, based on the experimental observations of Weller and many others, does not seem to apply to the photoinduced formation of radical ion pairs.

There is still some question regarding the dynamics of the electron transfer in these donor-acceptor systems. It is known that in non-polar solvents, some donor-acceptor pairs which lead to radical ion formation in polar solvents, show emission due to exciplex (or hetero-excimer) formation (11). It is accepted that exciplexes have some charge-transfer character, and, the wave function representing an exciplex includes contributions from locally excited states as well as the charge-transfer states (12, Equation 16). As

$$\psi_{ex} = c_1 \psi_1 (A^*,D) + c_2 \psi_2 (A,D^*) + c_3 \psi_3 (A^-,D^+)$$
$$+ c_4 \psi_4 (A^+,D^-) \qquad [16]$$

the polarity of the solvent increases, the exciplex emission becomes red-shifted and a decrease in the fluorescence quantum yield is observed (13). The decrease in the fluorescence quantum yield was attributed to the formation of

9

$$A^* + D \longrightarrow A^* \text{----} D \longrightarrow (A^- D^+)^*$$

$$\downarrow k_{ip}$$

$$A^- \text{----} D^{\cdot +} \xrightarrow{k_i} A^- + D^{\cdot +}$$
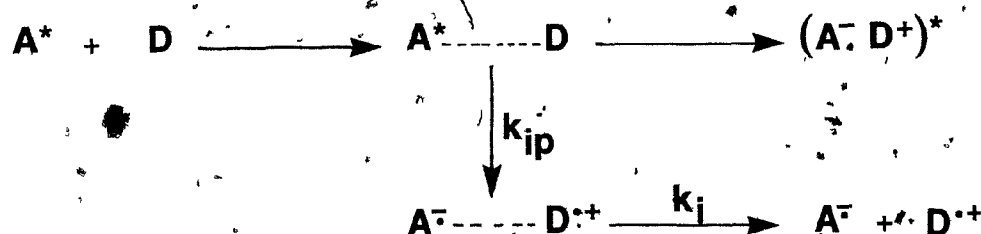
Scheme II.

solvated radical ion pairs (14, Scheme II). In this Scheme, it was assumed that the radical ion pair was formed from the initial encounter complex (k_{ip}) and that the fluorescent exciplex formation, $(A^- D^+)^*$ competes with electron transfer. In polar solvents, both k_{ip} and k_i (the rate of ionic dissociation) increase.

Ionic dissociation is an important factor in the study of radical ion reactions, especially the rate of ionic dissociation relative to the back electron-transfer process. Masuhara and Mataga (15) have studied the ionic dissociation of donor-acceptor systems in solution. In this study, an empirical relationship between the quantum yield for ionic dissociation (φ_1) and the dielectric constant of the solvent (ϵ) was developed (Equation 17), where p and q are constants. In acetonitrile, they found that the value of k_i was $> 10^8$ s^{-1}. Others (16) have found that the rate constant for this process in acetonitrile is typically 5×10^8 s^{-1}.

$$\log [\varphi_i^{-1}] = p/\epsilon + q \qquad [17]$$

The rate constant for back electron-transfer process, on the other hand, ranges from 2×10^{10} s^{-1} to approximately 10^9 s^{-1} (2a). Farid and coworkers have found that the quantum yield for formation of solvent separated radical ion pairs increases, with increasing exothermicity for back electron-transfer. This behaviour was explained in terms of the gap theory for radiationless decay and, was thought to correspond to the Marcus "inverted region" of electron transfer.(10).

Electrochemical methods also have become important to the study of radical cations. The electrode, simply, is an electron transfer agent and, as such, allows the formation of a radical cation in solution which is relatively isolated from protons or counter radical ions (2c). There are a large number of electrochemical techniques available (17). These can be separated into two classes: voltammetric techniques and bulk electrolysis techniques. The theory associated with these techniques is well developed (18) and so extensive that only a brief synopsis is possible.

Voltammetric techniques usually employ a three electrode cell: the working electrode, at which the electroanalytical measurements are made, the counter (or auxiliary) electrode, which is of opposite polarity to the working electrode, and, the reference electrode, which is a

stable half-cell and serves as an arbitrary zero to which all other potentials are compared.

The most frequently used voltammetric technique is cyclic voltammetry. This technique uses a stationary (platinum, gold or glassy carbon) electrode in an unstirred solution (17). In this technique (also referred to as triangular wave voltammetry) the potential at the working electrode is varied linearly with time and the current through the working electrode is measured. At some potential, E_s, the direction of the scan is reversed and, again, the current through the working electrode is measured. The result is a graph of current (i) versus potential (E) which is called a cyclic voltammogram.

For a reversible system (Figure 2, 19), the cyclic voltammogram exhibits several features. Consider, for example the reversible couple, $R \rightleftharpoons R^{\cdot +}$. On the initial forward scan, as the oxidation potential of R is approached, the anodic current increases. At some potential, E_{pa}, the current becomes limited by mass transport to the electrode (diffusion) and the anodic current decreases. When the direction of the scan is reversed, the radical cation will be reduced and, the resulting cathodic current will reach a diffusion controlled limit at potential, E_{pc}. For a completely reversible system, $E_{pa} - E_{pc} = 56$ mV and $i_{pa} = i_{pc}$ (17). Furthermore, the peak potentials are independent of the sweep rate (v) and, the peak current is proportional to $v^{1/2}$ (Equation 18). The peak potential, E_{pa}, is given by

12
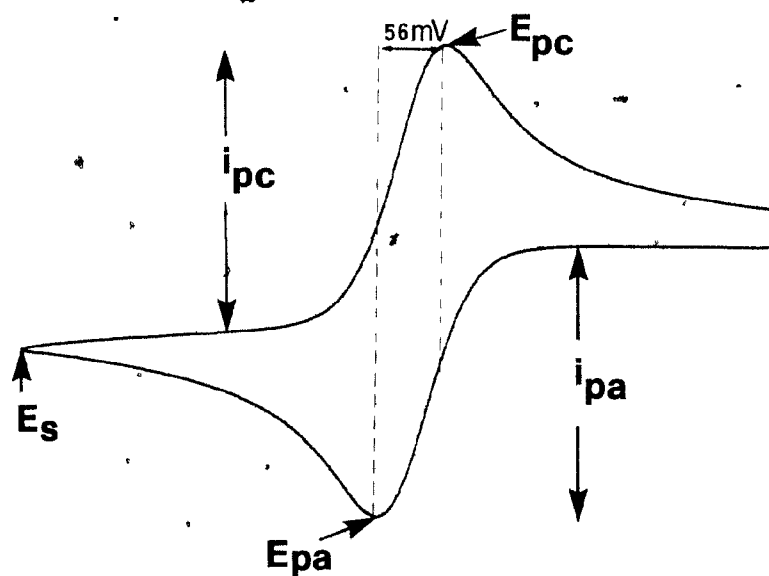
Figure 2. A typical cyclic voltammogram for a reversible electrochemical reaction $R \rightleftharpoons R^{\bullet+}$.

Equation 19 (the constants A, D_{ox}, and C_b refer to the electrode area, the diffusion coefficient of the electroactive species and the concentration of the electroactive species respectively), where $E_{1/2}$ is defined in Equation 20. A good approximation, however, is where the standard potential, E^O, which has thermodynamic significance, is given by Equation 21.

$$i_p = \pm 0.4463 (n^3 F^3/RT)^{1/2} AD_{ox}^{1/2} C_b v^{1/2} \qquad [18]$$

13

$$E_{pa} = E_{1/2} - 1.109RT/nF \qquad [19]$$

$$E_{1/2} = E^O + RT/2nF \ \ln(D_R/D_{R^{\cdot+}}) \qquad [20]$$

$$E^O = E_{1/2} \qquad [21]$$

Unfortunately, many organic molecules do not show reversible redox behaviour. There are two sources of irreversible behaviour to consider. If the oxidized or reduced form of the electroactive species is unstable (i.e. it reacts) then distortions of the cyclic voltammogram will result (17). This is known as chemical irreversibility (Scheme III). In this example, the electroactive species

$$R \xrightarrow{\ -e^-\ } R^{\cdot+} \qquad E$$

$$R^{\cdot+} \xrightarrow{\ k\ } P^{\cdot} \qquad C$$

$$P^{\cdot} \xrightarrow{\ -e^-\ } P^+ \qquad E$$
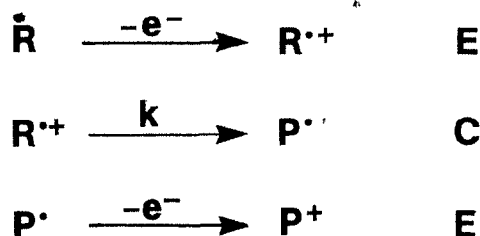
Scheme III.

undergoes what is known as an ECE reaction (E for electrochemical and C for chemical). The electrode kinetics associated with this type of irreversibility has been

discussed in detail (18). If the chemical step is competitive with the scan rates used, the rate constant associated with the chemical step can be determined (18a).

Another source of irreversibility is electrochemical irreversibility. This type of irreversible electrode process is related to the heterogeneous rate constant for electron transfer (18,20). In cyclic voltammetric measurements, this is manifested in several ways; primarily, sweep rate dependence on E_p (Equation 22) and, a half-width $(E_p-E_{p/2})$ which is generally greater than 56 mV (for a one-electron transfer, Equation 23, where n_a is the number of electrons transferred at the rate limiting step).

$$(E_p)_2 - (E_p)_1 = RT/\alpha n_a F \ln(v_1/v_2)^{1/2} \qquad [22]$$

$$E_p - E_{p/2} = 1.857RT/\alpha n_a F \qquad [23]$$

In both Equations 22 and 23, a new parameter has appeared, α. This is generally referred to as the transfer coefficient. The physical significance of the transfer coefficient has been addressed by several workers (21). Consider the rates of the forward and reverse electron transfer processes; there will be an activation energy associated with each. At equilibrium, the rates of the forward and reverse reactions are equal. If, for the redox

couple $R \rightarrow R^{\bullet +}$, the potential is displaced from its equilibrium value by an amount $-nF\Delta E$, then the activation energy for the forward reaction ($R \rightarrow R^{\bullet +}$) will only increase by some fraction of this. Similarly, the activation energy for the reverse reaction ($R^{\bullet +} \rightarrow R$) will decrease by some fraction of $-nF\Delta E$. The fraction is called the transfer coefficient and, is related to the shapes of the potential energy surfaces of R and $R^{\bullet +}$ at different potentials (19).

Bulk (controlled potential coulometric) electrolysis is usually carried out in a separated (H-type) cell in which the anode is separated from the cathode. The solutions are stirred and, generally, large surface area electrodes are used. The Nernst diffusion model (19) predicts that current (i) will decrease exponentially with time, (Equation 24). The time constant will depend on the surface area of the electrode (A), the diffusion coefficient of the electroactive species (D) and the volume of the cell (V) and the diffusion layer thickness (δ).

$$i = i_0 \exp(-ADt/V\delta) \qquad [24]$$

These two techniques, photosensitized (electron transfer) and electrochemical, have inherent advantages and disadvantages. However, from each method different

16

information can be gained about the system under study and, as such, the two methods complement one another.

1.1.2 1,n-Radical Ions

This section is concerned primarily with the chemistry of 1,n-radical ions; radical ions in which the radical centre and the ionic centre are separated by a saturated chain of n-2 carbons (22). The 1,2-radical ion has been generated by the one-electron oxidation or reduction of an olefin. The 1,3- and 1,4-radical ions are generated by the oxidation or reduction of cyclopropanes and cyclobutanes. The 1,4-radical ions can also be generated by the dimerization of a 1,2-radical ion with an olefin (2a). Reactions of 1,n-radical ions with n greater than 4 have not been reported.

The 1,n-radical ions are an interesting class of intermediates since the radical centre and the ionic centre will be separated from each other. Some of the questions that can be addressed are: (1) does the intermediate react as an ion or a radical or either; (2) does the radical centre interact with the ionic centre, i.e. how strong is the one-electron two-centre bond in a radical cation compared to the three-electron two-centre bond in the radical anion; (3) will the reactions of these intermediates

17

prove to be synthetically useful?

The first step in this general program has been to study the reactivity 1,3-radical cations generated by photosensitized (electron-transfer) and electrochemical methods. In particular, the focus is on the 1,3-radical cation obtained by the one-electron oxidation of 1,1,2,2-tetraphenylcyclopropane, and, the effect of the choice of sensitizer on the course of the reaction.
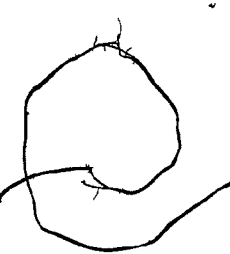
1.1.3 The Role of the Sensitizer

The primary role of the acceptor in photosensitization (electron-transfer) reactions is to absorb a photon and, generate an electronically excited state (22). Encounter of this electronically excited molecule with an appropriate donor molecule can lead to electron-transfer quenching and, subsequent formation of the radical-ion pair. Unfortunately, it is not always possible to study the intrinsic reactivity of isolated radical cations by this method. Although it has not been generally recognized, the nature of the acceptor radical anion often plays an important role. Several examples will illustrate this point.

The ultimate reaction of the 1,2-diphenylcyclopropane (1) radical cation/sensitizer radical anion pair depends upon the acceptor. When 1,4-dicyanonaphthalene (DCN) is used as the electron accepting sensitizer, cis-trans isomerization of 1 is observed (23). The proposed mechanism

18

for this reaction, based on photochemically induced dynamic nuclear polarization (CIDNP), indicates that back electron-transfer from the radical anion to the radical cation gives the triplet of 1 (the trimethylene) which subsequently isomerizes. The energy of the radical ion pair is greater than the triplet energy of 1. On the other hand, when chloranil (TCQ) is used as the electron acceptor, no cis-trans isomerization occurs; CIDNP studies indicate that $1^{\cdot+}$ is formed as before, but, in this case back electron-transfer only yields the ground state singlet of 1 (23b). Apparently, cis-trans isomerization of $1^{\cdot+}$ is slow enough that it cannot compete with the back electron-transfer process.

In a similar example, the photosensitized (electron-transfer) isomerization of quadricyclane (2) to norbornadiene (3, Scheme IV) has been studied by Roth and coworkers using CIDNP (24). It was found that with TCQ as the sensitizer, $2^{+\cdot}$ readily isomerized to $3^{+\cdot}$; while, the reverse reaction did not occur. However, if 1-cyanonaphthalene (CN) was used as the sensitizer (CN), the isomerization of 3 to 2 did occur. Roth concluded that isomerization of 3 to 2 proceded via the triplet of 3. The energy of the radical ion pair with TCQ as the sensitizer was below the triplet energy of 3. In the examples above, therefore, the critical factors which influence the reaction are the triplet energy of the radical ion pair and the triplet energy of the sensitizer relative to the triplet

19
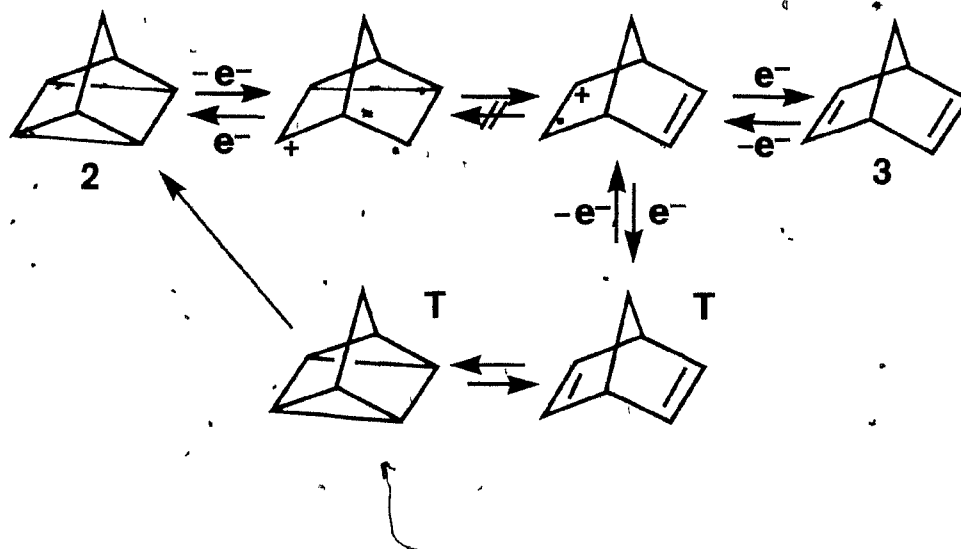
Scheme IV:

energy of the donor.

In another reaction, photosensitization (electron-transfer) of phenylcyclopropane (4, Scheme V) in methanol using 1,4-dicyanobenzene (DCB) as the acceptor, gives an almost equal mixture of the anti-Markownikoff addition product, methyl-3-phenylpropyl ether (5), and the photosubstitution product, 3-methoxy-1-(4-cyanophenyl)-1-phenylpropane (6) (25). When 1,1-diphenylcyclopropane (7) is subjected to these conditions, none of the analogous photosubstitution product is obtained; methyl-3,3-diphenylpropyl ether (8) is formed in almost quantitative

20

yield (Scheme VI).

In both cases the initial reaction of the radical cation is to add methanol to form the benzylic or diphenylmethyl type radical intermediate. In the case of **4**, coupling between the benzylic type radical and the DCB radical anion competes effectively with back electron-transfer; i.e. reduction of the radical. With **7**, coupling between the diphenylmethyl type radical and the DCB radical anion cannot compete with reduction of the radical. The difference in reactivity is attributed to the differences in the reduction potentials of the intermediate radicals. The diphenymethyl type radical is considerably easier to reduce than the benzyl type radical. While the reduction potential of this benzylic radical is not known, it will certainly be greater than that of benzyl (-1.43 V vs sce, HMPA-THF, 26) and may, in fact, be comparable to that of DCB (1.60 vs sce, acetonitrile, 2a). It therefore seems likely that the benzylic type radical and DCB radical anion will be in equilibrium with the benzylic type anion and DCB. In the diphenylmethyl analogue (the reduction potential of the diphenylmethyl radical is -1.16 V vs sce, HMPA-THF, 26) the equilibrium will be largely in favour of the anion. So, in this case, it is the reduction potential of the sensitizer that ultimately determines the reactivity of the radical ion pair (although steric factors also may play a role). A similar competition between addition of methanol and photosubstitution has been observed for olefin radical

21
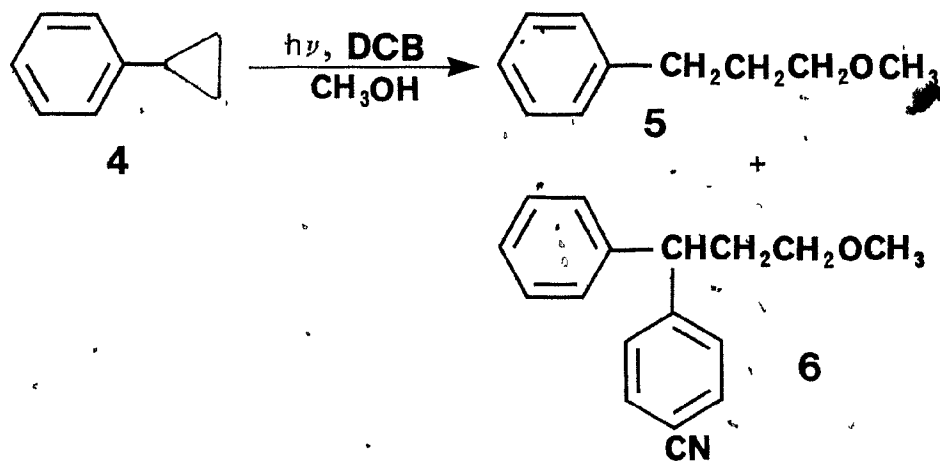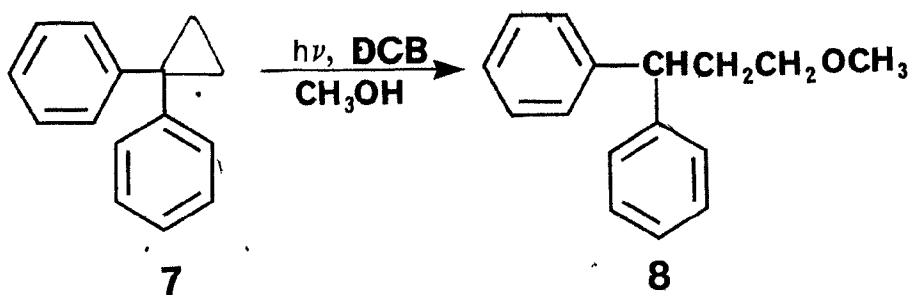
Scheme V.

Scheme VI.

cations (27).

There are other examples where the nature of the
sensitizer can influence the course of the reaction. The
product resulting from the anti-Markownikoff addition of
methanol to 1,1-diphenylethylene, methyl-2,2-
diphenylethylether (9) is isolated in good yield when CN is
the sensitizer (28a). On the other hand, with DCN as
sensitizer, the products obtained are diphenylmethane (10)
and the methylacetal of formaldehyde (28b, Scheme VII). The
difference in this case is in the free energy associated
with electron-transfer (calculated from Equation 11) between

$$\phi_2 C = CH_2 \xrightarrow[\text{CH}_3\text{OH}]{h\nu,\ \mathbf{A}} \phi_2 CH CH_2 O CH_3 \atop \mathbf{9}$$

$$\phi_2 CHCH_2 OCH_3 \atop \mathbf{9} \quad \xrightarrow[\text{CH}_3\text{OH}]{h\nu,\ \mathbf{A}} \phi_2 CH_2 \atop \mathbf{10} + CH_3 O CH_2 OCH_3$$
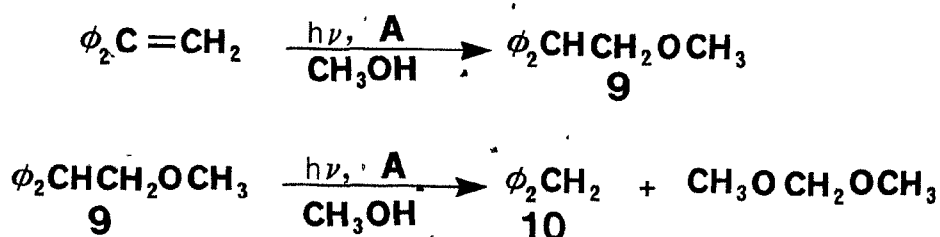
Scheme VII.

the excited state of the sensitizer and the donor; the
primary product, 9. With CN as sensitizer this is not a
favourable process (28b).

Another important characteristic of the sensitizer
radical anion that can influence the fate of the radical
cation is basicity; the radical cation may deprotonate with

the radical anion serving as the base (29). The observed

reaction will then depend on the reactivity of the radical

-pair. The electron transfer process greatly increases the

acidity of the donor (30) and the basicity of the acceptor;

so, proton transfer should frequently be favourable.

Apparently, proton transfer is not always rapid enough to

compete with other reactions or this process would be much

more common.

Awareness of the importance of these considerations

developed from the observations of the reactivity of the

1,1,2,2-tetraphenylcyclopropane (11) radical cation which

were apparently inconsistent. It has been reported that the

photosensitized (electron-transfer) reaction of 11 in

acetonitrile solution using DCN as the electron accepting

sensitizer, gave 1,1,3,3-tetraphenylpropene (12) in good

yield (31, Scheme VIII). In contrast, when

tetracyanoethylene (TCNE) was used as the acceptor, 1,3,3-

triphenylindene (13) was the only product (31, Scheme IX).

The formation of 13 was thought to involve the 1,1,3,3-

tetraphenylpropenyl cation, yet, it was known that this

cation, generated by treatment of the alcohol precursor with

acid, gave good yields of tetraphenylallene (14) (32, Scheme

X); and, the allene was not detected in either of the

photosensitized (electron-transfer) reactions.

A further complication was obvious from the work of

Hixson which was reported about the same time (25). As

mentioned above, 7 gives the methanol addition product upon

$$\text{11} \quad \underset{\text{Ph}_2 \quad \text{Ph}_2}{\triangle} \quad \xrightarrow[\text{CH}_3\text{CN}]{h\nu,\,\text{DCN}} \quad \text{Ph}_2\text{C}=\text{CHCH Ph}_2 \quad \text{12}$$

Scheme VIII.

$$\text{11} \quad \xrightarrow[\text{TCNE,CH}_3\text{CN}]{h\nu\,\rangle\,\textbf{400}\,\text{nm}}$$

13

Scheme IX.

$$\text{Ph}_2\text{C}=\text{CHC(OH)Ph}_2 \quad \xrightarrow[\text{CH}_3\text{COOEt}]{\textbf{HA}} \quad \text{Ph}_2\text{C}=\text{C}=\text{CPh}_2 \quad \text{14}$$
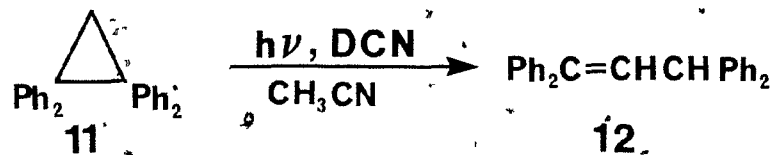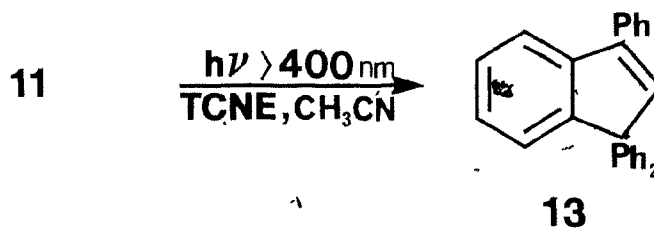
Scheme X.

irradition in methanol with DCB as the acceptor. Similar
irradiation of 11 gave good yields of 12; no 1-methoxy-
1,1,3,3-tetraphenylpropane (15) was detected. If the
1,1,3,3-tetraphenylpropenyl cation were involved in this
reaction, 3-methoxy-1,1,3,3-tetraphenylpropene (16) should
have been formed.

These results were particularly surprising, not only
because 15 was not formed, but also because 12 was
apparently stable under these conditions. It is well
established that 1,1-diphenylethylene and other arylalkenes
react to form the anti-Markownikoff addition products under
these conditions; by analogy, 12 should give 2-methoxy-
1,1,3,3-tetraphenylpropane (17). However, this product also
was not observed.

This large number of possible products from a
relatively simple substrate (11) may not be unusual for
electron-transfer reactions. An understanding of the
complex behaviour which determines the course of the
reaction is essential to the development of synthetically
useful reactions in this area.

This section describes the effect of different
sensitizers on the photosensitized (electron-transfer)
reactions of 11. These results are compared to the
electrochemical oxidation reactions of 11.

1.2   RESULTS

1.2.1 Photosensitized (electron-transfer) irradiation of 11

The pertinent characteristics of the electron accepting
sensitizers used in this study are listed in Table 1. The
reduction potentials were determined by cyclic voltammetry
and, since analysis of the waves indicates the electrode
processes are reversible, these values are thermodynamically
significant. The anodic oxidation of 11, however, is not
reversible; so, there is some uncertainty in the oxidation
potential. The free-energies for the electron transfer are
calculated using the Weller equation (8, Equation 11).

The results of the irradiations are summarized in Table
2. Sensitizers 1,4-dicyanobenzene (DCB), 1,4-
dicyanonaphthalene (DCN), 9, 10-dicyanoanthracene (DCA), and
methyl-4-cyanobenzoate (MCB) all lead to formation of
1,1,3,3-tetraphenylpropene (12) in acetonitrile solution
(Scheme VIII).

Hixson and his coworkers (25), have reported that 12 also
was formed from 11 upon irradiation in methanol solution.
This observation has been confirmed; when the
irradiation is carried out in acetonitrile-methanol (3:1,
v/v) only 12 is produced. No product resulting from the
addition of methanol (neither 15 nor 16) was detected. When
this irradiation is carried out in acetonitrile-methanol-Od,
the product (12) has deuterium (>95%) incorporated at the

27

Table 1. Calculated free energy change for electron transfer from 11[a].

Acceptor	E_{oo} (kcal mol^{-1})	E_{red} (V vs sce)	ΔG_{ET}[b] (kcal mol^{-1})
1,4-dicyano-benzene (DCB)	98.6[c]	-1.60	-31.7
1,4-dicyanonaphthalene (DCN)	79.6[c]	-1.28	-17.6
9,10-dicyanoanthracene (DCA)	66.6[c]	-0.89	-14.6
methyl-4-cyanobenzoate (MCB)	74.5[c]	-1.77	-23.7
tetracyanothethylene (TCNE)	d	-0.24	-15.5
chloranil (TCQ)	d	0.02	-20.5
2,3-dichloro-5,6-dicyano-benzoquinone (DDQ)	d	0.51	-31.8

[a]The oxidation potential of 11 is 1.36 V (E_p) in acetonitrile (1,2).

[b]Calculated for electron transfer from 11 using the Weller equation (12) using $e^2/\alpha\epsilon$ = 0.06 eV.

[c]Reference (3a)

[d]In these cases formation of a charge transfer complex was indicated by a new adsorption band at long wavelength. The energy at the onset of the long wavelength charge transfer absorption band is approximately 50 kcal mol^{-1}.

Table 2. Photosensitized (electron transfer) irradiation of **11**.

Acceptor	Product(s)	Yield(%)
DCB[a,b]	**12**	
DCN[a,b]	**12**	
DCA[a]	**12**	65–75
MCB[a]	**12**	
TCNE[a]	**13**(19):**14**(1)	71[c]
TCQ[a]	**13**(1) :**14**(9)	75[c]
DDQ[a]	**13**(1) :**14**(3.5)	47[c]
TCQ[b]	**16**	87[d]

[a] in acetonitrile

[b] in acetonitrile-methanol (3:1, v/v)

[c] combined yield of **13** and **14**

[d] combined yield of **14** and **18**; the decomposition products of **16** on a silica gel column.

allylic position. Extended irradiation of **12** under these conditions does not cause incorporation of deuterium nor methanol addition.

Using tetracyanoethylene (TCNE) as the acceptor, irradiation in acetonitrile, of the charge-transfer band leads to the formation of 1,3,3-triphenylindene (**13**) (31). Careful analysis of this reaction mixture by high pressure liquid chromatography (HPLC) indicates the presence of a trace of tetraphenylallene (**14**) (the ratio of **13** to **14** is 19:1) which was not detected in the previous work. Similar irradiation of this mixture, but with tetraethylammonium perchlorate (TEAP, 0.1 M) added, gives the same products in the same ratio.

On the other hand, with chloranil (TCQ) as the electron acceptor, irradiation of the charge-transfer complex in acetonitrile leads to the formation of tetraphenylallene (**14**) as the major product. Analysis of the reaction mixture by HPLC indicates the ratio of **13** to **14** is 1:9 with this sensitizer. This ratio also does not change when the irradiation is carried out in acetonitrile containing 0.1 M TEAP. When this irradiation was carried out in acetonitrile-methanol (3:1, v/v) the product is 3-methoxy-1,1,3,3-tetraphenylpropene (**16**).

When 2,3-dichloro-5,6-dicyanobenzoquinone (DDQ) is used as the electron accepting sensitizer, irradiation of the charge-transfer band, in acetonitrile solution, leads to the formation of substantial amounts of both **13** and **14**

(1:3.5).

1.2.2 Controlled potential electrolysis of 11

The results from the controlled potential oxidation of
11 under various conditions are summarized in Table 3. The
anodic oxidation of 11 in acetonitrile (0.1 M TEAP) at 1.3 V
(vs. sce) leads to the formation of 1,3,3-triphenylindene
(13); tetraphenylallene (14) was not detected. When the
electrolysis is carried out under similar conditions, but
with 2,6-lutidine (0.1 M) added to the anolyte, the product
is predominantly (14); only a trace (<3%) of 13 is present
under these conditions. Electrolysis of 11 in acetonitrile-
methanol (3:1, v/v) results in the formation of 3-methoxy-
1,1,3,3-tetraphenylpropene (16).

1.2.3 Electrochemical measurements of 11

Cyclic voltammetric studies were carried out in both
acetonitrile (0.1 M TEAP) and dichloromethane (0.1 M
tetrabutylammonium perchlorate TBAP). In acetonitrile,
two irreversible anodic waves are observed at $E_p = 1.36$ V
and $E_p = 1.58$ V, at a sweep rate of 400 mV s^{-1}. As the
sweep rate increases from 50 mV s^{-1}, the relative height of
the second wave decreases and it is not detected at sweep
rates faster than 1.0 V s^{-1} (Table 4).

The cyclic voltammogram of 1,3,3-triphenylindene (13)
reveals a sharp anodic wave ($E_p - E_{p/2} = 40$ mV) at 1.58 V at
a sweep rate of 400 mV s^{-1}. The cyclic voltammogram of this

31

Table 3. Controlled potential electrolysis of 11

Solvent[a]	Conversion(%)	Current Yield (%)[a]	Product(s)[c]	Yield(%)
CH₃CN	50	95	13	90
CH₃CN/0.1M 2,6-lutidine	25	70	13 14	2 55
CH₃CN/CH₃OH (3:1 V/V)	75	70	16	82

[a] 0.1M TEAP

[b] Based on recovered starting material

[c] These are the only products detected by HPLC at 5% conversion.

Table 4. Cyclic Voltammetric Data for 11[a]

Sweep Rate (V s⁻¹)	E_{P1}(V)[b]	i_{P1}(μA)	E_{P2}(V)[b]	i_{P2}(μA)
0.050	1.285	30	1.504	9
0.100	1.244	40	1.540	5
0.200	1.320	53	1.564	3
0.400	1.360	72	1.575	2

[a] in acetonitrile (0.1M TEAP)

[b] vs sce

solution after an equimolar amount of 11 has been added, does not exhibit the wave at 1.36 V. The peak current for the wave at 1.58 V, on the other hand, doubles in value for this mixture (Figure 3).

The cathodic sweep reveals the presence of a reversible wave at $E_{1/2}$ = 0.34 V and an irreversible wave at 0.17 V. The intensity of the reversible wave decreases if the cathodic sweep is delayed.

At the onset of oxidation of 11, the acetonitrile solution around the anode turns visibly purple. A solution of 1,1,3,3-tetraphenylpropenol (18) in acetonitrile (0.1 M TEAP) containing trifluoroacetic acid (5 x 10^{-3} M) turns the same colour. The cyclic voltammogram of this solution also reveals a reversible wave at $E_{1/2}$ = 0.34 V.

Cyclic voltammetric studies in dichloromethane (0.1 M TBAP) were similar to those in acetonitrile. The main difference being that while there is an anodic wave at 1.36 V, the second anodic wave at 1.58 V is not observed. There is a quasi-reversible wave at $E_{1/2}$ = 0.37 V. The onset of oxidation again is accompanied by the development of a purple colour near the surface of the electrode as was the case in acetonitrile.

1.2.4 Spectroelectrochemical measurements

The anolyte turns purple as soon as the potential is applied. The visible absorption spectrum of this solution shows three broad absorption maxima (λ_{max} = 568 nm, 459 nm,
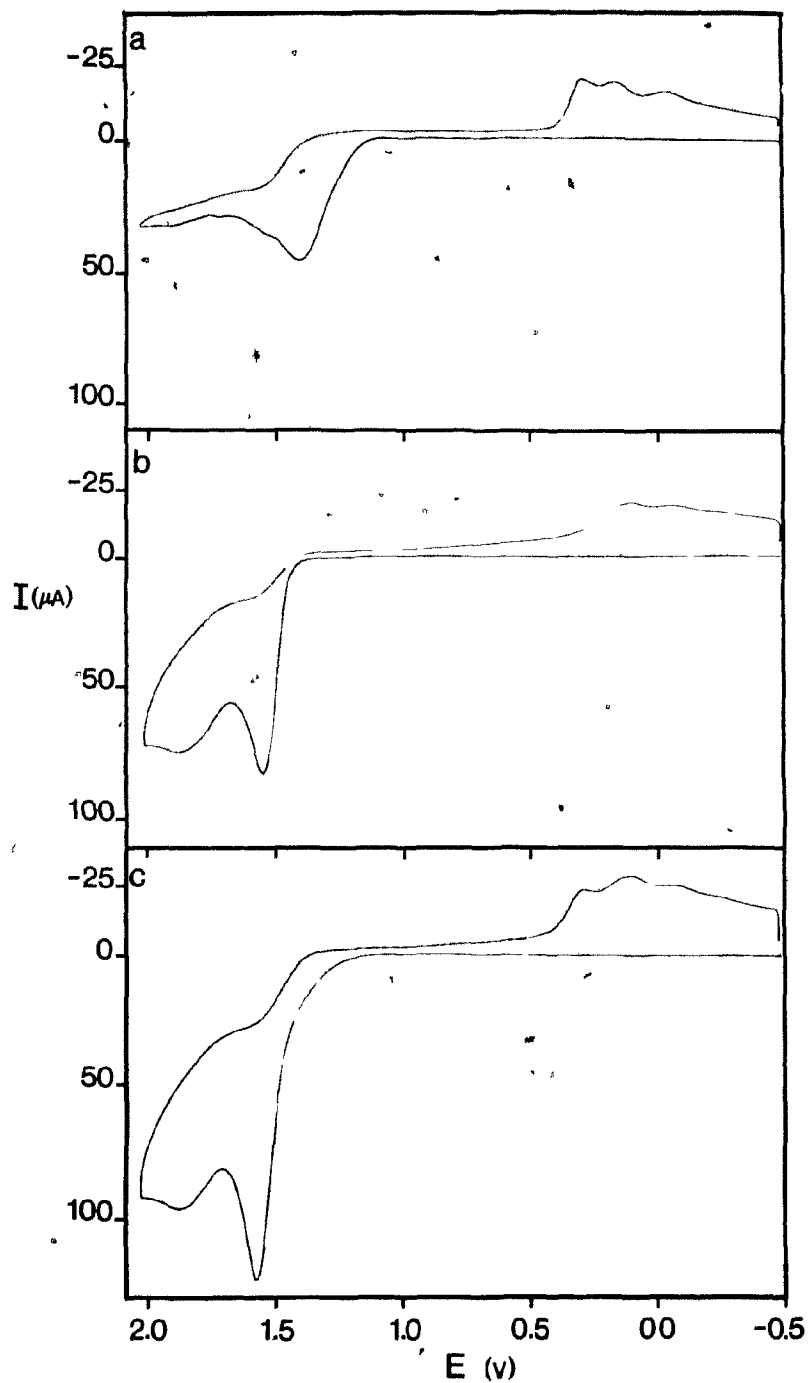
Figure 3. Cyclic voltammograms in acetonitrile, 0.1 M TEAP
at 400 mV s^{-1} of (a) 11 (1.5 x 10^{-3} M), (b) 23
(1.5 x 10^{-3} M) and (c) 11 (1.5 x 10^{-3} M and 13
(1.5 x 10^{-3}M).

34

382 nm) of approximately equal intensity. This spectrum is essentially identical to the spectrum obtained from the 1,1,3,3-tetraphenylpropenol (18) in acetonitrile (0.1 M TEAP) to which trifluoroacetic acid has been added. The irradiation of the charge-transfer band between 11 and TCNE, TCQ or DDQ results in the development of a coloured· intermediate with a similar visible absorption spectrum, within a few seconds of irradiation. This colour slowly disappears if the vessel is removed from the irradiation source.

The rate of disappearance of the coloured intermediate can be measured using an electrolysis cell fitted with Pyrex windows. The rate of disappearance of the colour follows first-order kinetics with a rate constant of 2.87 x 10^{-2} s^{-1} at 23 C. The same rate constant is obtained whether monitoring the absorption at 460 nm or 570 nm (at 380 nm background absorption interferes with the measurement). Furthermore, the rate is independent of electrolyte concentration over the range 0.1 to 0.001 M TEAP (cell resistance precluded measurements at lower concentrations).

The temperature dependence of the rate constant (Table 5) leads to an estimate of the activation energy for loss of the intermediate of 21.8±0.2 kcal mol^{-1} and a preexponential factor (log A) of 14.5±0.3.

1.2.5 Solvent and acid effects on the ratio 13 : 14

The products obtained by treatment of 18, in mixtures of

Table 5. Effect of temperature on the rate of the unimolecular reaction of 1,1,3,3-tetraphenylpropenyl cation in acetonitrile (0.1 M TEAP).

T(C)	$k_{obs}(s^{-1})$
37.6	$0.15\pm.01$
33.2	$0.092\pm.001$
28.3	$0.053\pm.001$
23.2	$0.029\pm.002$
19.6	$0.017\pm.002$
11.9	$0.0063\pm.0001$

acetonitrile and carbontetrachloride, with an acid are **13** and **14.** These products are obtained in chemical yields greater than 90%. The ratio of **13** to **14** is independent of acid concentration at concentrations greater than 5×10^{-3} M (Figures 4 and 5), and, independent of alcohol concentration at concentrations less than 2×10^{-4} M (Figures 6 and 7). The ratio (**3:4**) decreases as the percentage of acetonitrile decreases (Figure 8). While there appears to be no significant differences between trifluoroacetic acid and trichloroacetic acid, 4-toluenesulphonic acid gives a significantly higher ratio (**13:14**) in all solvent mixtures.

1.2.6 Oxidation potentials of 1,1,2,2-tetraaryl-cyclopropanes (11a-h) in dichloromethane

The oxidation potentials ($E_{1/2}$, cyclic voltammetry) of a series of 1,1,2,2-tetraarylcyclopropanes are listed in Table 6. All are irreversible with $E_p - E_{p/2}$ ranging from 30 to 240 mV. The reduction potentials of the corresponding 1,1,3,3-tetraarylpropenyl cations (**19$^+$a-f,h**) are listed in Table 7. These redox couples are all quasireversible in this solvent system with $E_{pa} - E_{pc}$ ranging from 70 to 90 mV.

Correlations of $E_{1/2}$ vs $\Sigma \sigma^+$ for **11a-h** and **19$^+$a-f,h** are shown in Figures 9 and 10 respectively. For **11a-h**, the correlation coefficient is 0.976 with a slope (0.059 $\rho/\alpha n$) of 0.19 V. For **19$^+$a-f,h**, the correlation coefficient is 0.985 with a slope of 0.19 V.
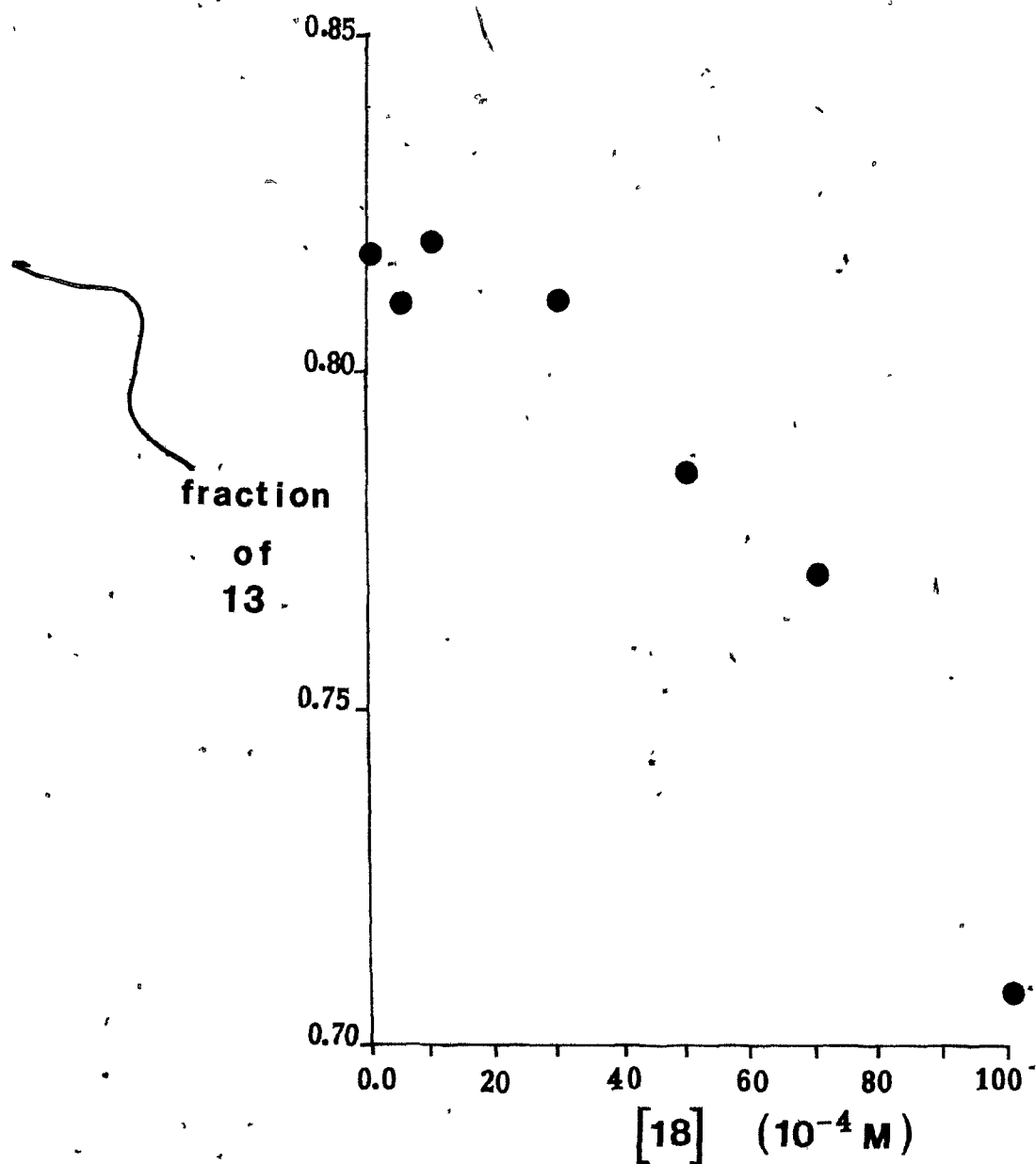
Figure 4. Mole fraction of **13** (the remainder being **14**)
versus [**18**] from the reaction of **18** with
trifluoroacetic acid $(1 \times 10^{-2}$ M) in acetonitrile.
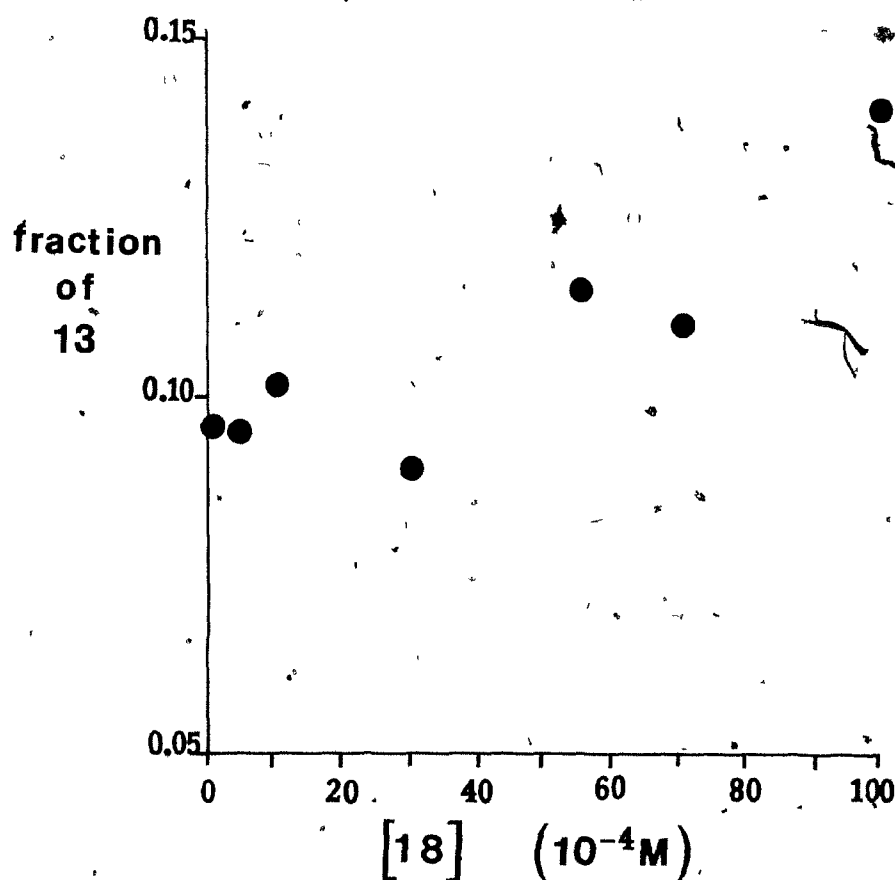
Figure 5. The mole fraction of **13** (the remainder being **14**) versus [**18**] from the reaction of **18** with trifluoroacetic acid (1 x 10^{-2} M) in carbontetrachloride.
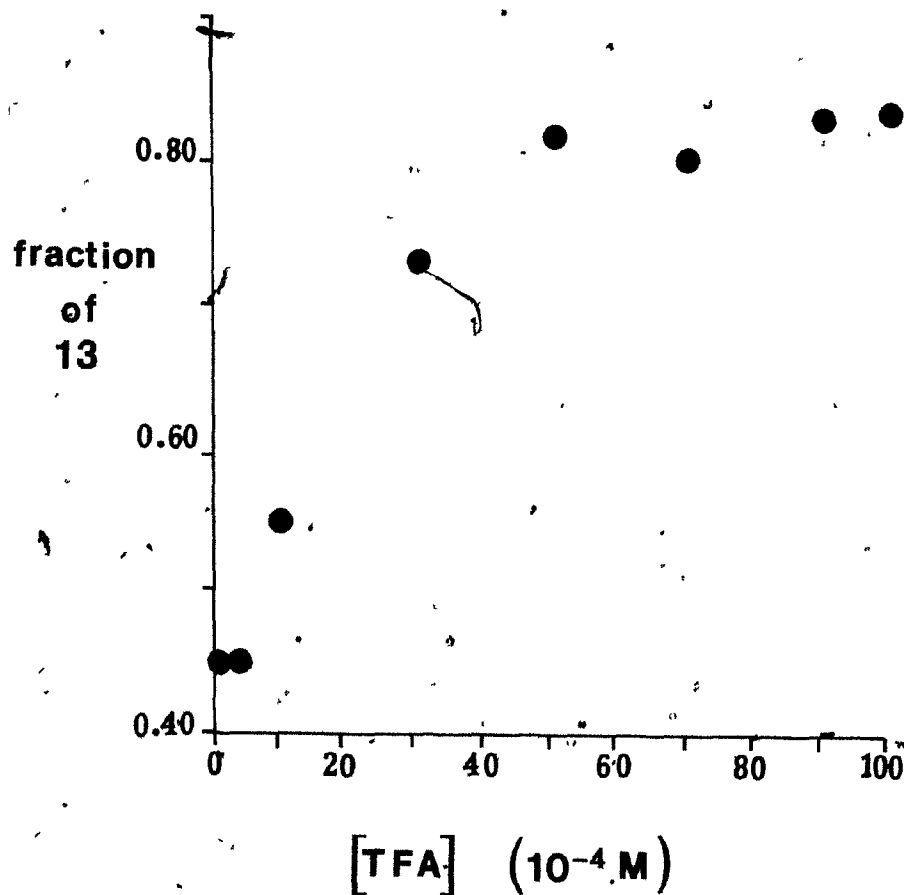
Figure 6. The mole fraction of 13 (the remainder being 14) versus the concentration of trifluoroacetic acid from the reaction of 18 (5×10^{-4} M) with trifluoroacetic acid in acetonitrile.

40
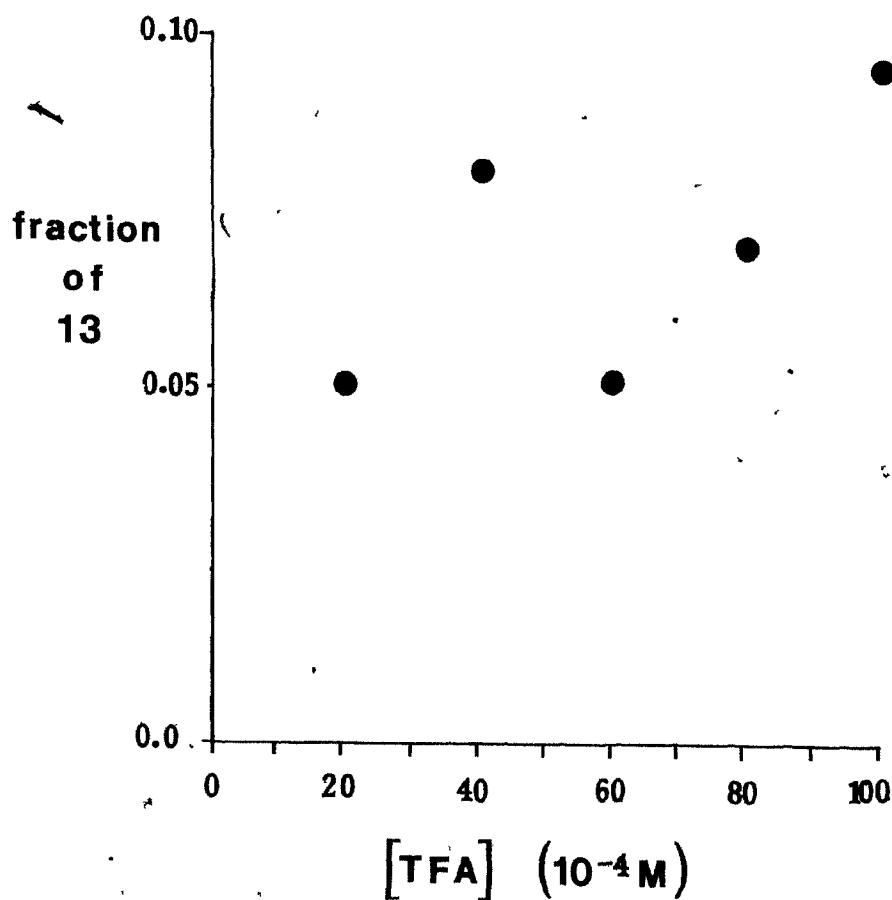
Figure 7. The mole fraction of **13** (the remainder being **14**) versus the concentration of trifluoroacetic acid from the reaction of **18** (5 x 10^{-4} M) and trifluoracetic acid in carbontetrachloride.
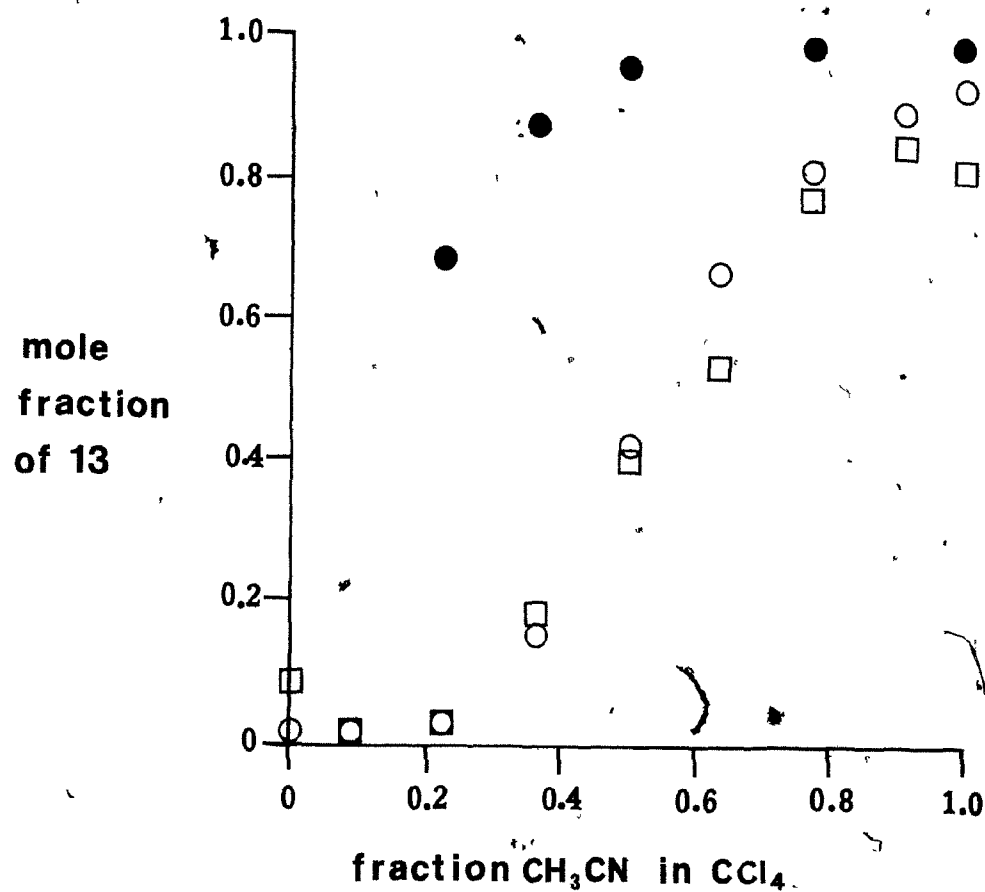
Figure 8. The mole fraction of 13 (the remainder being 14) versus the fraction (by volume) of acetonitrile in carbontetrachloride from the reaction of 18 with (a) ● 4-toluenesulphonic acid, (b) □ trifluoroacetic acid, and, (c) ○ trichloroacetic acid.

42

Table 6. Oxidation Potentials of 1,1,2,2-tetraaryl-cyclopropanes in dichloromethane 0.1M TBAP

11		X_1	X_2	Y_1	Y_2	$E_{1/2}$ (V)[a]	$E_p-E_{p/2}$ (mV)
a		H	H	H	H	1.23	130
b		OCH_3	H	H	H	1.14	160
c	cis	OCH_3	H	OCH_3	H	0.96	140
	trans	OCH_3	H	H	OCH_3	0.96	140
d		OCH_3	OCH_3	OCH_3	OCH_3	0.88	150
e		CN	CN	H	H	1.52	170
f	cis	CN	H	CN	H	1.51	240
	trans	CN	H	H	CN	1.51	240
g		CN	CN	CN	CN	1.80	150
h		OCH_3	OCH_3	CN	CN	1.14	220

[a] volts versus sce.
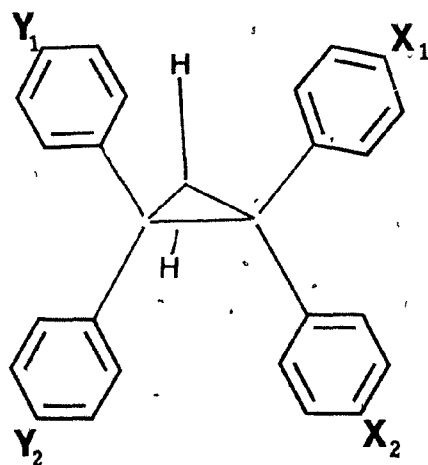
Table 7. The reduction potentials of 1,1,3,3-tetraaryl-propenyl cations (19^+)[a] in dichloromethane 0.1 M TBAP.

19	X_1	X_2	Y_1	Y_2	$E_{1/2}(V)$[b]	$E_p-E_{p/2}$ (mV)
a	H	H	H	H	0.37	90
b	OCH_3	H	H	H	0.22	90
c	OCH_3	H	OCH_3	H	0.12	90
	OCH_3	H	H	OCH_3	0.12	90
d	OCH_3	OCH_3	OCH_3	OCH_3	-0.04	90
e	CN	CN	H	H	0.65	70
f	CN	H	CN	H	0.66	80
	CN	H	H	CN	0.66	80
g	CN	CN	CN	CN	not observed	
h	OCH_3	OCH_3	CN	CN	0.31	80

[a]Generated at the anode from the anodic oxidation of 11a-h.

[b]Volts versus sce.
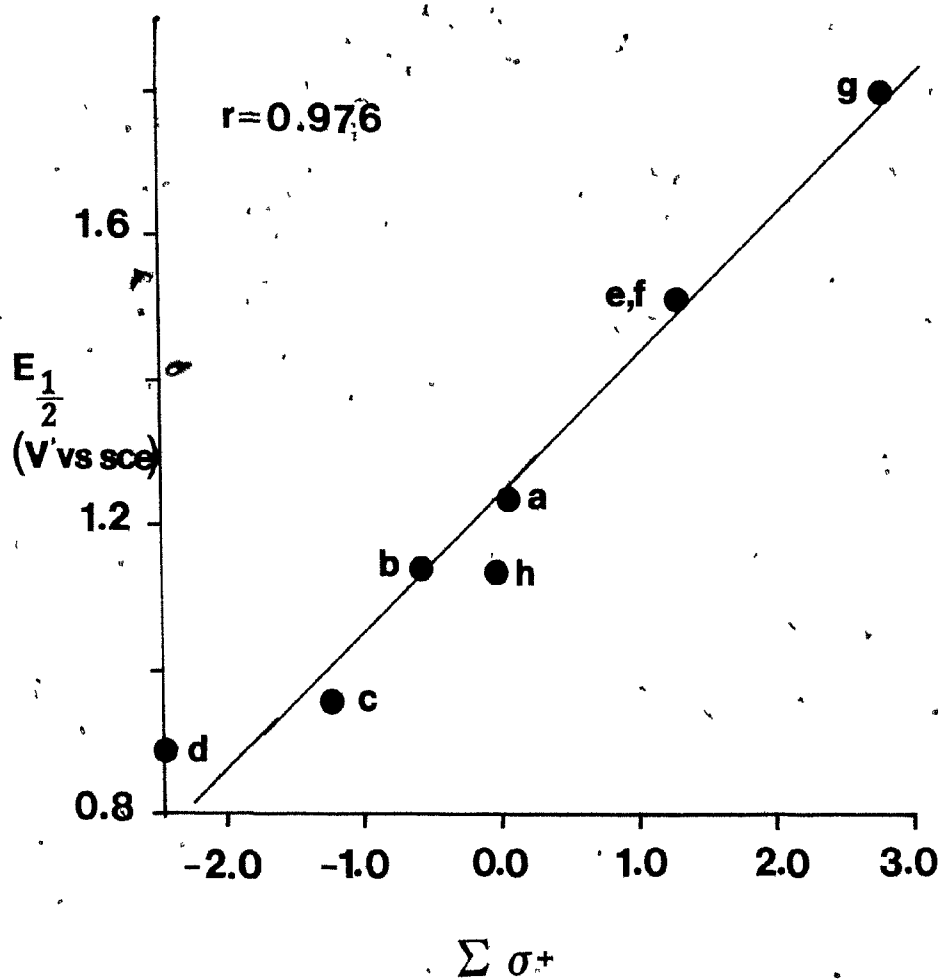
Figure 9: Hammett plot of $E_{1/2}$ of **11a-h** versus $\sum \sigma^+$.

45
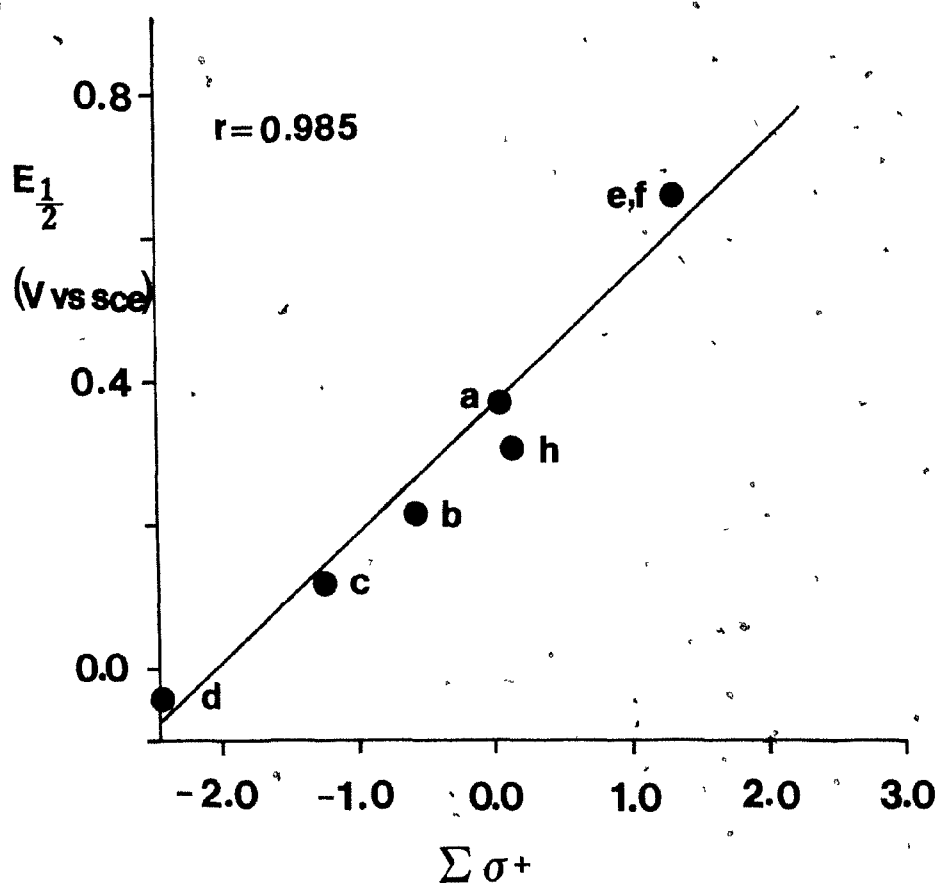
Figure 10. Hammett plot of $E_{1/2}$ of $19^{\ddagger}$a–f,h versus $\sum \sigma^+$.

1.3 DISCUSSION

1.3.1 Photosensitized and electrochemical reactions of 11

The products obtained upon photosensitized (electron-transfer) oxidation of 11 are remarkably dependent upon reaction conditions, particularly solvent and sensitizer. Although some of these observations were reported several years ago (25,31), the mechanism has never been discussed in detail. The sequence outlined in Scheme XI accounts for all the results.

The first two steps, initial excitation of the electron accepting sensitizer and electron transfer to give $11^{\cdot+}$ and $A^{\cdot-}$ are well established and have been discussed in Section 1.1.1. All of the irradiations were carried out through Pyrex so, wavelengths shorter than 290 nm are absorbed by the vessel. The sensitizers have appreciable absorption at longer wavelengths, while 11 is essentially transparent beyond 300 nm. The electron-transfer step is thermodynamically favourable in every case. Table 1 lists the free-energy change for this process as estimated by the Weller equation (Equation 11). With the quinone sensitizers (DDQ and TCQ) the triplet state is undoubtedly involved because of the rapid intersystem crossing in these cases (33). When the sensitizer forms a charge-transfer complex with 11 (TCNE, TCQ, DDQ), irradiation in the wavelength region of the charge-transfer transition can lead directly to the radical ion pair.

47

$$A \xrightarrow[[1]]{h\nu} A^*$$

$$11 + A^* \xrightarrow[[2]]{} Ph_2\overset{+}{\wedge}\cdot Ph_2 + A^{\bar{\cdot}}$$

$$Ph_2\overset{+}{\wedge}\cdot Ph_2 \xrightarrow[[3]]{B(A^{\bar{\cdot}})} Ph_2\overset{}{\wedge}Ph_2 + BH^+(HA^\cdot)$$

$$Ph_2\overset{\cdot}{\wedge}Ph_2 \begin{cases} \xrightarrow[[4]]{A^{\bar{\cdot}}} Ph_2\overset{-}{\wedge}Ph_2 \xrightarrow[[5]]{H^+(D^+)} Ph_2C=CHCXPh_2 \\ \qquad\qquad\qquad\qquad X= H \text{ or } D \\[2em] \xrightarrow[[6]]{HA^\cdot} Ph_2\overset{+}{\wedge}Ph_2 + HA^- \end{cases}$$

$$Ph_2\overset{+}{\wedge}Ph_2 \xrightarrow[[9]]{B} Ph_2C=C=CPh_2 + BH^+$$

$$Ph_2\overset{+}{\wedge}Ph_2 \xrightarrow[[10]]{CH_3OH} Ph_2C=CHC(OCH_3)Ph_2 + H^+$$

Scheme XI.

48
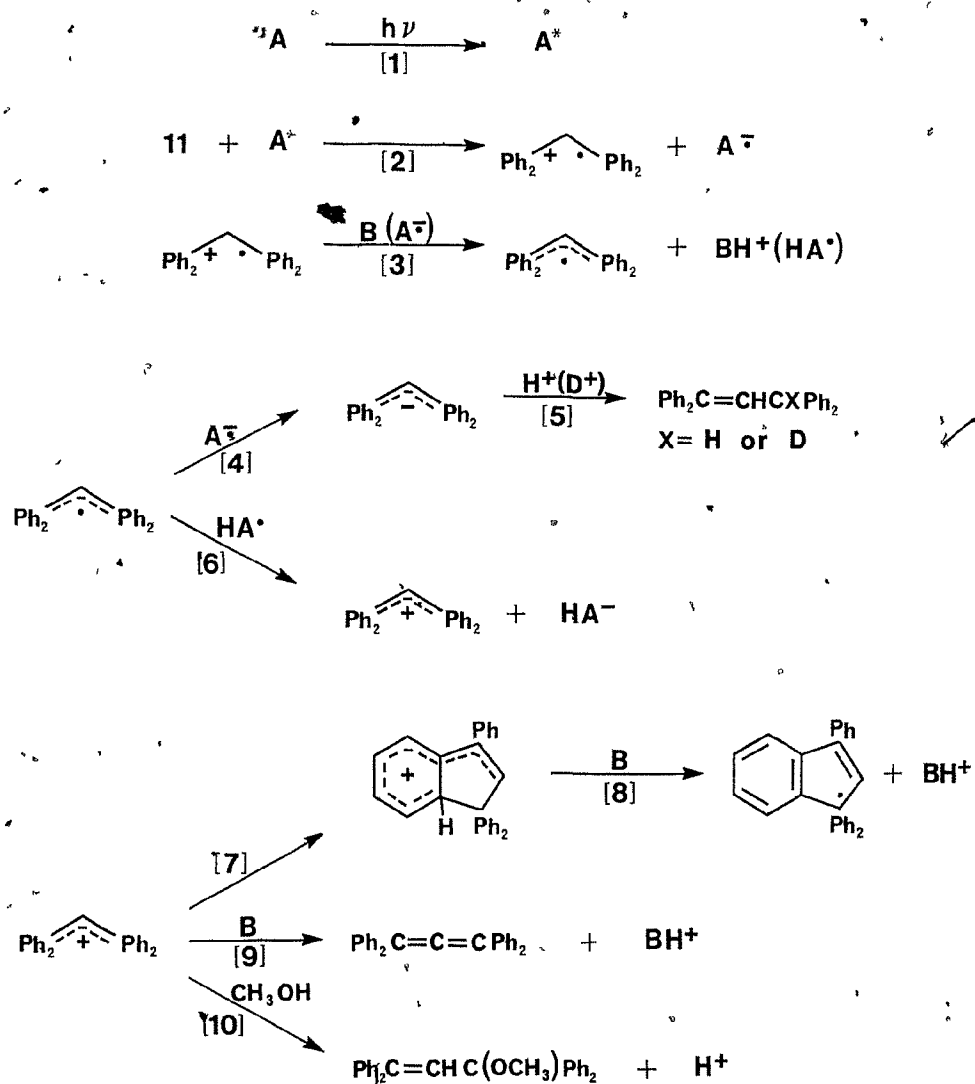
The deprotonation of $11^{\cdot+}$ (Scheme XI, Step 3) dominates the chemistry after the electron transfer has occurred. In many instances in the literature, when a mechanism involving the deprotonation of a radical cation is proposed, the fate of the proton is ignored until it is needed again to protonate another intermediate. In some cases the deprotonation does not seem to occur when it is predicted that it should (34), while in other cases, the anion radical is thought to serve as the base (2a). It is of fundamental importance to understand what is occurring and why. The first requirement is to estimate the pKa of $11^{\cdot+}$.

Several thermochemical cycles have been developed which can be used to estimate the pKa of a radical cation from available thermochemical data (35) . An estimate can be made if the oxidation potential of RH (E^O_{RH}) and the bond dissociation energy of RH (ΔG_{BDE}) are known. In this case, Equation 25 can be used,

$$pKa = 0.73(-FE^O_{RH} + \Delta G_{BDE} + \Delta G_{tr(H^+)} + \Delta G_{f(H)} + \Delta G_{isom}) \quad [25]$$

where $\Delta G_{tr(H+)}$ is the free-energy change associated with the transfer of a proton from water to the solvent of interest, $\Delta G_{f(H)g}$ is the free-energy of formation of a hydrogen atom and, ΔG_{isom} is the free-energy change associated with the isomerization of the cyclopropyl radical to the allyl radical, Figure 11.
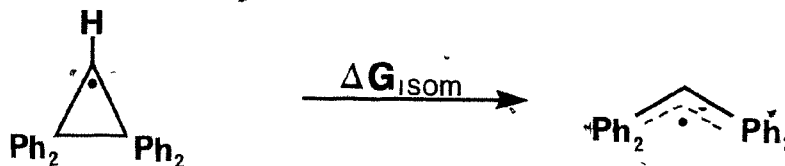
Figure 11. The isomerization of 2,2,3,3-tetraphenyl-cyclopropyl radical to 1,1,3,3-tetraphenyl-propenyl radical.

To determine the pKa of $11^{\cdot+}$, the value of E^O_{RH} is estimated from the E^{OX} (1.48V vs NHE) of the cyclic voltammogram; $\Delta G_{tr(H+)}$ is 11 kcal mol^{-1} for acetonitrile (36); $\Delta G_{f(H)g}$ is 48.6 kcal mol^{-1} and, $\Delta G_{BDE(RH)}$ is approximately 96 ± 3 kcal mol^{-1} (37). The free-energy change associated with the isomerization from the cyclopropyl to the allylic structure (Figure 11), must also be estimated. In the unsubstituted c-C$_3$H$_5$$^{\cdot}$ radical this value is approximately -25 kcal mol^{-1} (14). The extra stabilization associated with the four phenyl groups should not account for more than -14 ± 3 kcal mol^{-1} (based on the ΔG_{BDE}(C-H) for diphenylmethane (84 kcal mol^{-1}) relative to the ΔG_{BDE}(C-H) for ethane (98 kcal mol^{-1})) so, ΔG_{isom} should then be approximately -39 ± 3 kcal mol^{-1}. Substitution of these values into Equation [2] gives an estimate of -11 ± 4 for the pKa of $11^{\cdot+}$.

50

Another approach can be used to obtain an estimate of this number. The pKa of the 1,1-diphenylethyl cation (in water) is approximately -6 (38). The pKa value in acetonitrile, based on the free-energy of transfer of the proton (11 kcal mol^{-1}) and the hydrocarbon fragments (-2±2 kcal mol^{-1}, 39), should be about 0.6±1. This number must be corrected for the allylic stabilization gained upon deprotonation (-14±3 kcal mol^{-1}) and the strength of the one-electron two-centre bond being broken. An estimate of the strength of this bond may be obtained from the cycle shown in Figure 12. The value of ΔG_{BDE}(C-C) is estimated from the

Figure 12. Thermochemical cycle to estimate the strength of the one-electron two-centre bond in 11$^{\cdot+}$.

activation barrier to thermal isomerization which is about

30 kcal mol^{-1} (17). The oxidation potential E^O_2 should be

approximately the same as the oxidation potential of the

1,1-diphenylethyl radical (about 0.5 V vs NHE)(40) and the

oxidation potential of **11** is given above. The sum of the

$G_{BDE(C-C)}$ and FE^O_2 is greater than FE^O_1. Consequently,

the strength of the one-electron two-centre bond of **11**$^{\cdot+}$

should be about 8 kcal mol^{-1}. Therefore, the pKa

of **11**$^{\cdot+}$ should be -4 ± 3 by this method.

It is, therefore, not surprising that **11**$^{\cdot+}$ deprotonates.

Furthermore, this process should be rapid because the C-H

bond being broken can be parallel to the vacant p-orbital.

It is reasonable to assume that the sensitizer radical

anion could serve as the base for the deprotonation of **11**$^{\cdot+}$.

In those cases where the sensitizer is reduced (TCNE, TCQ

and DDQ) this occurs. In fact, even in those cases where

the sensitizer is not reduced (DCN, DCB, DCA AND MCB), and

12 is the product, protonation of the sensitizer radical

anion still may be favourable. However, in these cases,

the radical anion is required to reduce **19**$^{\cdot}$ (Scheme XI, Step

4). Even if the proton transfer to this radical anion is

slow, the radical cation, **11**$^{\cdot+}$, is acidic enough to

protonate the solvent. But, consider briefly, the

protonation of DCN $^-$ by **11**$^{\cdot+}$. The required values of

ΔG^O_{BDE}, ΔG^O_{isom} and E^O have been discussed above. The value

of E_{red} for DCN is in Table 1. Therefore, only an estimate

of ΔG_{BDE}(C-H) of the C-H bond to be made in DCNH$^{\cdot}$ is

required (Figure 13). The enthalpy of reaction for 1,4-dihydronaphthalene to give naphthalene and two hydrogen atoms can be calculated (109.9 kcal mol^{-1}) from information in standard tables (41). The BDE of the C-H bond in 1,4-dihydronaphthalene is approximately 75±2 kcal mol^{-1} (42a). This would give a BDE of 35±2 for the second C-H bond. It is estimated that an α-cyano group decreases the C-H BDE by approximately 6 kcal mol^{-1} (42b). On the other hand, the other cyano group will stabilize the radical (DCNH·) to some degree, and both cyano groups will be conjugated in the product. The overall effect on the BDE may be as much as 4±2 kcal mol^{-1}. This would give a value of 22±3 kcal mol^{-1} for ΔG^o_{BDE}(DCNH·). The ΔG^o for protonation of DCN·$^-$ by 11·$^+$ would then be -27±6 kcal mol^{-1}. Similar reasoning suggests that protonation of the radical anion of DCB, DCA and MCB is also favourable.

Figure 13. Thermochemical cycle to estimate the ΔG^o for protonation of DCN·$^-$ by 11·$^+$.

There are other possible mechanisms for the formation of 12 which involve HA·, disproportionation of the radical 19·, for example. However, the observed deuterium incorporation in 12, from methanol-Od, argues against this.

The next step in the reaction scheme, Step 4, involves a reduction of 19· by the sensitizer radical anion. The reduction potential of 19· is known (-0.94 V, DMF vs sce, 43). Table 1, which lists the reduction potentials of the sensitizers, indicates that the radical anions of all of the aromatic nitriles are capable of reducing 19· to 19⁻; even DCA, where the electron transfer may be slighty endothermic. Furthermore, the radical anions of the other sensitizers (TCNE, TCQ and DDQ), which do not give 12 as a product are not capable of reducing 19·. Following the reduction of 19·, protonation (Scheme XI, Step 5) completes the mechanism for the formation of 12.

The reduction of 19· and subsequent protonation of the carbanion explains the high degree of incorporation of deuterium at the allylic position with no scrambling. The absence of observable isotopic scrambling in 12 also rules out reversibility for the deprotonation of $11^{·+}$ (35).

An alternative mechanism for the incorporation of deuterium in 12 could be via deprotonation of $12^{·+}$ to form 19· followed by reduction and subsequent deuteration. However, when a solution of 12 and 1,4-dicyanonaphthalene (DCN) are irradiated in acetonitrile-methanol-Od (3:1, v/v), no deuterium exchange is observed.

54

These results raise several new questions. Since the formation of the highly delocalized radical, 19•, should be a driving force for deprotonation of 12•+, it is not immediately obvious why 11•+ deprotonates while 12•+ does not. Using a thermochemical cycle similar to that above (Equation 25), the pKa of 12•+ also may be calculated. The oxidation potential (E_{ox}) of 12 is 1.80 V (vs NHE) and the free-energy associated with the bond dissociation is about 72 kcal mol^{-1} (42a). The estimated pKa of 12•+ is −5±2. Therefore, 12•+ should deprotonate in methanol. Since deprotonation of 12•+ appears to be favourable from thermochemical considerations, the reason for the lack of apparent acidity must be kinetic in nature. The relevant C-H bond in 12•+, is perpendicular to the π-system in the preferred conformation. Evidence for this conformational preference is based on observed vicinal ^1H-^1H coupling constants (44). In ^1H-^1H coupling in 12 is 10 Hz while, in an analogous compound, 1,3-diphenylindene, where the dihedral angle between the C-H bond and the adjacent p-orbital is approximately 60 degrees, the ^1H-^1H coupling constant is only 2 Hz (45). The proton chemical shifts for the allylic and vinyl protons in 12 are $\delta 4.75$ and $\delta 6.45$ respectively. Those for 1,3-diphenylindene are $\delta 4.55$ and $\delta 6.49$ respectively. Under these conditions it is not surprising that 12•+ does not deprotonate rapidly.

The inability of both 11•+ and 12•+ to react with methanol also is unexpected (2a,27); especially in the case

of $12^{\cdot+}$ since 1,1-diphenylethylene, under similar conditions, reacts to form the anti-Markownikoff addition product in·high yield (28). Also, 1,1-diphenylcyclopropane (7) and phenylcyclopropane (4) react to add methanol. Products resulting from the deprotonation of the radical cation of 4 or 7 were not reported in either of these cases (25). The radical cation $11^{\cdot+}$ must preferentially deprotonate. The bulky phenyl groups will inhibit the addition of methanol, allowing the deprotonation to compete effectively. The addition of methanol to $12^{\cdot+}$ must also be hindered. It is known that the rate of addition of methanol to olefin radical cations decreases markedly as the olefin becomes more heavily substituted (3a,46). The preferred conformation of the diphenylmethyl group in 12 (and presumably $12^{\cdot+}$) has the C-H bond perpendicular to the olefinic π-bond. The phenyl groups, therefore, effectively hinder the addition of methanol. This conformational preference also accounts for the apparent lack of acidity of $12^{\cdot+}$ and, has been observed in other systems (47).

Consider next, Scheme XI, Step 6, the oxidation of $19^{\cdot}$. The deprotonation of $11^{\cdot+}$ to $A^{\cdot-}$ (Step 3) and the electron-transfer (Step 6) can occur simultaneously and, this process is equivalent to hydrogen atom transfer from $11^{\cdot+}$ to $A^{\cdot-}$ (Scheme XII). In essence, the transition state can be more or less polar. Nevertheless, it is useful to consider these various steps independently in order to assess the energetics of the overall process.

$$11^{\bullet+} + A^{\bullet-} \longrightarrow \left[19\colon\!\text{---}H\text{---}A^{\bullet} \longleftrightarrow 19^{+}\text{---}H\text{---}A^{-} \right]^{\ddagger}$$

$$\left[19\colon\!\text{---}H\text{---}A^{\bullet} \longleftrightarrow 19^{+}\text{---}H\text{-}\!\!\!\!\diagup\!A^{-} \right]^{\ddagger}$$

$$19^{\bullet} + HA^{\bullet}$$

$$19^{+} + HA^{-}$$

Scheme XII.

If proton transfer were to occur between $11^{\bullet+}$ and $A^{\bullet-}$, and if the reduction potential of $HA^{\bullet}$ is greater than the oxidation potential of $19^{\bullet}$ (i.e., $E_{ox}(19^{\bullet}) - E_{red}(HA^{\bullet}) < 0$) then the subsequent electron transfer to form 19^{+} would be fast. On the other hand, if $E_{ox}(19^{\bullet}) - E_{red}(HA^{\bullet}) > 0$; then, even if hydrogen atom transfer were to occur, the ion-pair would undergo an electron transfer to generate the radical-pair.

There is independent evidence, at least in the case of TCQ, where 19^{+} is observed, that $E_{ox}(19^{\bullet}) - E_{red}(HA^{\bullet}) < 0$. The electrochemistry of several quinones and hydroquinones (not DDQ or TCQ) has been studied previously. (48). The oxidation of hydroquinones in the presence of bases such as

pyrrolidine, 2,6-lutidine and pyridine results in a new wave at about 0.7 V below the oxidation potential of the hydroquinone (49). In the case of 1,4-hydroquinone (QH$_2$), the anodic wave for the oxidation of the hydroquinone disappears upon addition of two equivalents of 2,6-lutidine to the anolyte (49b). Under these conditions, a new wave at E_p=0.67 V, was attributed to the oxidation of QH$^-$ $\rightleftharpoons$ Q + H$^+$ + 2e$^-$ (recently, Laviron (50) has measured the E^0 value for the oxidation QH$^-$ $\rightleftharpoons$ QH$\cdot$ in an aqueous medium; 0.22 V vs sce). Similarly, the oxidation of TCQH$_2$ in acetonitrile occurs at E_p=1.56 V. Addition of 2,6-lutidine (1.5 equivalents) to the anolyte produces a new wave at E_p=0.60 V attributable to the oxidation of TCQH$^-$. Addition of 2,6-di-t-butylpyridine has a similar effect, except, forty equivalents must be added before the wave at E_p=1.56 V is not observed. The new wave occurs at E_p=0.87 V. These differences can be attributed to a steric effect with this hindered base (51). Since E_{ox}(19$\cdot$) $-$ E_{red}(TCQH$\cdot$) = -0.24 V, the observation of 19$^+$ is expected.

Irradiation of the charge-transfer complex between 11 and TCNE, DDQ or TCQ results in the formation of mixtures of 13 and 14 as well as the reduced acceptors. The mechanism for the formation of 13 and 14 via 19$^+$ is shown in Scheme XI, Step 7-9.

The proposed cyclization of the cation 19$^+$ is in apparent contradiction of reported behavior. Treatment of 1,1,3,3-tetraphenylpropenol (18) with 4-toluenesulphonic

acid in ethylacetate gave an almost quantitative yield of **14**
(32). With acetonitrile as solvent, however, treatment of
18'with 4-toluenesulphonic acid leads to an almost
quantitative yield of **13**. As the percentage of
carbontetrachloride in acetonitrile increases, the
proportion of **14** progressively increases (Figure 8). A
weaker acid (trifluoroacetic acid or trichloroacetic acid)
produces a much more dramatic effect than the strong acid
(4-toluenesulphonic acid).

These results are rationalized by considering the
effect of the solvent polarity on the strength of the acid
(or its conjugate base)(52). The dielectric constant of
binary solvent mixtures of carbontetrachloride and
acetonitrile as a function of mole fraction of
carbontetrachloride is almost linear. As the solvent
polarity decreases, the strength of the conjugate base
increases so the deprotonation of 19^+ by the conjugate base
becomes more favourable. The strong acid (4-
toluenesulphonic acid) results in a higher ratio of **13:14**.
The pKa of trichloroacetic acid is similar to that of
trifluoroacetic acid, so it is not surprising that the plots
obtained in Figure 8 are similar.

This explanation may be over-simplified. Acid-base
equilibria in aprotic solvents are complex. Besides the
equilibrium for salt formation, equilibria for acid
dimerization, $(HA)_2$, homoconjugate ion formation, $(A-H--A)^-$,
and, in the case of **18**, the pK_R^+, are also important. In

general, weaker acids dimerize more readily in aprotic media. On the other hand, homoconjugate ion formation is more favourable with stronger acids. The ability of the conjugate base to accept a proton, however, depends on its charge, size, polarizability and, to some extent, steric factors (ie. the same factors that are important in aqueous media). In the reaction of 19^+ in ethylacetate, the solvent apparently acts as the base.

Examples of the formation of indenes from the allylic cations also have been reported. Pittman and Miller (53) found that allylic cations such as the 1,1,3-triphenylpropenyl cation are stable at low temperature in strong acid. Warming these solutions induces cyclization to form stable solutions of the indanyl cation. Quenching with base leads to an almost quantitative yield of the corresponding indene. In these solutions, the intermediate cyclohexatrienyl cations were not observed, which implies that Scheme XI, Step 8 is rapid; probably a result of the driving force for aromatization upon proton loss.

It is clear, therefore, that the ratio of 13 to 14 is sensitive to the basicity of the medium. The observed dependence of the ratio of 13 to 14 on the sensitizer (Table 2) may be explained on this basis. The ratio of 13 to 14 from the photosensitized (electron-transfer) irradiation decreases in the order TCNE > TCQ > DDQ. This follows expected base strength of the anions HA$^-$. The difference in base strength of the anions (HA$^-$) can also account for the

qualitative observation that the steady state concentration of 19^+ is greater with TCNE as the sensitizer than with TCQ. The possibilty that $19 \cdot$ may cyclize to lead, ultimately, to 13, or, that $19 \cdot$ may disproportionate to give 14 should be considered. Dietz, Peover and Wilson (43) found that a stable solution of $19^{\pm}$ could be oxidized to form a stable solution of $19 \cdot$ (which gave a well resolved esr spectrum). The solution of $19 \cdot$ could be reduced back to 19^- with no apparent reaction. Furthermore, if $19 \cdot$ could cyclize to lead ultimately, to 13, it would then be surprising that 13 was not observed as a product in the photosensitized (electron-transfer) reactions with the aromatic nitriles as sensitizers.

The irradiation of the charge-transfer complex between 11 and TCQ in acetonitrile-methanol (3:1, v/v) leads to the formation of 16 in good yield (based upon HPLC analysis of the crude reaction mixture). The isolation of 16 is not straightforward; only half of this ether was eluted from a silica gel flash chromatographic column even though the compound was on the column for less than 30 minutes. The remainder of the material was recovered as 18 on elution with methanol. The formation of 16 is consistent with the existence of 19^+ along the reaction pathway. Treatment of 18 in acetonitrile-methanol (3:1, v/v) with trifluoroacetic acid (10^{-2} M) produces 16 in good yield based upon proton magnetic resonance (^{1}Hmr) spectroscopy and HPLC.

Strong support for many of the mechanistic

considerations proposed in Scheme XI can be obtained from the study of the electrochemical oxidation of **11**. The oxidation of **11** at a spherical platinum electrode occurs at Ep = 1.36 V in acetonitrile (0.1M TEAP) using a sweep rate of 400 mV s^{-1}. At sweep rates less than 1.0 V s^{-1} a second anodic wave (Ep = 1.58 V at 400 mV s^{-1}) is observed. The relative height of the second wave increases as the sweep rate decreases (Table 4). The second wave is attributable to the oxidation of **13**, adsorbed on the working electrode. The sweep rate dependence is a result of a slow chemical step. The strong adsorption of **13** to the working electrode is evident from Figure 3. The sharp anodic wave at Ep = 1.58 V is obtained for the cyclic voltammogram of **13**. Addition of an equivalent amount of **11** to this solution only results in an increase in the peak current for the second anodic wave. The first wave at Ep = 1.36 V is not observed, indicating that the working electrode is insulated from the solution until the discharge potential of **13** is reached.

The appearance of an anodic wave attributable to the oxidation of **13** indicates that the anodic wave at Ep = 1.36 V represents a two-electron process. Radical cations generally are more stable in dichloromethane than in acetonitrile (54), so, this solvent was used in an attempt to detect the individual one electron transfer steps upon oxidation of **11**. The first wave at Ep = 1.36 V in dichloromethane appears to be identical to the wave in acetonitrile. Even at sweep rates as fast as 20 V s^{-1}, no

evidence for two one-electron transfers is obtained.

At the onset of oxidation (in acetonitrile), the solution near the surface of the electrode becomes visibly purple. The cathodic sweep reveals two waves. The first cathodic wave is reversible with $E_{1/2} = 0.34$ V. The second wave is at $E_p = 0.17$ V and is irreversible. The irreversible wave may be the reduction of a proton which occurs at $E_{1/2} = 0.24$ V (55) in water, ie., the normal hydrogen electrode (NHE). A likely candidate for the coloured intermediate is 19^+. When the cation 19^+ is generated in the electrolysis cell from the alcohol 18 by the addition of trifluoroacetic acid, the voltammogram of the resulting purple solution has the same reversible reduction wave at $E_{1/2} = 0.34$ V.

Some uncertainty still remains regarding the mechanistic sequence of the anodic oxidation of 11 to 19^+. Two possible pathways are the ECE and the EEC process (Figure 14). For the ECE mechanism the deprotonation of $11^{\cdot +}$ is thermodynamically feasible even considering acetonitrile as the base (35) and, the oxidation of $19^{\cdot}$ would be rapid at 1.1 V. The alternative pathway (EEC) requires that the oxidation of $11^{\cdot +}$ to 11^{++} occurs at 1.1 V (the onset of oxidation), followed by deprotonation to give 19^+. An estimate of the oxidation potential of $11^{\cdot +}$ can be made; it should be between the oxidation potential of tetraphenylethylene radical cation (1.45 V) (56) and the oxidation potential of the 1,1-diphenylethyl radical (0.3 V

(40)). The strength of the one-electron two-centre bond in $11^{\cdot+}$ is small (see Section II) so the oxidation potential of $11^{\cdot+}$ should be closer to the value for the 1,1-diphenylethyl radical. Obviously, both pathways are thermodynamically feasible.

$$\text{Ph}_2\!\!\overset{\cdots\cdot}{\frown}\!\!\text{Ph}_2$$

$-H^+$ **a** $-e^-$

C   **E**

$$\text{Ph}_2\!\cdot\ \ +\text{Ph}_2 \qquad\qquad \text{Ph}_2\!\!\overset{\cdots+}{\frown}\!\!\text{Ph}_2$$

E   **C**

$-e^-$ **b** $-H^+$

$$\text{Ph}_2\!+\ \ +\text{Ph}_2$$

Figure 14. The CE mechanism (path a) and the EC mechanism (path b) for the formation of 19^+ from $11^{\cdot+}$.

Controlled potential electrolysis of **11** gives further support to the suggestion that 19^+ lies on the reaction pathway (Table 3). Electrolysis in acetonitrile (0.1 M TEAP) gives **13** in good yield. Addition of a base (2,6-lutidine) diverts the reaction from the original pathway and

64

14 is now the major product (only a trace of **13** is detected). In acetonitrile-methanol (3:1, v/v) (0.1 M TEAP) the product obtained is **16**. This, of course, parallels the expected behavior of **19$^+$**.

It is interesting to compare the controlled potential electrolysis (in methanol) of **11** to that reported for 1,2-diphenylcyclopropane (cis- and trans-**1**)(57). In the case of 1,2-diphenylcyclopropane (**1**) the product from the electrolysis was 1,3-dimethoxy-1,3-diphenylpropane (**21**). It was proposed that the radical cation of the cyclopropane reacted with methanol to form the benzylic radical which was then oxidized to the cation and reacted once again with methanol (ECEC). The radical cation of **1** showed no propensity for deprotonation under these conditions (the allylic ether analogous to **16** was not detected). This, of course, is consistent with the photosensitized (electron-transfer) results (25,31).

The isolation of **16** from the electrolysis of **11** does not confirm unambiguously the intermediacy of **19$^+$**. If methanol were to react with **11$^{\cdot+}$** (or **11^{++}**), the resulting diphenylethyl type cation could simply deprotonate to give **16**. Furthermore, since an excess of protons is produced in this reaction, 1,3-dimethoxy-1,1,3,3-tetraphenylpropane may be produced, and subsequently react via an acid catalyzed elimination of methanol. Analysis of the reaction by HPLC indicates that **16** is the only product formed, even at low conversion (<5%). The photosensitized (electron-transfer)

reaction of 11 in acetonitrile-methanol (3:1, v/v) indicates
that $11^{\cdot+}$ deprotonates much faster than it reacts with
methanol. Certainly the dication 11^{++} will be as, or more,
acidic under similar conditions. The formation of 16, via
19^{+} under the electrolysis conditions is, therefore,
reasonable.

Treatment of 18, in acetonitrile (0.1 M TEAP), with
trifluoroacetic acid, produces a coloured solution which
exhibits three broad absorption maxima at 568 nm, 459 nm and
382 nm attributed to 19^{+}. This spectrum can be compared to
the spectrum of 19^{-} which exhibits visible absorption maxima
at 564 nm and 463 nm (43). This similarity is expected; the
energy difference between the HOMO and the NBMO (non-
bonding molecular orbital) in the cation is the same as the
difference between the NBMO and the antibonding MO in the
anion (58).

Electrolysis of a solution of 11 gives a coloured
solution which exhibits absorption maxima at 570 nm, 461 nm
and 381 nm. Similarly, irradiation of the charge-transfer
band between 11 and TCNE, DDQ or TCQ in acetonitrile produces
a coloured solution with absorption maxima at 566 nm and 458
nm. It is reasonable to suggest that all three spectra
represent the same intermediate, 19^{+}

The stability of 19^{+}, the ease with which it is
generated electrochemically from 11, and the ease with which
it is detected spectrophotometrically, makes it possible to
measure the rate of disappearance as a function of

temperature (Table 5). The rate of disappearance of 19^+ (measured at either 570 nm or 460 nm) follows first order kinetics. The temperature dependence gives an apparent activation energy of 21.8 ± 0.2 kcal mol^{-1} and a preexponential factor, log A, of $14.5\pm.3$. It is clear from the simple mechanism in Scheme XI, Step 7-8, that this rate constant represents the rate of formation of 13. The rate at 23 C is independent of the concentration of electrolyte, between 0.1 and 0.001 M TEAP. The ratio of 13:14 with TCNE as acceptor does not change significantly when 0.1 M TEAP is added to the solution. Similarly, the product ratio is the same with or without 0.1 M TEAP when TCQ is the acceptor. It is likely, therefore, that the rate constant for the formation of 13 will be the same in the photochemical experiments.

It is interesting to consider the activation parameters obtained for the reaction of 19^+. The activation energy of 21.8 kcal mol^{-1} is expected for a reaction of this type. The cyclization of the highly delocalized cation is essentially an electrophilic aromatic substitution on an electron deficient ring. The activation energies for the electrophilic aromatic substitution on benzene (in nitrobenzene) by several alkylchlorides (catalysed by $AlCl_3$) fall in the range 11 kcal mol^{-1} to 20 kcal mol^{-1} (59). In these reactions, the activation entropies (ΔS^o) are all approximately -12 e.u. (i.e. large negative numbers). It is puzzling, therefore, to find that in the reaction of 19^+,

the activation entropy is positive (5.9±1 e.u.).

There is a way to estimate the activation entropy for this cyclization reaction. Intuitively, the activation entropy for a intramolecular reaction should be more positive than the activation entropy for an analogous intermolecular reaction. This is because the order of the transition state for both reactions should be similar, however, in the case of the intramolecular reaction, there is more order in the starting material. Consider an analogous cyclization; the cyclization of the pentadienyl radical to the 2-cyclopentenyl radical. The activation entropy for this reaction can be calculated using Benson's group additivities (60). Since the starting material is essentially rigid, the overall entropy change for this reaction is only -6.34 e.u. (group additivities for cationic groups are not available so a free radical reaction has been used in this example). This will be a reasonable estimate (probably too negative) for the activation entropy.

In the reaction of 19^+, however, there are additional corrections. Rotation of the phenyl rings in 19^+ are restricted and generally, these systems (e.g. triphenylmethyl) are thought to take on a propeller-like preferred conformation. At the transition state (as well as in the product) rotation of the three remaining phenyl rings is not as restricted. The entropy associated with the single bond rotation of a phenyl ring is 8.6 e.u. (61) and, for three phenyl rings, this would account for 25.8 e.u. Of

68

course, the phenyl rings will not be free rotating in the product. However, even if only one-forth of this entropy is attained at the transition state, the total entropy change would be positive.

1.3.2 Substituent effects on the oxidation of 11a-h

The oxidation potentials ($E_{1/2}$) of several substituted 1,1,2,2-tetraarylcyclopropanes (11a-h) are listed in Table 6. While the unsubsituted derivative has been referred to as 11 in the above discussion, in the ensuing discussion, this compound will be referred as 11a, to distinguish it from the other substituted derivatives. Similarly, the 1,1,3,3-tetraphenylpropenyl cation, 19$^+$, will be referred as 19a$^+$ (Table 7).

All of the anodic oxidations of 11a-h are irreversible. The Hammett equation for electrochemical reactions (Equation 26) is often used to describe the effect on the equilibrium constants (E^O) for a series of structurally related compounds in which the electron demand at the reactive centre is varied. In general, these plots have slopes in the range 0.1 to 0.8 V (19, 62). While this relationship is meaningful for reversible processes, for irreversible processes the analysis is not as straightforward.

$$E_{1/2} = (RT/\alpha n_a F)\rho\sigma \qquad [26]$$

Analysis of the oxidation of 11a-h by the Hammett approach gives a slope of 190±20 mV, an intercept of 1.25±.04 V and a correlation coefficient, r, of 0.976 (Figure 9). There has been some controversy over the ability of a cyclopropane ring to transmit electronic effects (63). It is somewhat surprising that the oxidation potentials correlate as well as they do with the $\Sigma \sigma^+$. It is tempting to conclude that this correlation is evidence for transmission of substituent effects through the cyclopropane ring. However, this ring in the radical cation will not be intact and, the substituent effect is probably derived from the interaction of the aryl ring in this open chain species with the vacant p-orbitals. This idea of a product-like transition state is compatible with a slow electron transfer (i.e. Hammond postulate).

Shono and Matsumura have measured the half-wave oxidation potentials of some 4-substituted arylcyclopropanes (57). In this work, a slope of 730 mV was obtained from the Hammett plot of $E_{1/2}$ versus σ^+. The slope of the line from the Hammett plot for 11a-h is expected to be one-forth of the slope obtained for the arylcyclopropanes only if the charge can be delocalized into all of the aryl rings at the transition state. One forth of the line reported by Shono and Matsumura is 183 mV; remarkably close to the slope obtained in this work of 190 mV for 11a-h. Some caution should be exercised since, for irreversible systems, the slope depends on αn_a as well as the traditional ρ value

(Equation 26), where α is the transfer coefficient and n_a is the number of electrons transfered at the rate limiting step. Furthermore, a limited number of substituents were used in this study so , the slope of the line may be biased in one direction.

The Hammett plot of the reduction potentials ($E_{1/2}$) of 19^+a-f,h has a slope of 190 ± 20 mV, an intercept of $0.38\pm.03$ mV and a correlation coefficient, r, of 0.985 (Figure 10). In the case of 11a-h, the oxidations are totally irreversible in contrast to the reductions of 19^+a-f,h which are quasireversible in this solvent. The equivalence of the slopes may be fortuitous. The Hammett equation for an irreversible electrochemical reaction (Equation 27, 19) includes the term αn_a. The value of αn_a can be estimated from the shape of the voltammetric wave (17, Equation 23) or from the sweep rate dependence of the peak potential (Equation 22). For 11a, the value of αn_a is estimated to be 0.35 by both methods (see Table 4). However, the value of αn_a does not appear to be constant for all of the tetraarylcyclopropanes studied. An average value is 0.28, which leads to an estimate of 0.89 for ρ. On the other hand, the value of αn_a for the quasi-reversible reduction of 19^+ is 0.53, giving an estimate of 1.72 for ρ. Therefore, while the slopes of the original Hammett plots appear to be the equivalent, the sensitivity of the transition state to changes in electron demand (as measured by ρ) is, as should be expected, much greater for 19^+ than

71

for **11**.

1.4   CONCLUSIONS

One of the objectives of this study was to understand the apparently inconsistent reactions of **11** under photosensitized (electron-transfer) conditions. Some of the factors which influence the reactions of **11**$^{\bullet+}$ have been identified. The reactivity of **11**$^{\bullet+}$ is dominated by its acidity. The calculated thermodynamic acidity of **11**$^{\bullet+}$ is consistent with this conclusion, however, the kinetic factors which influence the deprotonation are not completely understood. The implication from this work is that geometric (including conformational) considerations are important, i.e. the C-H bond being broken must have at least partial overlap with the p-orbitals of the aromatic radical cation. Very recent results from this laboratory support this conclusion.

There are several properties of the sensitizer which also have an influence on the course of the reaction. The reduction potential of the sensitizer not only is important to the initial electron-transfer step but, in the system studied, the ability to reduce the intermediate radical, **19**$^{\bullet}$, is the factor which determines whether an oxidation (to form **13** or **14**) or a rearrangement (to form **12**) occurs. Strong evidence (deuterium incorporation in **12**) supports the mechanism proposed for the formation of **12**.

The oxidation products (13 and 14) are formed via the carbocation 19^+. This intermediate cation has been observed spectroscopically in the photosensitized (electron-transfer) reaction. The results from the controlled potential electrolysis of 11 (in which 19^+ is also identified as an intermediate) is also very strong evidence in support of the proposed mechanism.

The effect of the sensitizer on the formation of 19^+ is not completely understood. While it is clear that only those sensitizer radical anions which are not capable of reducing $19\cdot$ lead to the formation of 19^+, the sequence of reactions need not include $19\cdot$ as an intermediate. In these cases, the sensitizer radical anion may be serving as a hydrogen atom acceptor. Since electron transfer in the radical pair (after protonation of the sensitizer radical anion by $11^{\cdot +}$) will be spontaneous, these differences are probably only differences in the degree of electron-transfer at the transition state for the transfer of the hydrogen atom.

The ratio of 13 to 14 is shown to be sensitive to the basicity of the medium. This product ratio from the photosensitized (electron-transfer) reactions is consistent with the expected basicities of the reduced acceptors (HA^-). The sensitivity of the ratio to the basicity of the medium and, the solvent effect on the basicity of acids, may be useful in the future for the determination of relative pKa's of strong acids in aprotic solvents.

The complex behaviour observed in this system must pertain to photosensitized (electron-transfer) reactions in general. There are few, if any, reported reactions of this type where the variation of the sensitizer has a dramatic effect on the products or product ratios. Now that the possibility has been recognized, there is an opportunity to learn much more about these systems and, to increase the synthetic utility of photosensitized (electron-transfer) reactions.

The substituent effects on the oxidation of **11a-h** indicate that all of the aryl groups can interact with the incipient ionic centre. Since it is not expected that the substituent effects will be transmitted through the intact cyclopropyl ring, this result is best interpreted in terms of a slow electron-transfer leading to a product like transition state.

1.5 EXPERIMENTAL

General

Acetonitrile (Fisher ACS grade) for preparative photolysis and electrolysis as well as for electrochemical measurements was distilled successively from sodium hydride (1g/L) and phosphorous pentoxide (2g/L), followed by passing through a column of basic alumina (100g/L), refluxing over calcium hydride for 24 hours in an inert atmosphere and, finally, fractional distillation. Acetonitrile for the

electrochemical measurements was used immediately after distillation while that for preparative work was stored over 3A molecular sieves. Tetraethylammonium perchlorate (Aldrich) was recrystallized three times from 90% ethanol and dried in a vacuum dessicator. Tetracyanoethylene (Aldrich) was sublimed and recrystallized three times from chlorobenzene. Chloranil (Eastman) was purified by recrystallization four times from benzene. 2,3-Dichloro-2,6-dicyanobenzoquinone (Aldrich) was purified by recrystallization four times from chloroform-benzene (4:1). 1,4-Dicyanobenzene (Aldrich) was purified by sublimation followed by recrystallization three times from ethanol. 1,4-Dicyanonaphthalene was prepared by the method of Heiss, Paulus and Rehling (64) from the reaction of o-phenylenediacetonitrile and N,N'-di-tert-butylglyoxaldiimine. The 1,4-dicyanonaphthalene was purified by column chromatography followed by recrystallization from methanol (three times). Methyl-4-cyanobenzoate was prepared by the acid catalysed esterification of 4-cyanobenzoic acid (Aldrich) and purified by recrystallization (ethanol). 9,10-Dicyanoanthracene was prepared by the reaction of cuprous cyanide with 9,10-dibromoanthracene (65) and was purified by column chromatography followed by recrystallization (twice from benzene). The preparation of 1,1,2,2-tetraphenylcyclopropane (66), 1,3,3-triphenylindene (67) and tetraphenylallene (32) have been described.

[1]Hmr spectra were recorded on a Varian T60 spectrometer or a Nicolet 360 MHz nmr spectrometer and are reported in parts per million downfield from TMS. [13]Cmr spectra were recorded on a CFT-20 nmr spectrometer and are reported in parts per million downfield from TMS. Infrared spectra were recorded on an air-purged Perkin-Elmer 180 grating infrared spectrometer or a Pye-Unicam SP-1000 infrared spectrometer and are reported in wavenumbers (calibrated against the 1601.8 cm^{-1} absorption of polystyrene). Ultraviolet-visible absorption spectra were recorded on a Cary-Varian 219 absorption spectrometer and are reported in nm followed by the molar extinction coefficient. Elemental analyses were carried out by Chemianalytics Inc. and agreed to within 0.3% of the calculated values. Melting points were obtained on a Sybron Corporation Thermodyne hot stage and are uncorrected. HPLC analysis was performed using a Waters Associates M-45 solvent delivery system in conjunction with a Tracor 970 variable wavelength absorbance detector. The column (Merck, Lichrosorb RP-18) was prepared by suspending the packing (1.1 g) in a mixture of carbontetrachloride (10 mL) and tetrabromoethane (8 mL) by sonication for 3 minutes. The slurry was poured into a precolumn (18 cm x 1.5 dia.) and immediately packed into the analytical column (10 cm x .6 cm dia.) with n-heptane at a pressure of 3450 psi (using a Haskel air driven fluid pump). The eluant was progressively changed to chloroform then methanol. The analysis was done at a flow rate of 1.2 mL per minute with 83% methanol-water.

The absorbance was monitored at 247 nm (the isobestic point of 13 and 14).

To calibrate the HPLC, the apparent mole fraction of 13 (based on relative peak heights) was converted to a true mole fraction with a working curve. The working curve was a plot of apparent versus true mole fraction, constructed with ten accurately weighed samples of mixtures of 13 and 14 and is linear between 5% and 95% 13.

Electrochemical cell and apparatus

Cyclic voltammetric measurements were performed in a three electrode cell (10 mL volume) fitted with a cooling jacket and a scintered glass frit through which nitrogen was passed in order to deoxygenate and stir the solution prior to measurement. The working electrode was a spherical platinum electrode (1 mm diameter) embedded in soft glass and contacted with a Nichrome wire through a mercury pool. The counter electrode was a platinum coil embedded in soft glass and inserted through a sidearm of the cell. The reference electrode was a saturated calomel electrode (sce) which was isolated from the solution by a glass tube (inserted in another sidearm) which ended in a luggin capillary placed 0.5 mm from the surface of the working electrode. The working electrode was immersed in concentrated nitric acid for thirty minutes prior to use, washed with 5% bicarbonate, water and methanol then dried in

an oven at 60 C. The electrochemical cell was cleaned by immersion in concentrated nitric acid (2 hours), followed by rinsing with water, 5% sodium bicarbonate, water and acetone and dried at 100 C.

Solutions were degassed with dry nitrogen (presaturated with solvent) for five minutes prior to each measurement, and, during the measurement, the nitrogen atmosphere was maintained above the solution. Substrate concentrations were typically 0.001 M in a total volume of 7 mL.

The spectroelectrochemical cell consisted of a 4 cm cylinder (2 cm diameter) with optically flat Pyrex windows sealed at each end. The cell was surrounded by a water jacket. The temperature of the solution in the cell was maintained using a Polyscience Corporation, Model 90 temperature controlled circulating bath. The solution in the cell was continuously stirred with a magnetic stirring bar, placed in a shallow well below the light path. The working electrode, (platinum mesh, 4 cm x 0.5 cm) inserted via an opening in the top of the cell, was held against the inside wall of the cell in order to keep it out of the light path. A thermistor probe (Cary 219 spectrophotometer accessory) was placed in a second opening in the top of the cell and, protruded only slightly (by approximately 2 mm) into the light path. The reference electrode and counter electrode were isolated from the solution in a separate compartment which contacted the working compartment through a scintered glass frit. This compartment was inserted

through an opening in the side of the cell, ending with a ground glass joint. The entire assembly was placed in the sample compartment of a Varian-Cary ·219 spectrophotometer.

The substrate concentrations were 2.9×10^{-3} M. During each run, approximately 0.5 C were passed at constant current (.05 equivalents). The cell was then open circuited, and, the absorbance of the solution monitored as a function of time. The solution was replaced with fresh solution after every third measurement. The temperature did not vary by more than ± 0.1 degree during any given measurement.

Controlled potential electrolysis was performed with a standard H-cell (total volume 100 mL). Both the working electrode and counter electrode were platinum mesh (9 cm^2). The reference electrode was introduced via a luggin capillary.

Cyclic voltammetric measurements were obtained with a PAR (Princeton Applied Research) 173 potentiostat in combination with a PAR 175 universal programmer and a PAR 179 digital coulometer. Controlled potential electrolyses and spectroelectrochemical measurements were performed with the use of the PAR 173 potentiostat.

Irradiations were carried out in acetonitrile or acetonitrile-methanol (3:1) at a substrate concentration of 0.1 M. Solutions were degassed by bubbling dry nitrogen for 10 minutes prior to irradiation. Irradiations were carried out in 2 cm I.D. Pyrex tubes (large scale) or 5 mm Pyrex nmr

tubes. Two irradiation systems were employed. A 1 kW
medium pressure mercury lamp (General Electric Co.) with a
quartz cooling jacket which was immersed in a constant
temperature bath at 10 C and, a Hanovia 450 W lamp with a
quartz cooling jacket. When the Hanovia lamp was used the
irradiation tubes were contained in a Pyrex cooling jacket
connected to a Polyscience Model 90 Temperature controlled
circulating bath. This jacket also served as a short
wavelength (< 290 nm) filter. Reaction mixtures were
chromatographed on a flash chromatographic column or with a
medium pressure (15 psi, helium) LC system (27).

Photosensitized (electron-transfer) irradiation of 11 using 1,4-dicyanonaphthalene in acetonitrile

11 (100 mg, 2.9×10^{-4} mole) and 1,4-dicyanonaphthalene
(10 mg, 5.8×10^{-5} mole) were dissolved in acetonitrile (3.0
mL), degassed by bubbling nitrogen for 10 minutes, and,
irradiated at 10 C (through a Pyrex filter) with a 1 kW lamp
for 4 hr. HPLC indicated only one major product. The
solvent was evaporated under reduced pressure and the
reaction mixture separated by medium pressure chromatography
(silica gel, hexanes-dichloromethane gradient). 12 (66 mg,.
73%) was isolated and recrystallized from absolute ethanol
to give colourless crystals which melted at 126-128 C (lit.
127-128 (66)). ^{1}Hmr spectrum was identical to an authentic
sample (δ, CDCl$_3$, 7.20 (m, 20 H), 6.52 (d, J=10 Hz, 1H),
4.75 (d, J=10 Hz, 1H)).

Other compounds isolated from the column were unreacted starting material (11, 10 mg) and unreacted sensitizer (DCN, 8 mg, 80 percent recovery).

Photosensitized (electron-transfer) irradiation of 11 using 1,4-dicyanonaphthalene in acetonitrile-methanol-Od

11 (30 mg, 8.7 x 10^{-5} moles) and DCN (3 mg, 1.7 x 10^{-5} mole) were dissolved in a mixture of acetonitrile and methanol-Od (3:1, v/v, 1.0 mL), degassed by bubbling nitrogen for 5 min.; and, irradiated (through Pyrex) with a 1 kW lamp for 1.5 hr (at 10 C). The solvent was removed under reduced pressure, and, 12 was isolated by medium pressure chromatography (silica gel, hexanes-dichloromethane gradient). ^{1}Hmr (Nicolet 360 MHz NMR spectrometer) showed only the resonances at δ7.20 (m, 20H) and δ6.52 (s, 1H). ^{2}Dmr spectrum showed only a singlet at δ4.78.

Photosensitized (electron-transfer) irradiation of 11 using tetracyanoethylene

11 (100 mg, 2.9 x 10^{-4} mole) and tetracyanoethylene (38 mg, 3.0 x 10^{-4} mole) in acetonitrile (3.0 mL), were degassed by bubbling nitrogen for 10 min. and then, irradiated through a sodium nitrite filter (> 400 nm) at 10 C for 72 hrs. Within a few seconds of irradiation, the solution became dark purple. This colour slowly faded when the tube was removed from the irradiation bath. After the

irradiation was complete (monitored by HPLC) a colourless solid, which had precipitated, was filtered and, the solvent was evapourated under reduced pressure.

The residue, after evapouration, exhibited an [1]Hmr spectrum (δ, CDCl$_3$, 4.90(s)) and an ir spectrum (KBr (cm^{-1}), 2819, 2606, 2484, 2274, 1620, 1302, 1201, 996, 908, 561) identical to an authentic sample of dihydrotetracyanoethylene (68). The crude yield was 28 mg (74%).

The precipitate was combined with the residue from the evaporation of solvent and separated by medium pressure chromatography (silica gel, hexanes-dichloromethane gradient) to give 13 (58 mg, 67%), 14 (3 mg, 4%) and 11 (14 mg). The identity of 13 and 14 was confirmed by comparison to authentic samples of each (67, 32).

Photosensitized (electron-transfer) irradiation of 11 using chloranil in acetonitrile

11 (100 mg, 2.9 x 10^{-4} mole) and chloranil (63 mg, 3.0 x 10^{-4} mole) in acetonitrile (4.0 mL) were degassed by bubbling nitrogen for 10 min. then, irradiated through a sodium nitrite filter solution (> 400 m) at 10 C for 4 hrs. The solution became only slightly purple within a few seconds of irradiation. HPLC indicated that 13 (minor) and 14 (major) were formed. The solvent was evapourated under reduced pressure, and, the residue was dissolved in dichloromethane, and the tetrachlorohydroquinone (insoluble

82

in dichloromethane) was filtered (42 mg, 67%) and identified by mass spectrometry ($M^+(246)$, and, characteristic M+2, M+4, M+6) and ir (KBr (cm^{-1}), 3410(s), 1415(s), 1312(s), 1205(s), 888(s), 720(m), 708(m)).

The dichlormethane was evapourated under reduced pressure and, the residue was separated by medium pressure chromatography (silica.gel, hexanes-dichloromethane gradient). Isolated from the column were, 14 (47 mg, 67%), 13 (5 mg, 7%) and 11·(30 mg).

Photosensitized (electron-transfer) irradiation of 11 using 2,3-dichloro-5,6-dicyanobenzoquinone in acetonitrile

11 (100 mg, 2.9 x 10^{-4} mole) and 2,3-dichloro-5,6-dicyanobenzoquinone (68 mg, 3.0 x 10^{-4} mole) in acetonitrile (3.0 mL) were degassed by bubbling nitrogen for 10 min.; then, irradiated, through a sodium nitrite filter solution (> 400 nm) at 10 C for 4 hrs. The solution became dark purple within a few seconds of irradiation. The solvent was evapourated and the residue extracted into dichloromethane. The hydroquinone precipitate (reduction product) was filtered to give a crude yield of (32 mg, 47%), and, identified by mass spectrometry ($M^+(228)$, and, characteristic M+2, M+4) and ir (KBr (cm^{-1}), 3260(s), 2260(m), 1578(m), 1455(s), 1360(m), 1280(s), 1200(s), 1078(m), 892(s), 778(m), 748(m), 703(w), 690(w)).

The dichloromethane was evapourated under reduced pressure and the residue was separated by medium pressure

chromatography (silica gel, hexanes-dichloromethane gradient) to give 13 (7 mg, 10%), 14 (25 mg, 35%) and 11 (29 mg).

Photosensitized (electron-transfer) irradiation of 11 using chloranil in acetonitrile-methanol (3:1, v/v)

11 (100 mg, 2.9×10^{-4} mole) and chloranil (63 mg, 3.0×10^{-4} mole) in acetonitrile-methanol (3:1, v/v, 3.0 mL) were degassed by bubbling nitrogen for 10 min., then, irradiated through a sodium nitrite filter solution (> 400 nm) at 10 C for 5 hr. The solvent was evapourated under reduced pressure, and, the residue was extracted with dichloromethane (to separate the hydroquinone from the reaction mixture). The hydroquinone precipitate was filtered (43 mg, 68%), and characterized as above.

The dichloromethane was removed under reduced pressure and separated by medium pressure chromatography (silica gel, hexanes-dichloromethane gradient) to give 14 (7 mg, 10%), 18 (54 mg, 77%) and 11 (33 mg). Analysis (HPLC) of the original reaction mixture indicated that only 16 was present; neither 14 nor 18 were detected indicating that these products were a result of decomposition of 16 on the silica gel column.

Controlled potential electrolysis of 11 in acetonitrile

Into the anodic compartment of the electrolysis cell, containing acetonitrile (0.1 M TEAP, 100 mL), 11 (250 mg, 7.2

x 10^{-4} mole) was dissolved. The solution was stirred and a constant potential of 1.3 V (vs sce) was applied. When 90.8 C had been consumed, the reaction was stopped. The solvent was removed under reduced pressure, and, the residue taken up into benzene to remove the electrolyte. After gravity filtration and removal of the benzene the mixture was separated, by medium pressure LC (silica gel, hexane-dichloromethane gradient). The compounds isolated were 11 (84 mg) and 13 (142 mg, 85%). The indentity of 13 was confirmed by comparison to an authentic sample (67).

Controlled potential electrolysis of 11 in the presence of base

11 (100 mg, 2.9 x 10^{-4} moles) was added to the anodic compartment of the electrolysis cell containing acetonitrile 100 mL (0.1 M TEAP) and 0.1M 2,6-lutidine. The solution was stirred and a controlled potential of 1.4 V was applied until 19.9 C were consumed. The solvent was removed under reduced pressure, and, the residue was dissolved in benzene. This solution was filtered (to remove TEAP) and the benzene was removed under reduced pressure. The mixture was separated by medium pressure chromatography (silica gel, hexane-dichloromethane gradient). The compounds isolated were 11 (77 mg) and 14 (13 mg, 57%). HPLC analysis of the fractions containing 14 indicated the presence of a trace (<3%) of 13. The identity of 14 was confirmed by comparison to an authentic sample (32).

85

Controlled potential electrolysis of 11 in acetonitrile-methanol.

11 (100 mg, 2.9 x 10^{-4} mole) was added to the anodic compartment of the electrolysis cell containing a mixture of acetonitrile and methanol (3:1, V/V, 0.1M TEAP). The solution was stirred and a controlled potential of 1.4 V was applied until 60.1 C had been consumed. The solvent was evapourated and the residue dissolved in benzene. The benzene solution was filtered and the solvent was removed under reduced pressure. The mixture was separated by flash chromatography (silica gel, hexane—dichloromethane gradient). The products isolated were 11 (27 mg) and 16 (43 mg, 55%). Elution of the flash chromatographic column with methanol gave 18 (20 mg, 27%). 18 was not detected by HPLC analysis or ^{1}Hmr of the reaction mixture.

Solvent and acid effect on the ratio 13:14

Stock solutions of acid (1.1 x 10^{-1} M) and 18 (5 x 10^{-3} M) in acetonitrile and carbontetrachloride were prepared. The samples for each run were prepared by adding 1.0 mL of the stock solution of 18 to each test tube followed by the appropriate volumes of acetonitrile and carbontetrachloride (Table 8) to a total of 9.0 mL. These solutions were equilibrated for 30 min. (in a Polyscience Corporation Model 90 Temperature Controlled Circulating Bath) and finally, to these tubes, 1.0 mL of stock solution of acid was added.

The tubes were replaced in the temperature controlled bath. The reaction was quenched with 2 g of anhydrous potassium carbonate (BDH), the solution was decanted, and the solvent was evapourated. The residue was dissolved in dichloromethane, filtered and, the samples were analysed by HPLC.

Table 8. Preparation of solutions for the study of the solvent and acid effect on the ratio of 13:14.

Volume of Acid (mL)[a]	Volume of 18 (mL)[b]	Volume of CH_3CN (mL)	Volume of CCl_4 (mL)	%CH_3CN
1.0	1.0	9.0	0.0	100.0
1.0	1.0	8.0	1.0	90.9
1.0	1.0	6.5	2.5	77.2
1.0	1.0	5.0	4.0	63.6
1.0	1.0	3.5	5.5	50.0
1.0	1.0	2.0	7.0	36.3
1.0	1.0	0.5	8.5	22.7
1.0[c]	1.0	0.0	9.0	9.1
1.0[c]	1.0[c]	0.0	9.0	0.0

[a]1.1×10^{-1} M stock solution in acetonitrile.

[b]5.0×10^{-3} M stock solution in acetonitrile.

[c]stock solution in carbontetrachloride.

The runs with trichloroacetic acid and trifluoroacetic acid were allowed to react for 15 hr. However, the reaction with 4-toluenesulphonic acid was quenched after only 20 min. since, in this solvent, **14** is slowly converted to **13**.

Preparation of 11a-h

The 1,1,2,2-tetraarylcyclopropanes were prepared by the addition of a diarylcarbene to a corresponding 1,1-diarylethylene in benzene. The diarylcarbenes were generated by the photolysis of the corresponding diaryldiazomethanes through a sodium nitrite filter solution. To reduce the formation of tetraarylazines, the diaryldiazomethanes were added to the olefin solutions in ten equal aliquots allowing the colour to disappear between each addition. The preparation of the diaryldiazomethanes and the diarylolefins from the corresponding benzophenones have been described (69,70,71). The tetraarylcyclopropanes were isolated by medium pressure chromatography (silica gel, hexanes-dichloromethane gradient) and purified by recrystallization. The preparation of **11a** has been reported (66). Details of the preparation, separation and purification of **11b-h** are described below.

1-(4-methoxyphenyl)-1,2,2-triphenylcyclopropane (11b)

Diphenyldiazomethane (0.9 g, 0.0046 mole) in benzene (10 mL) was added to 1-(4-methoxyphenyl)-1-phenylethylene (1.0 g, 0.0048 mole) in benzene (20 mL) as described above.

88

The solvent was evapourated and the reaction mixture was separated by medium pressure chromatography. The product recrystallized from chloroform-methanol to give colourless plates (mp 145-6 C). Ir (KBr): 3050(m), 2839(w), 1608(m), 1512(s), 1290(m), 1246(s), 1172(s), 1028(s), 798(m), 699(s); uv (ethanol): 237(20000); ^{1}Hmr (CDCl$_3$): 2.48(s,2H), 3.69(s,3H), 6.80(m, 4H), 7.05(m, 15H); anal. calcd. for $C_{28}H_{24}O$: C 89.32, H 6.43; found C 89.50, H 6.38.

1,2-di(4-methoxyphenyl)-1,2-diphenylcyclopropane (11c)

(4-Methoxyphenyl)phenyldiazomethane (1.5 g, 0.0067 mole) in benzene (10 mL) was added to 1-(4-methoxyphenyl)-1-phenylethylene (1.5 g, 0.0071 mole) in benzene (20 mL). The solvent was then evapourated and the reaction mixture separated by medium pressure chromatography. The cis isomer was recrystallized from chloroform-ethanol to give colourless prisms (mp 139-41 C). Ir (KBr): 3040(w), 2833(w), 1608(m), 1510(s), 1495(m), 1477(m), 1245(s), 1033(m), 826(m), 697(s); uv (ethanol): 236(17000); ^{1}Hmr (CDCl$_3$): 2.43(ABdd, 2H, J=5Hz), 3.69(s, 3H), 6.80(m, 8H), 7.02(m, 10H); anal. calcd. for $C_{29}H_{26}O_2$: C 85.68, H 6.45; found C 85.69, H 6.56.

The trans isomer was recrystallized from chloroform-ethanol to give colourless prisms (mp 205-6 C). Ir (KBr): 3030(w), 2830(m), 1606(s), 1509(s), 1457(m), 1289(m), 1241(s), 1031(s), 831(m), 692(m); uv (ethanol): 235(17000); ^{1}Hmr (CDCl$_3$): 2.44(S, 2H), 3.68(S, 6H), 6.78(m, 8H),

7.04(m, 8H); anal. calcd. for $C_{29}H_{26}O_2$: C 85.69, H 6.45; found: C 85.48, H 6.30.

1,1,2,2-tetra(4-methoxyphenyl)cyclopropane (11d)

Di(4-methoxyphenyl)diazomethane (1.0 g, 0.004 mole) in benzene (10 mL) was added to 1,1-di(methoxyphenyl)ethylene (2.0 g, 0.008 mole) in benzene (20 mL). The solvent was evapourated and the reaction mixture was separated by flash chromatography (silica gel, dichlormethane). The product contained a trace amount of fluorescent impurity which could be removed only by careful chromatography of the product (collecting the last few fractions as the compound eluted; basic alumina, haxanes-dichloromethane gradient). The product was recrystallized from chloroform-hexanes to give colourless needles (mp 215-15.5 C). Ir (KBr): 3030(w), 2832(m), 1605(s), 1507(s), 1461(m), 1290)m), 1241(s), 1105(m), 1031(s), 837(m), 748(m); uv (ethanol): 233 (32000); ^{1}Hmr (CDCl$_3$): 2.34(s, 2H), 3.70(s, 12H), 6.74(m, 16H); anal. calcd. for $C_{31}H_{30}O_4$: C 79.83, H 6.45; found: C 79.81, H 6.37.

1,1-di(4-cyanophenyl)-2,2-diphenylcyclopropane (11e)

Di(4-cyanophenyl)diazomethane (1.3 g, 0.0053 mole) in benzene (10 mL) was added to 1,1-diphenylethylene (1.0 g, 0.0056 mole) in benzene (20 mL). The solvent was then evapourated and the reaction mixture was separated by medium pressure chromatography. The product was recrystallized

from chloroform-ethanol to give colourless needles. (mp 217-19 C). Ir (KBr): 2222(s), 1600(s), 1495(s), 1448(m), 1398(w), 828(m), 738(m), 705(m), 569(m); uv (ethanol): 243 (26000), 260 (20000); ^{1}Hmr (CDCl$_3$): 2.64 (s, 2H), 7.10 (m, 10H), 7.26(m, 8H); anal. calcd. for C$_{29}$H$_{20}$N$_2$: C 87.85, H 5.08; found: C 87.96, H 5.28.

1,2-(Dicyanophenyl)-1,2-diphenylcyclopropane (11f)

4-(cyanophenyl)phenyldiazomethane (0.2 g, 0.0009 mole) in benzene (5 mL) was added to 1-(4-cyanophenyl)-1-phenylethylene (0.2 g, 0.001 mole). The solvent was evapourated and the reaction mixture separated by medium-pressure chromatography. The cis isomer was recrystallized from chlorform-ethanol to give colourless needles (mp 201-202 C). Ir (KBr): 3060(w), 2227(s), 1605(s), 1496(s), 1449(m), 1400(w), 1008(m), 833(m), 761(m), 695(s), 628(m); uv (ethanol): 241 (27000), 255(22000); ^{1}Hmr (CDCl$_3$): 2.64(ABdd, 2H, J=6Hz), 7.10(m, 10H), 7.32(m, 8H); anal. calcd. for C$_{29}$H$_{20}$N$_2$: C 87.85, H 5.08; found: C 87.72, H 5.01.

The trans isomer was recrystallized from chloroform-ethanol to give colourless plates (mp 106-109 C). Ir (KBr): 3060(w), 2227(s), 1606(s), 1501(m), 1444(w), 1400(w), 1008(w), 849(m), 701(s), 675(m), 621(m); uv (ethanol): 241 (27000), 255 (20000); ^{1}Hmr (CDCl$_3$): 2.65(s, 2H), 7.15(m, 10H), 7.22(m, 8H); anal. calcd. for C$_{29}$H$_{20}$N$_2$: C 87.85, H 5.08; found: C 87.69, H 4.99.

1,1,2,2-tetra(4-cyanophenyl)cyclopropane (11g)

Di(4-cyanophenyl)diazomethane (0.5 g, 0.0020 mole) in
benzene (10 mL) was added to 1,1-di(4-cyanophenyl)ethylene
(0.5 g, 0.0022 mole). The solvent was evapourated and the
reaction mixture was separated by medium pressure
chromatography. The yellow solid was recrystallized three
times from chloroform-haxanes to give colourless plates (mp
233-44 C). Ir (KBr): 3060(w), 2227(s), 1605(s), 1502(s),
1448(w), 1405(m), 1178(w), 1005(w), 851(w), 752(m), 630(w);
uv (ethanol): 243 (56000), 260 (38000); ^{1}Hmr (CDCl$_3$):
2.68(s, 2H), 7.20(m, 16H); anal. calcd. for $C_{31}H_{18}N_4$: C
83.41, H 4.04, N 12.56; found: C 83.11, H 3.82, N 12.51.

1,1-Di(4-cyanophenyl)-2,2-di(4-methoxyphenyl)cyclopropane (11h)

Di(4-cyanophenyl)diazomethane (1.2 g, 0.0049 mole) in
benzene (10 mL) was added to 1,1-di(4-methoxyphenyl)ethylene
(1.2 g, 0.005 mole) in benzene (20 mL). The solvent was
then evapourated and the reaction mixture separated by
medium pressure chromatography. The product was
recrystallized from chloroform-ethanol to give colourless
needles (mp 203-4 C). Ir (KBr): 2840(w), 2230(s), 1608(s),
1510(s), 1452(s), 1290(m), 1250(s), 1112(w), 1028(s),
850(m), 756(m); uv (ethanol): 233 (37000), 270 (14000);
^{1}Hmr (CDCl$_3$): 2.53(s, 2H), 3.71(s, 6H), 7.00(m,16H); anal.
calcd. for $C_{31}H_{24}N_2O_2$: C 81.55, H 5.33; found: C 81.24, H
5.39.

PART II.   1,n-RADICAL IONS.   THE NATURE OF THE ONE-ELECTRON
TWO-CENTRE BOND IN CYCLOPROPANE RADICAL CATIONS:
AN SCFMO APPROACH.

2.1   INTRODUCTION

2.1.1 Molecular Orbital Theory

A major goal of physical organic chemistry is the study
of the relationship between structure and reactivity. In a
superficial sense, structural information may only mean
molecular geometry and, there are many methods available to
elucidate molecular geometries in the solid, liquid or gas
phase. Normally, however, it is the electronic structure
that is important in determining the reactivity of a
molecule. For ionic or free radical reactions the
relationship between structure and reactivity is well
understood. In these cases the observed reactivity of a
molecule can have specific structural implications. In the
case of radical ions, however, the relationship is not as
well developed. While the study of the reactivity of
radical ions is relatively straightforward (see Part I), the
study of the structure of these intermediates is not always
possible. Experimental techniques used in the study of the
electronic structure of radical ions include esr
spectroscopy (3,72) and CIDNP (23,24,73). Molecular orbital
theory also is an important method for the study of the
electronic structure of radical ions.

93

The fundementals of quantum mechanics are described in detail in several excellent books (74). This introduction will not dwell on the mathematical development of the pertinent equations since only a qualitative understanding of the self-consistent field molecular orbital (SCFMO) is necessary.

The electronic energy expectation value of a system of interacting particles is given by the Schroedinger equation (Equation 27)

$$\hat{H}\Psi(1,2,...,n) = \mathcal{E}\Psi(1,2,...,n) \qquad [27]$$

where H is the Hamiltonian operator, E is the electronic energy and $\Psi(1,2,...,n)$ is the wavefunction describing the spatial motion of all of the electrons moving in a potential field. The wavefunction for a many electron system can be expressed as a product of one-electron wavefunctions (Equation 28). This is known as a Hartree product.

$$\Psi(1,2,...,n) = \psi_1(1)\psi_2(2)...\psi_n(n) \qquad [28]$$

Each of the one-electron molecular orbitals can be expressed as a linear combination of atomic orbitals (LCAO).

$$\psi_i = \sum_j c_{ji} \phi_j \qquad\qquad [29]$$

The objective of molecular orbital theory is to solve the Schroedinger equation by finding a solution for the wavefunction. If the Hamiltonian operator can be expressed as a sum of one-electron Hamiltonian operators then the solution for the one-electron wavefunctions, ψ_i, would be straightforward. Unfortunately, the electron-electron repulsion is a two electron term and as such, the Hamiltonian operator cannot be expressed as a sum of one-electron operators. However, each electron can be treated as if it were interacting with the average of the instantaneous field presented by the other n-1 electrons and the potential field of the nuclei. This treatment leads to a new operator which can be written as an "effective" one-electron Hamiltonian operator. The set of resulting equations is known as the Hartree-Fock equations (Equation 30).

$$\hat{F}\psi_i = \epsilon_i \psi_i \qquad i = 1, n \qquad\qquad [30]$$

The Fock Hamiltonian operator, $\hat{F}$, has the form

$$\hat{F} = H^{core} + \sum_j (2J_j - K_j) \qquad\qquad [31]$$

where H^{core} is the one-electron Hamiltonian operator for an electron moving in the the potential field of the bare nucleus; J_J is the coulomb operator which represents the electron-electron repulsion that results if the electrons are constrained to the orbitals in which they are originally assigned (i.e. it assumes that the electrons can be distinguished from each other); and, K_J is the exchange operator which is a consequence of the antisymmetry principal (i.e. electrons are indistinguishable). It is a stabilizing term resulting from partial correlation of electrons of parallel spin. The solution to obtain ψ_i from the Hartree-Fock equations cannot be obtained directly. The best MO's are eigenfunctions of the Fock Hamiltonian operator. However, this operator is defined in terms of the coulomb and exchange integrals which, in turn, depend on the MO's (ψ_i). Therefore, the solutions must be obtained by some iterative procedure.

One method to determine the MO's (ψ_i) would be to evaluate the coefficients, c_{ji}, from Equation 29. This LCAO approach is also an iterative procedure. The equations used in this case are known as the Roothaan equations. These equations differ from the Hartree-Fock equations in that they are algebraic, not differential equations. The matrix elements of the Hartree-Fock operator (from the Roothaan equations) has the form

$$F_{\mu\nu} = H_{\mu\nu} + \sum P_{\lambda\sigma}\left((\mu\nu|\lambda\sigma) - \frac{1}{2}(\mu\lambda|\nu\sigma) \right) \qquad [32]$$

96

where $H_{\mu\nu}$ is the core Hamiltonian operator; $P_{\lambda\sigma}$ is an element of the density function matrix (Equation 33);

$$P_{\mu\nu} = \sum_{I}^{OCC} c_{\mu I} c_{\nu I} \qquad [33]$$

and, $(\mu\nu|\lambda\sigma)$ is a two electron integral (Equation 34).

$$(\mu\nu|\lambda\sigma) = <\varphi_\mu(1)\varphi_\nu(1)|\frac{1}{r_{12}}|\varphi_\lambda(2)\varphi_\sigma(2)> \qquad [34]$$

Again, this is a situation in which the coefficients being evaluated $(c_{\mu\nu})$ are terms in the Hartree-Fock operator. The iteritive procedure involves guessing at the initial set of coefficients (using the core Hamiltonian operator only), then calculating the density matrix elements and hence evaluate the electronic energy and obtain the Hartree-Fock Hamiltonian operator. The eigenvectors of F are used to get a second approximation of the density matrix and, the procedure is repeated until the variation in the electronic energy falls within a preset threshold.

For open shell systems the procedure is similar. However, the electrons with α-spin and β-spin are treated independently. This gives rise to a set of α-MO coefficients and a set of β-MO coefficients. In this case, it is possible to define not only electron density associated with each nucleus, but unpaired spin density as

well. The full density matrix is defined as

$$P = P^\alpha + P^\beta \qquad\qquad [35]$$

and the spin density matrix is defined as

$$P = P^\alpha - P^\beta \qquad\qquad [36]$$

2.1.2 Basis Sets

Molecular orbitals may be obtained to essentially any accuracy desired by altering the number of basis functions in the LCAO expansion. The best basis set is not necessarily the largest basis set for a given problem. The larger basis sets require more computing time and the benefits of the increased accuracy of the MO must be balanced against the increasing demand on the computing system. Several types of basis sets are available which vary in sophistication:

(1) π-Basis set.

This basis set consists of a single p-atomic orbital on each heavy atom perpendicular to the molecular plane. This type of basis set is used in Huckel MO theory.

98

(2) Valence basis set.

This basis includes all of the AO's in the valence shell (e.g. carbon requires 2s, $2p_x$, $2p_y$ and $2p_z$ orbitals). The semi-empirical molecular orbital methods use this basis set.

(3) Minimal basis set.

This basis set includes the core electrons as well as the valence electrons. This is the minimum number of basis functions per atom required to describe all of the occupied AO's of each atom. Because this basis set is so small for __ab initio__ calculations, quantitatively accurate results are not usually obtained. However, the essential bonding interactions and many useful qualitative properties can be obtained with this basis set.

(4) Extended basis sets.

These basis sets use more basis functions than is necessary to describe all of the occupied AO's. Included in this class of basis sets is the split valence basis set in which the number of basis functions in the valence shell is increased. Also included are the double zeta basis set which uses twice as many basis functions as the minimal basis set and, the polarized basis set which uses basis functions of higher angular momentum than the highest occupied AO.

The minimal and extended basis sets are employed in _ab_ _initio_ molecular orbital theory. These wavefunctions take into account electron interactions only in an average way. The effect of this is that the calculated energies are in error, typically by one percent. On an absolute basis this is not much, however, for some problems it is too large. For example, the total energy of a carbon atom is approximately 1000 eV. Chemical bond energies involving carbon are typically 100 kcal mol^{-1}, which is about 5 eV per bond. Attempting to calculate a bond energy by taking the difference between the Hartree-Fock molecular and atomic energies can lead to results with large errors. The difference between the exact energy and the Hartree-Fock energy is known as the correlation energy.

2.1.3 Basis Functions

The two most common basis functions employed are the Slater type orbital (STO) which has the form exp(-ar) and the Gaussian type orbital (GTO) which has the form exp(-ar^2). In both cases, r refers to the radial distance from the nucleus. The evaluation of two-electron integrals involving STO's is expensive in terms of computing time. A solution to this problem is to use GTO's for the basis functions since the evaluation of the two-electron integrals is much faster. The GTO, however, is more rounded in the region of the nuclear cusp and it falls off more rapidly at

100

large distances from the nucleus in comparison to an STO. As a result, more GTO's must be used in order to adequately describe each atomic orbital.

A typical example is the STO-NG basis set, a minimal basis set in which N GTO's are used to approximate each STO. Similarly, a split valence basis set such as the K-LMG basis set uses K GTO's to approximate the STO's for the core, atomic orbitals, L GTO's to approximate each STO for the valence atomic orbitals at a small distance from the nucleus and, M GTO's to approximate each STO for the valence atomic orbitals at large distances from the nucleus. More GTO's are needed to approximate the inner GTO's since in this region the GTO is much less adequate.

2.1.4 Bonding in Cyclopropane

It is useful to review the models of bonding in cyclopropane (75) and how these models are used to rationalize the chemical and physical properties observed. The bonding arrangement of cyclopropane resembles the bonding in ethylene more closely than it resembles the bonding in alkanes insofar as they undergo analogous reactions (e.g. acid catalysed addition, cycloadditions, catalytic hydrogenation).

The most simple model (conceptually) that has been used to describe the bonding in cyclopropane was proposed by Walsh in 1949 (76). In the Walsh model the three ring carbons are sp^2 hybridized. Three occupied MO's determine

the nature of the C-C bonds (Figure 15a). One sp^2 orbital
points toward the centre of the ring; the other two sp^2
orbitals are used to form the C-H bonds. This leaves a p-
orbital in the plane of the ring from which symmetric (e'_s)
and antisymmetric (e'_a) combinations are formed. The
analogy to bonding in olefins can be understood with this
model; the orbital of a'_1 symmetry is analogous to the σ-
bond in the σ-π description of olefins while the two
orbitals of e' symmetry are analogous to the π-MO of
olefins.

a   **b**

e'_a e'_s π

a'_1 σ
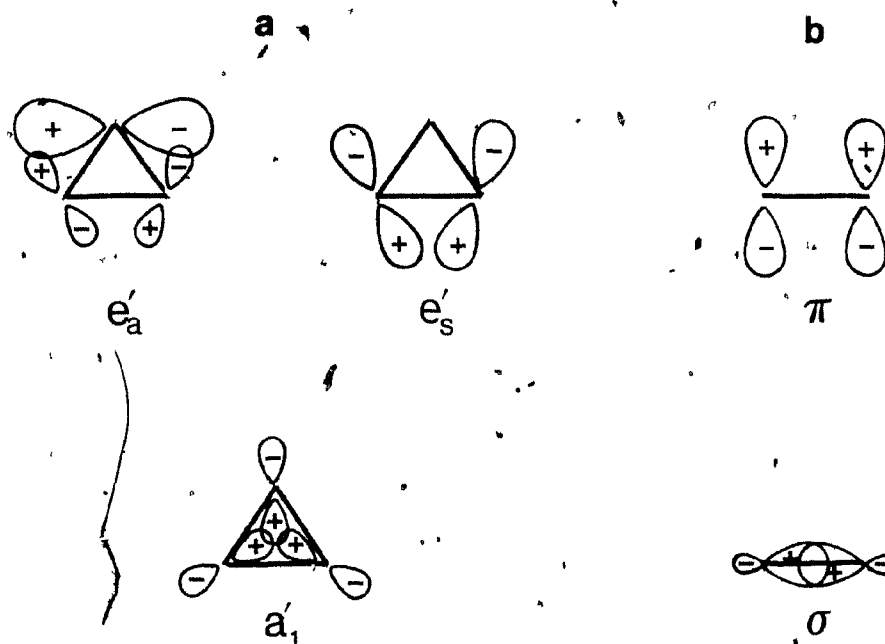
Figure 15. (a) The Walsh model of bonding in cyclopropane
and (b) the σ-π description of bonding
in olefins.

102

An alternative model for bonding in cyclopropane is the valence bond model proposed by Coulson (77). In this model, the C-C bonds are formed from the overlap of two sp^5 orbitals. The sp^5 orbitals are formed from the rehybridization of a p-orbital with a sp^2 orbital. The direction of the sp^5 orbital is not in the same direction as the internuclear axis and, hence, the term "bent bond" has been applied to this model. As in the Walsh model, the valence bond model requires that the C-H bond be formed from an sp^2 orbital on the carbon atom. Olefins have an analogous bent bond description (Figure 16).
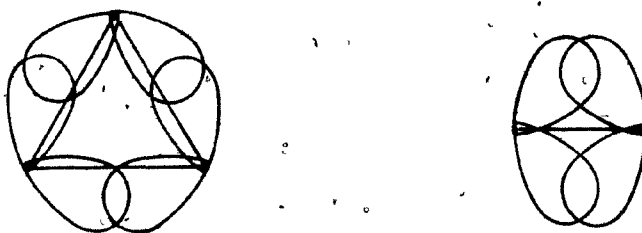
Figure 16. Valence bond model for bonding in (a) cyclopropane and (b) ethylene.

It should be pointed that the Walsh model and the valence bond model are merely different interpretations of the same molecular orbital (78). Both models predict correctly the experimental fact that the locus of maximum electron density does not lie along the internuclear axis. The cyclopropane C-H bond lengths are shorter than normal aliphatic bonds and, the ^{13}C-H spin-spin coupling constants

measured for some cyclopropane derivatives (79) indicate
that the cyclopropane ring carbons have 32 percent "s"
character. This is also predicted by both models (actually
the models predict the "s" character to be 33 percent).

The mechanism by which the cyclopropyl group interacts
with an adjacent π-system has been one of continuing
controversy. If the Walsh model is considered, it is
apparent that the most stable conformation should be when
the π-system lines up parallel to the plane of the ring.
This is known as the "bisected conformation". On the other
hand, in the valence bond model, a wider range over which
effective overlap is possible is predicted (Figure 17).
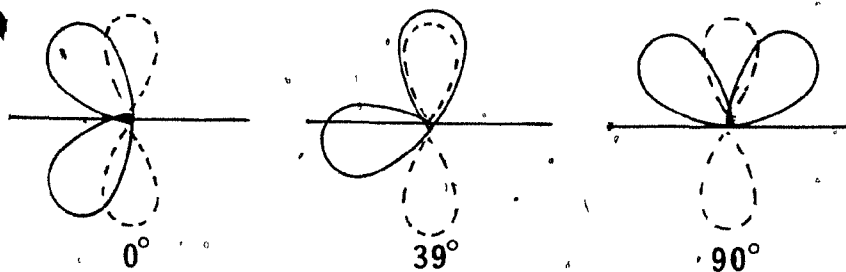
Figure 17. The overlap of adjacent sp^5 and p orbitals as a
function of dihedral angle.

If this type of overlap is present in cyclopropane
derivatives, then conjugative transmission of electronic
effects through the cyclopropane ring should be possible.
However, experimental results (often contradictory) have
only prolonged the controversy (63,79). The general
consensus that has emerged is that the cyclopropyl group can

·effectively stabilize a positive charge but cannot extend conjugation. This may be understood qualitatively since there is a larger coefficient in the Walsh orbital of the cyclopropyl carbon adjacent to the π-centre (80). This concentration of electron density helps to stabilize a positive charge by depleting electron density at other sites, electronic effects may not be transmitted.

2.1.5 The Cyclopropane Radical Cation

The structure and reactivity of the radical cations of cyclopropane and its derivatives are of considerable interest and have been the subject of both experimental and theoretical investigation. Most of the theoretical studies (81) have been directed toward the interpretation of the photoelectron spectrum of the parent molecule. In cyclopropane, removal of the electron from either of the two degenerate Walsh MO's of e' symmetry (76) leads to two possible structures of $C_{2}v$ symmetry for the radical cation (Figure 18). One of these species, having the trimethylene type structure, will have a $^2A_1$ ground state while the other, which resembles the π-complex between ethylene and CH_2^+ will have a $^2B_2$ ground state. Recent calculations by Collins and Gallup (81a) using the method of targeted correlation, suggest that these two species correspond to saddle points on the radical cation surface. The minimum, having C_s symmetry, is approximately half way between these structures on the surface. This result has been criticized

by Radom and coworkers (82) who questioned whether or not the effect was real.

Although these theoretical studies have been useful in explaining the photoelectron spectrum of cyclopropane, they generally have not provided information that can be used to understand the reactivity of the radical cation. Evidence obtained from chemically induced dynamic nuclear polarization (CIDNP) spectra (23) indicates that most radical cations of alkyl and aryl substituted cyclopropanes tend to favour the $^2A_1$ type structure. There is evidence, however, that in some special cases, such as the radical cation of benzonorcaradiene, the radical cation may assume the $^2B_2$ structure (83).

Theoretical calculations investigating some of the reactions of $C_3H_6^+$ (84) have yielded estimates of the activation energies for the loss of H, H_2, H_2^+ and CH_2^+. One important reaction, which has received little attention from a theoretical point of view, is the thermal cis-trans isomerization of the cyclopropane radical cation. This reaction is particularly interesting because information about the nature of the one-electron two-centre bond can be obtained from an investigation of this kind.

Much that is known about the nature of bonding in cyclopropanes (85) and olefins (86) comes from experimental investigation of their thermal reactions, particularly cis-trans isomerization. Since direct observation of the parent cyclopropane radical cation is difficult, similar data for

106

this system is not available. There is evidence, however, that the radical cation of 1,2-diphenylcyclopropane (23) does not rapidly isomerize. In this work, however, the radical cations were generated by photosensitization (electron-transfer). Under these conditions, all other reactions must compete with back electron-transfer. Since it is unlikely that there is a significant activation barrier for this process (the rate constant for back electron-transfer will be $> 10^{10}$, 2a), it is impossible to determine the lower limit for the barrier to cis-trans isomerization.

The purpose of this section is to investigate the nature of the one-electron two-centre bond in the cyclopropane radical cation. Ab initio calculations have been used to obtain equilibrium geometries for the cyclopropane radical cation (22^+) in the 90,90 conformation (both $^2A_1$ and $^2B_2$ states), the 90,0 conformation, and in the 0,0 conformation. The conformers are named according to the convention established by Hoffmann (87) in which the two numbers represent the rotational angles of the two principal methylene groups relative to the plane of the three carbons. The partial surface for twisting of one of the methylenes in the $^2A_1$ state to the transition state for cis-trans isomerization (the 90,0 conformer) is also studied. The energy difference between the 90,0 conformer and the 90,90 conformer ($^2A_1$) is an estimate of the barrier to cis-trans isomerization, while the energy difference between the 0,0

conformer and the 90,90 ($^2A_1$) conformer is an estimate of the barrier to racemization. This study has been extended to the 1,2-divinylcyclopropane radical cation; the results are pertinent to the 1,2-diphenyl derivative for which some experimental data are available.

2.2   Details of Calculations

Standard ab initio SCFMO calculations were carried out
with the GAUSSIAN 80 system of programs (88a) on a Perkin-
Elmer 3230 minicomputer or the GAUSSIAN 76 program (88b) on
a Control Data CYBER 170-720 mainframe computer system.
Gradient techniques (89) were used for geometry
optimizations. Calculations were performed with STO-3G, 4-
31G and 4-31G* basis sets with valence electron correlation
incorporated by using Møller-Plesset perturbation theory
(90) terminated at the second- (MP2) and third- (MP3) order.
The energies of the radical cations were computed using the
open-shell, spin-unrestricted (UHF) procedure (91).
Complete geometry optimizations of **22** and **22$^+$** (a maximum of
21 degrees of freedom) in the 90,0; 90,10; 90,20; 90,30;
90,60; 90,90; and 0,0 conformations were carried out at the
4-31G level (Table 9).

Calculations on the 1,2-divinylcyclopropane radical
cation (**23$^+$**) were carried out only using the STO-3G basis
set. A complete geometry optimization was not feasible.
The 4-31G optimized geometry for **22$^+$** ($^2A_1$) was used as a
model for the cyclopropane group while the STO-3G optimized
geometry for the allyl cation (92, Figure 18a) was used to
represent the vinyl groups. The vinyl groups were placed in
the plane of the corresponding methylene to ensure maximum
overlap through the π-system. In trans-**23$^+$**, the C_2 axis was
maintained and in cis-**23$^+$** the plane of symmetry was
maintained. The conformers are best described using the

nomenclature derived for conjugated polyenes (in this case 1,3,5-hexatriene) since 23^+ is structurally similar. Four conformers in the 90,90 conformation were considered (Figure 19): 2s-trans-4s-trans-3-trans (23a$^+$), 2s-cis-4s-cis-3-trans (23b$^+$), 2s-trans-4s-trans-3-cis (23c$^+$) and 2s-cis-4s-cis-3-cis (23d$^+$). The geometry for 23^+ in the 90,0 conformation was derived using a similar approach. In this case, however, the STO-3G geometry for the allyl radical (92, Figure 18b) was used as a model for the vinyl group on C_2, which was twisted into the plane of the cyclopropane group (vide infra). In all cases, the $C_1C_3C_2$ angle of the cyclopropane group was optimized.
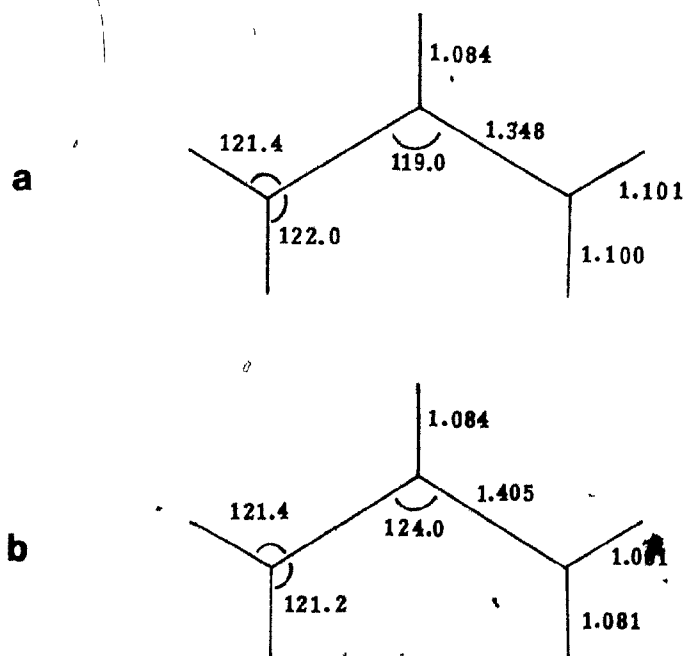
Figure 18. Equilibrium geometry (STO-3G) for (a) the allyl cation and (b) the allyl radical (reference 92).
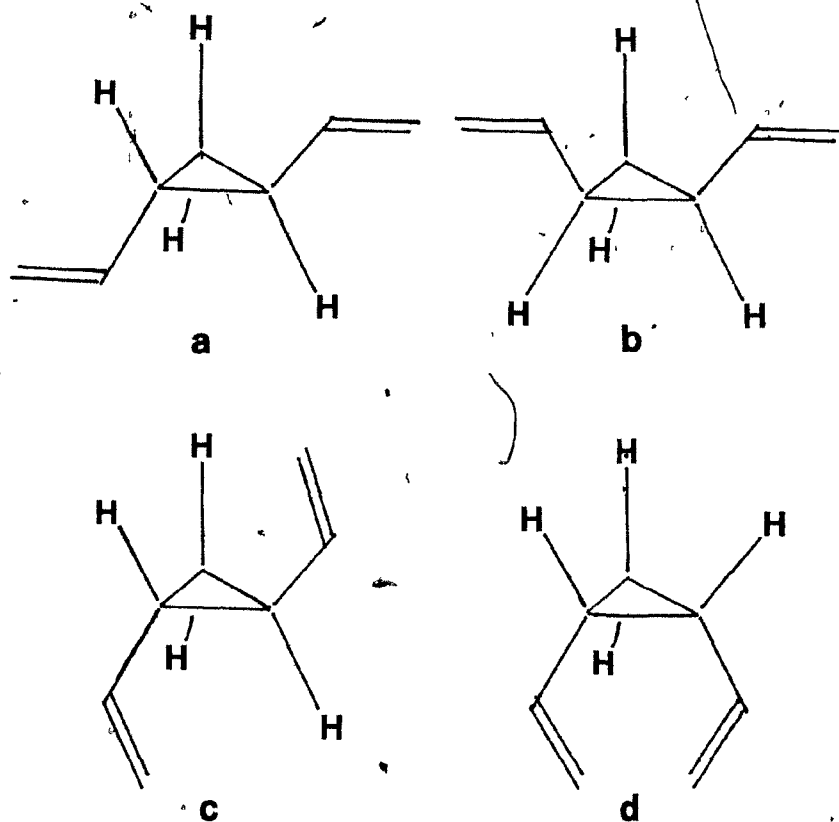
Figure 19. Comformers of 23^{+} in the 90,90 conformation.
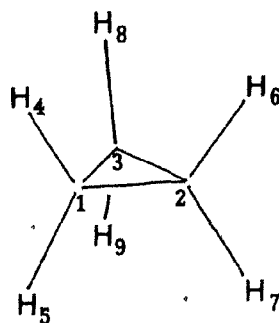
Diagram to accompany Table 9.

Table 9. Equilibrium geometries of **22** and **22**[+] (4-31G)[a].

Parameter	**22**	**22**[+] $90,90(^2A_1)$	**22**[+] $90,90(^2B_2)$	**22**[+] $90,0(^2A'')$	**22**[+] $0,0(^2A)$
r_{12}	1.503	1.941	1.400	(2.322)[b]	(2.535)[b]
r_{13}	1.503	1.483	1.720	1.434	1.430
r_{23}	1.503	1.483	1.720	1.569	1.430
r_{14}	1.072	1.072	1.072	1.076	1.072
r_{15}	1.072	1.072	1.072	1.076	1.071
r_{26}	1.072	1.072	1.072	1.071	1.072
r_{27}	1.072	1.072	1.072	1.070	1.071
r_{38}	1.072	1.075	1.069	1.080	1.119
r_{39}	1.072	1.075	1.069	1.080	1.119
$\angle HC_1H$	113.7	118.2	117.2	117.2	117.8
$\angle HC_2H$	113.7	118.2	117.2	120.9	117.8
$\angle HC_3H$	113.7	113.6	120.6	111.3	93.0
$\angle C_1C_2C_3$	60.0	81.7	48.0	101.2	124.8
α_1[c]	150.0	179.9	126.7	175.0	180.0
α_2[c]	150.0	179.9	126.7	179.5	180.0
α_3[c]	0.0	0.0	0.0	5.8	0.0
ω_1[d]	0.0	0.0	0.0	0.0	1.5
ω_2[d]	0.0	0.0	0.0	5.3	-1.5
ω_3[d]	0.0	0.0	0.0	0.0	0.0
θ_1[e]	90.0	90.0	90.0	90.0	0.0
θ_2[e]	90.0	90.0	90.0	0.0	0.0
θ_3[e]	90.0	90.0	90.0	90.0	90.0

[a]All bond lengths are in Å and all angles are in degrees.

[b]Internuclear distance.

[c] α_i is the angle representing the wagging motion of the C_i methylene. It is the angle between the C_iC_3 bond and the intersection of the plane of the C_i methylene with the plane of the carbons. α_3 is measured with respect to the C_1C_3 bond.

[d] ω_i is the angle representing the rocking motion of the C_i methylene. It is the angle between the line which bisects the HC_iH methylene and the line which is the intersection of the plane of the methylene and the plane of the carbons.

[e] θ_i is the angle representing the tortional motion of the C_i methylene. It is the angle between the plane of the C_i methylene and the plane of the carbons.

2.3   DISCUSSION

2.3.1 Structure of 22$^+$

'The equilibrium geometries (4-31G) of the 22 and 22$^+$ in the 90,90 conformation ($^2A_1$ and $^2B_2$ states) the 90,0 (pseudo $^2A''$) conformation and the 0,0 conformation (^2A) are shown in Table 9. The symmetries and energies of all of the occupied MO's of 22 and 22$^+$ are shown in Table 10. The structures for the $^2A_1$ and $^2B_2$ states are qualitatively similar to those using semi-empirical (81b,c,d,84) and other ab initio methods (81a). The equilibrium geometry of the 90,0 conformer and the 0,0 conformer have not been reported previously. While the structures of these species are of great interest, the spin and charge distributions are the important factors in the study of reactivity.

An interesting feature of the $^2A_1$ structure is that the value of α_1 (defined in Table 9, Figure 20) indicates that C_1, C_3, H_1 and H_2 lie in one plane while C_2, C_3, H_3 and H_4 lie in another plane (indicative of sp^2 hybridization at C_1 and C_2). This geometry allows effective bonding between C_1 and C_2 even though $\angle C_1C_3C_2$ has increased relative to that of cyclopropane. Another interesting aspect of this structure is the geometry at C_3. Although substantial changes have occurred at C_1 and C_2 virtually no change (relative to cyclopropane) in the C_3H bond length or the HC_3H angle occurs. This may be rationalized using the Walsh

113

Table 10. Orbital energies[a] and symmetry labels of the occupied MO's of **22** and **22$^+$**.

Molecule or Ion	MO	4-31G//4-31G[b]	MO	4-31G*//4-31G[b]
22	$1a'_1$	-11.2009	$1a'_1$	-11.2005
	$1e'_a$	-11.2004	$1e'_1$	-11.2046
(D$_3$h)	$1e'_s$	-11.2004	$1e'_a$	-11.2046
	$2a'_1$	-1.1400	$2a'_1$	-1.1282
	$2e'_s$	-0.8199	$2e'_a$	-0.8180
	$2e'_a$	-0.8199	$2e'_s$	-0.8180
	$1a''_2$	-0.6729	$1a''_2$	-0.6664
	$3a'_1$	-0.6283	$3a'_1$	-0.6280
	$1e''_s$	-0.5106	$1e''_a$	-0.5116
	$1e''_a$	-0.5106	$1e''_s$	-0.5116
	$3e'_a$	-0.4118	$3e'_s$	-0.4163
	$3e'_s$	-0.4118	$3e'_a$	-0.4163
	α-MO		α-MO	
22$^+$	$1a_1$	-11.5345	$1a_1$	-11.5389
	$1b_2$	-11.5344	$1b_2$	-11.5387
(90,90)	$2a_1$	-11.4708	$2a_1$	-11.4754
	$3a_1$	-1.3087	$3a_1$	-1.3876
(C$_2$v)	$2b_2$	-1.1598	$2b_2$	-1.1550
	$4a_1$	-1.0820	$4a_1$	-1.0792
	$1b_1$	-0.9468	$1b_1$	-0.9402
	$5a_1$	-0.8644	$5a_1$	-0.8656
	$1a_2$	-0.8381	$1a_2$	-0.8360
	$3b_2$	-0.7889	$3b_2$	-0.7879
	$2b_1$	-0.7640	$2b_1$	-0.7661
	$6a_1$	-0.6433	$6a_1$	-0.6438
	β-MO		β-MO	
	$1b_2$	-11.5220	$1a_1$	-11.5270
	$1a_1$	-11.5219	$1b_2$	-11.5269
	$2a_1$	-11.4750	$2a_1$	-11.4793
	$3a_1$	-1.3660	$3a_1$	-1.3562
	$2b_2$	-1.1063	$2b_2$	-1.1055
	$4a_1$	-1.1054	$4a_1$	-1.0523
	$1b_1$	-0.9372	$1b_1$	-0.9318
	$5a_1$	-0.8512	$5a_1$	-0.8537
	$1a_2$	-0.8284	$1a_2$	-0.8281
	$3b_2$	-0.7690	$3b_2$	-0.7661
	$2b_1$	-0.7589	$2b_1$	-0.7611

114

	α–MO			α–MO	
22⁺	1a₁	-11.5291		1a₁	-11.5352
	2a₁	-11.5129		2a₁	-11.5157
(90,90)	1b₂	-11.5121		1b₂	-11.5146
	3a₁	-1.4142		3a₁	-1.4017
(C₂v)	4a₁	-1.1430		4a₁	-1.1387
	2b₂	-1.0955		2b₂	-1.0925
	1b₁	-0.9556		1b₁	-0.9479
	5a₁	-0.8833		5a₁	-0.8831
	2b₁	-0.8275		2b₁	-0.8261
	1a₂	-0.7851		1a₂	-0.7855
	6a₁	-0.7556		6a₁	-0.7553
	3b₂	-0.6810		3b₂	-0.6818
	β–MO			β–MO	
	1a₁	-11.5018		1a₁	-11.5166
	1b₂	-11.5099		1b₂	-11.5137
	2a₁	-11.5096		2a₁	-11.5125
	3a₁	-1.3787		3a₁	-1.3669
	4a₁	-1.0777		3a₁	-1.0794
	2b₂	-1.0681		2b₂	-1.0647
	1b₁	-0.9469		1b₁	-0.9402
	5a₁	-0.8674		5a₁	-0.8681
	2b₁	-0.8167		2b₁	-0.8172
	1a₂	-0.7798		1a₂	-0.7805
	6a₁	-0.7286		6a₁	-0.7296

	α–MO			α–MO	
22⁺	1a'	-11.5984		1a'	-11.6053
	2a'	-11.4619		2a'	-11.4679
(90,0)	3a'	-11.4495		3a'	-11.4549
	4a'	-1.3570		4a'	-1.3503
(Cₛ)	5a'	-1.1711		5a'	-1.1675
	6a'	-1.0648		6a'	-1.0622
	1a"	-0.9433		1a"	-0.9407
	7a'	-0.8804		7a'	-0.8770
	2a"	-0.7945		2a"	-0.7967
	8a'	-0.7768		8a'	-0.7766
	9a'	-0.7618		9a'	-0.7616
	3a"	-0.5875		3a"	-0.5866
	β–MO			β–MO	
	1a'	-11.5987		1a'	-11.6056
	2a'	-11.4647		2a'	-11.4703
	3a'	-11.4213		3a'	-11.4282
	4a'	-1.3482		4a'	-1.3417

115

5a'	−1.1304		5a'	−1.1289
6a'	−1.0127		6a'	−1.0137
1a"	−0.9395		1a"	−0.9365
7a'	−0.8734		7a'	−0.8728
2a"	−0.7761		2a"	−0.7778
8a'	−0.7621		8a'	−0.7638
9a'	−0.7477		9a'	−0.7489

	α-MO		β-MO	
22^+	1b	−11.4970	1b	−11.5038
	1a	−11.4970	1a	−11.5038
(0,0)	2a	−11.4780	2a	−11.4838
	3a	−1.3572	3a	−1.3519
(C_2)	2b	−1.1992	2b	−1.1957
	4a	−1.0460	4a	−1.0416
	5a	−0.9030	5a	−0.8999
	3b	−0.8638	3b	−0.8617
	4b	−0.8169	4b	−0.8146
	5b	−0.7942	5b	−0.7957
	6a	−0.7593	6a	−0.7610
	7a	−0.5304	7a	−0.5324

	α-MO		β-MO	
	1a	−11.4827	1a	−11.4897
	1b	−11.4819	1b	−11.4895
	2a	−11.4817	2a	−11.4875
	3a	−1.3352	3a	−1.3294
	2b	−1.1354	2b	−1.1351
	4a	−1.0318	4a	−1.0319
	5a	−0.8930	5a	−0.8918
	3b	−0.8518	3b	−0.8513
	4b	−0.8241	4b	−0.8219
	5b	−0.7824	5b	−0.7854
	6a	−0.7611	6a	−0.7648

[a]Atomic units.

[b]The basis set on the left refers to the basis used for the single point calculation; the basis set on the right refers to the basis set used to optimize the geometry.
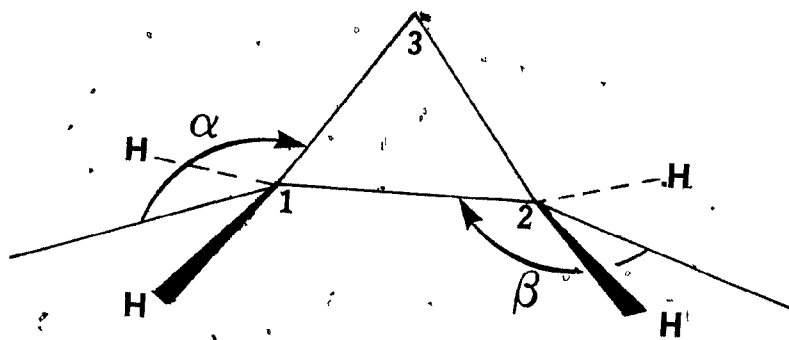
Figure 20. Pictorial representation of the angles α and β.

model for bonding; since the electron has been removed from a molecular orbital which is bonding between C_1 and C_2, large changes at C_3 are not expected if there is still substantial bonding between C_1 and C_2 in the radical cation. The magnitude of $\angle C_1 C_3 C_2$ (only 81.7 degrees) is an indication that there is considerable $C_1 C_2$ bonding interaction in this species. Furthermore, the Mulliken overlap population (Table 11) between C_1 and C_2 is another indication that there is bonding overlap between these atoms. However, this overlap is very much reduced in comparison to the overlap between the carbon atoms in 22.

The value of α in the $^2B_2$ structure is much smaller than that in the $^2A_1$ state. Since this structure is

Table 11. Mulliken overlap populations for the carbons in 22 and 22^+.

Molecule or Ion	Basis Set	Overlap		
		C_1C_2	C_1C_3	C_2C_3
22	4-31G//4-31G	0.1705	0.1705	0.1705
	4-31G*//4-31G	0.2646	0.2646	0.2646
22^+ ($^2A_1$)	4-31G//4-31G	0.0226	0.1922	0.1922
	4-31G*//4-31G	0.0597	0.2608	0.2608
22^+ ($^2B_2$)	4-31G//4-31G	0.2060	0.0883	0.0883
	4-31G*//4-31G	0.3057	0.1332	0.1332
22^+ (90,0)	4-31G//4-31G	-0.0326	0.2557	0.2097
	4-31G*//4-31G	-0.0169	0.3297	0.2508
22^+ (0,0)	4-31G//4-31G	-0.0609	0.3025	0.3025
	4-31G*//4-31G	-0.0588	0.3654	0.3654

described as a π-complex between ethylene and CH_2^+, it is useful to consider an angle β which is defined as the angle between the C_1C_2 bond and the intersection of the plane of the methylene with the plane of the carbons (Figure 20). In this case, β has a value of 167.2 degrees (for ethylene the corresponding angle would be 180.0 degrees). The lengthening of the C_1C_3 and C_2C_3 bonds and concurrent shortening of the C_1C_2 bond are consistent with the structure predicted by the Walsh model. The Mulliken overlap between C_1 and C_2 has increased relative to **22**, while the overlap between C_1 and C_3 and between C_2 and C_3 has decreased. The overlap between the carbons, however, is still large compared to the overlap between C_1 and C_2 in the $^2A_1$ state. The antisymmetric MO extends over all three carbons, consequently, the equilibrium geometries of all three methylenes in this state differ substantially from those in cyclopropane.

The equilibrium geometry of **22**$^+$ in the 90,0 conformation is very close to the C_s point group (α_2 is 179.5 degrees). Consequently, the symmetry label of the singly occupied state is "pseudo"-$^2A''$ (Table 10). The C_1C_3 bond has shortened while the C_2C_3 bond (the plane of the C_2 methylene has rotated 90 degrees) has lengthened. The C_1H and C_2H bond lengths, the HCH angles and the value of α_1 and α_2 are those expected for sp^2 hybridized carbons. On the other hand, the longer C_3H bond, the larger value of $\angle C_1C_3C_2$ and the smaller HC_3H angle are characteristic of a

normal alkane bond (i.e. sp^3 hybridized). Further investigation, in fact, reveals that the C_1C_3 and C_2C_3 bond lengths are similar to those calculated for the 1-propyl cation (92). In the case of the 1-propyl cation, the C_1C_3 and C_2C_3 bond lengths (using a 3-21G basis set) were found to be 1.438A and 1.536A respectively. In contrast, for the 90,0 conformer of **22**, the C_1C_3 and C_2C_3 bonds are almost equal in length (93).

The 0,0 conformer of $\mathbf{22}^+$ has C_2 symmetry and exists as a ^2A ground state. However, since the value of α_1 and α_2 in this conformer are very close to 180.0 degrees (actually 179.95 degrees), it could be classified in the C_{2v} point group and, as such would have a $^2A_1$ ground state. While there is substantial overlap between C_1 and C_3 and between C_2 and C_3, there is no bond between C_1 and C_2 (Table 11). The CH bond lengths, the HCH angles and the value of α_1 and α_2 are consistent with sp^2 hybridization at C_1 and C_2. The geometry at C_3, however, is very different. The value of $\angle C_1C_3C_2$ is anomalously large (124.8 degrees), the C_3H bonds are anomalously long and the HC_3H angle is smaller than expected (Table 9). This unique geometry can be understood. The steric repulsion between the hydrogens on C_1 and C_2 could be responsible for the unusually large value of $\angle C_1C_3C_2$. The value of 124.8 degrees is close to the value expected for a bond angle in an sp^2 hybridized carbon. If it is assumed that the hybridization at C_3 is sp^2 then, each C-C bond would be formed with one of the three available sp^2

120

orbitals on C_3. This arrangement would leave one sp^2 and one p orbital to form the two C-H bonds. Rehybridization of the sp^2 and p orbitals leads to the formation of two sp^5 orbitals. The increased "p" character of these new orbitals leads to much longer C-H bonds (e.g. $C(sp^3)$-H bonds are longer than $C(sp^2)$-H bonds). Furthermore, the angle between two sp^5 orbitals is 101.2 degrees (78) which is larger than the 93.0 degrees obtained for the 0,0 conformer but, nevertheless, is in the right direction.

The charge and spin distributions in each of these structures are shown in Table 12 and 13 respectively. In the $^2A_2$ structure only 20% of the charge is delocalized to the C_3 methylene. Similarly, most of the spin density remains between C_1 and C_2. This, of course, is consistent with the Walsh model described previously. The electron density distribution in 22 (Figure 21) is symmetrical around the three carbons. However, the electron density distribution in 22^+ ($^2A_1$) illustrates the decreased electron density between C_1 and C_2 and, in fact, resembles very closely the distribution expected for a trimethylene type structure (Figure 22).

In the $^2B_2$ structure the charge is almost equally distributed between the three methylenes; 30% on the C_3 methylene and 35% on each of the C_1 and C_2 methylenes. The spin density, however, is almost entirely localized on C_3. It is interesting that while there is excess spin density on C_1 and C_2, the Fermi contact is negative. This is

Table 12. Atomic charge densities of **22** and **22**$^{+a}$.

Molecule or Ion	Atom	4-31G//4-31G	4-31G*//4-31G
22	C_1	6.346	6.352
	C_2	6.346	6.352
	C_3	6.346	6.352
	H_4	0.827	0.824
	H_5	0.827	0.824
	H_6	0.827	0.824
	H_7	0.827	0.824
	H_8	0.827	0.824
	H_9	0.827	0.824
22$^+$ ($^2A_1$)	C_1	6.210	6.243
	C_2	6.210	6.243
	C_3	6.393	6.359
	H_4	0.696	0.687
	H_5	0.696	0.687
	H_6	0.696	0.687
	H_7	0.696	0.687
	H_8	0.701	0.702
	H_9	0.701	0.702
22$^+$ ($^2B_2$)	C_1	6.269	6.275
	C_2	6.269	6.275
	C_3	6.316	6.327
	H_4	0.688	0.687
	H_5	0.688	0.687
	H_6	0.688	0.687
	H_7	0.688	0.687
	H_8	0.688	0.687
	H_9	0.688	0.687
22$^+$ (90,0)	C_1	5.946	5.992
	C_2	6.298	6.365
	C_3	6.512	6.477
	H_4	0.676	0.663
	H_5	0.676	0.663
	H_6	0.722	0.710
	H_7	0.762	0.747
	H_8	0.703	0.706
	H_9	0.703	0.706

22^+ (0,0)	C_1	6.126	6.191
	C_2	6.126	6.191
	C_3	6.613	6.521
	H_4	0.723	0.707
	H_5	0.725	0.712
	H_6	0.723	0.707
	H_7	0.725	0.707
	H_8	0.618	0.629
	H_9	0.618	0.629

[a]Atomic units.

Table 13. Atomic spin densities and Fermi contact in 22^{+}[a].

		4-31G//4-31G		4-31G*//4-31G	
Ion	Atom	spin density	Fermi contact	spin density	Fermi contact
22^+ ($^2A_1$)	C_1	0.677	0.106	0.652	0.080
	C_2	0.677	0.106	0.652	0.080
	C_3	-0.218	-0.057	-0.186	-0.048
	H_4	-0.050	-0.017	-0.043	-0.015
	H_5	-0.050	-0.017	-0.043	-0.015
	H_6	-0.050	-0.017	-0.043	-0.015
	H_7	-0.050	-0.017	-0.043	-0.015
	H_8	0.031	0.016	0.027	0.015
	H_9	0.031	0.016	0.027	0.015
22^+ ($^2B_2$)	C_1	0.112	-0.002	0.112	-0.006
	C_2	0.112	-0.002	0.112	-0.006
	C_3	0.923	0.152	0.902	0.117
	H_4	0.000	0.004	0.000	0.003
	H_5	0.000	0.004	0.000	0.003
	H_6	0.000	0.004	0.000	0.003
	H_7	0.000	0.004	0.000	0.003
	H_8	-0.074	-0.026	-0.063	-0.023
	H_9	-0.074	-0.026	-0.063	-0.023
22^+ (90,0)	C_1	-0.012	0.001	-0.027	0.002
	C_2	1.318	0.265	1.271	0.214
	C_3	-0.153	-0.050	-0.121	-0.040
	H_4	0.001	0.000	0.001	0.000
	H_5	0.001	0.000	0.001	0.000
	H_6	-0.107	-0.036	-0.092	-0.032
	H_7	-0.106	-0.036	-0.094	-0.032
	H_8	0.036	0.020	0.031	0.018

	H_9	0.036	0.020	0.031	0.018
22^+ (0,0)	C_1	0.797	0.137	0.760	0.107
	C_2	0.797	0.137	0.760	0.107
	C_3	-0.187	-0.041	-0.141	-0.026
	H_4	-0.063	-0.022	-0.054	-0.019
	H_5	-0.058	-0.021	-0.049	-0.019
	H_6	-0.063	-0.022	-0.054	-0.019
	H_7	-0.058	-0.021	-0.049	-0.019
	H_8	-0.083	-0.047	-0.086	-0.050
	H_9	-0.083	-0.047	-0.086	-0.050

[a]Atomic units.

because the α spin density on these two atoms is in the p orbitals which form the "π-bond" of the ethylene part of the complex. There is excess spin in the other orbitals. Since a p-orbital has no Fermi contact with the nucleus, the net Fermi contact (from the "s" character of the orbitals) has a slight excess of β-spin (94). The similarity of the $^2B_2$ state of 22^+ to a π-complex is supported by the electron density distribution for this species (Figure 23). Thus, the description of the $^2B_2$ state as complex between CH_2^+ and ethylene is appropriate.

The charge and spin distributions in the 90,0 conformer are unusual. The charge is localized essentially on the C_1 methylene (71%) and to a lesser extent on C_2 and C_3 (21% and 8% respectively, Table 12). The spin, on the other hand (Table 13), is localized almost completely on C_2; the remainder is on C_3. These spin and charge distributions may be understood qualitatively by considering two
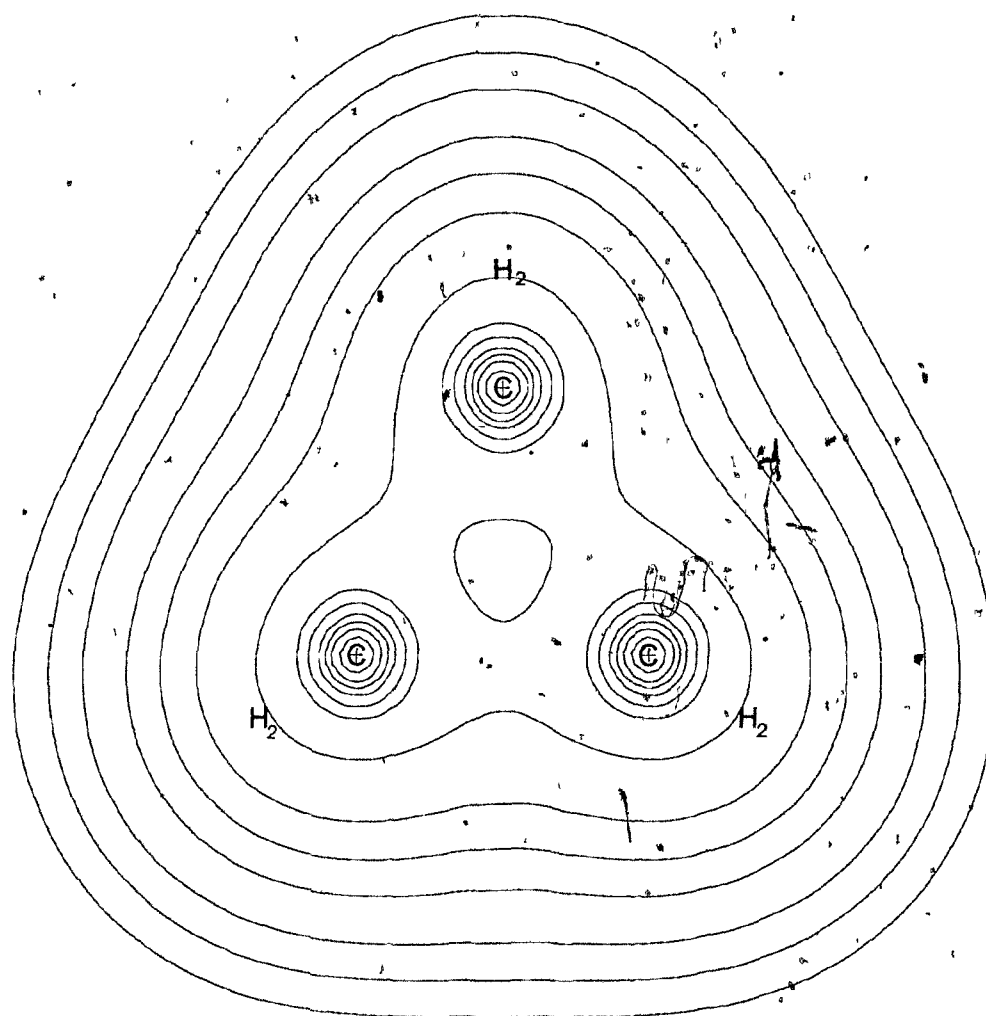
Figure 21. Electron density distribution in **22.** The
contour values in atomic units are 0.002, 0.004
and 0.008 increasing in powers of 10. The
outermost contour in this and the following two
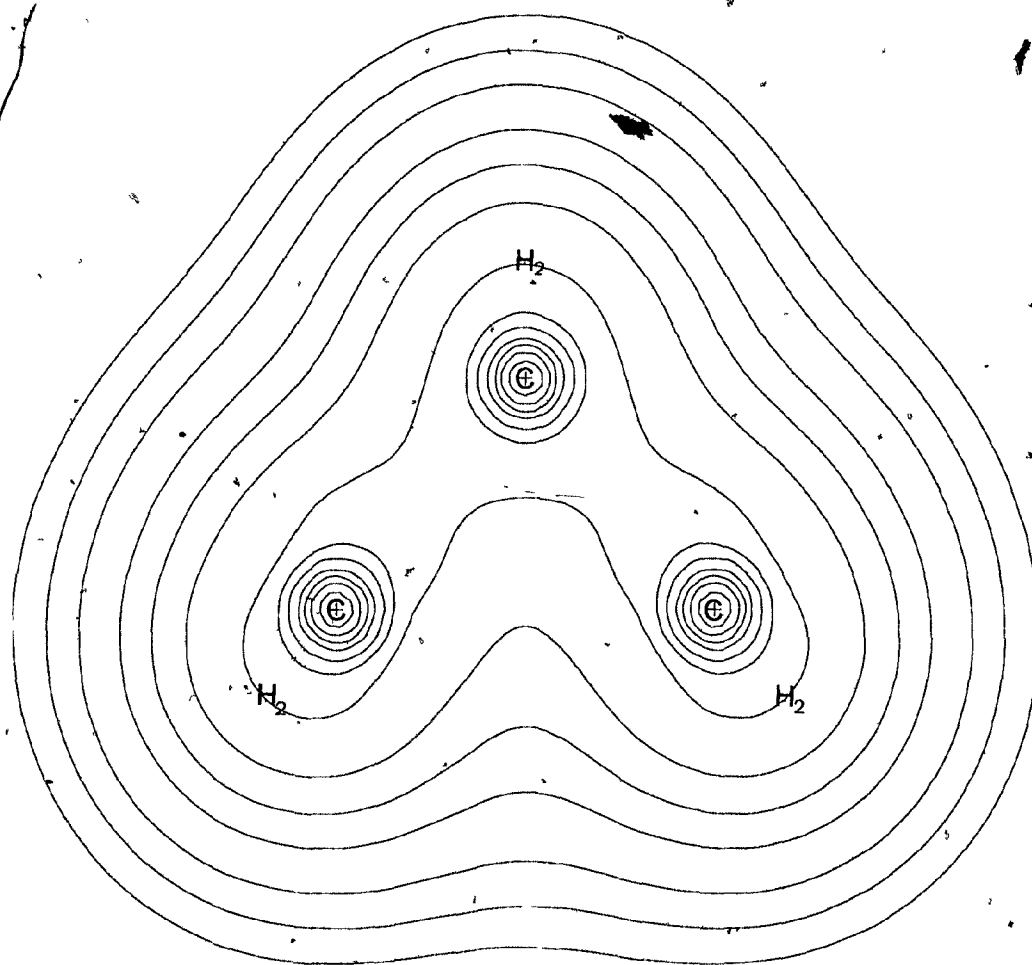figures is 0.002 au.

Figure 22. Electron density distribution in 22^+ (90,90 conformer, $^2A_1$ state).
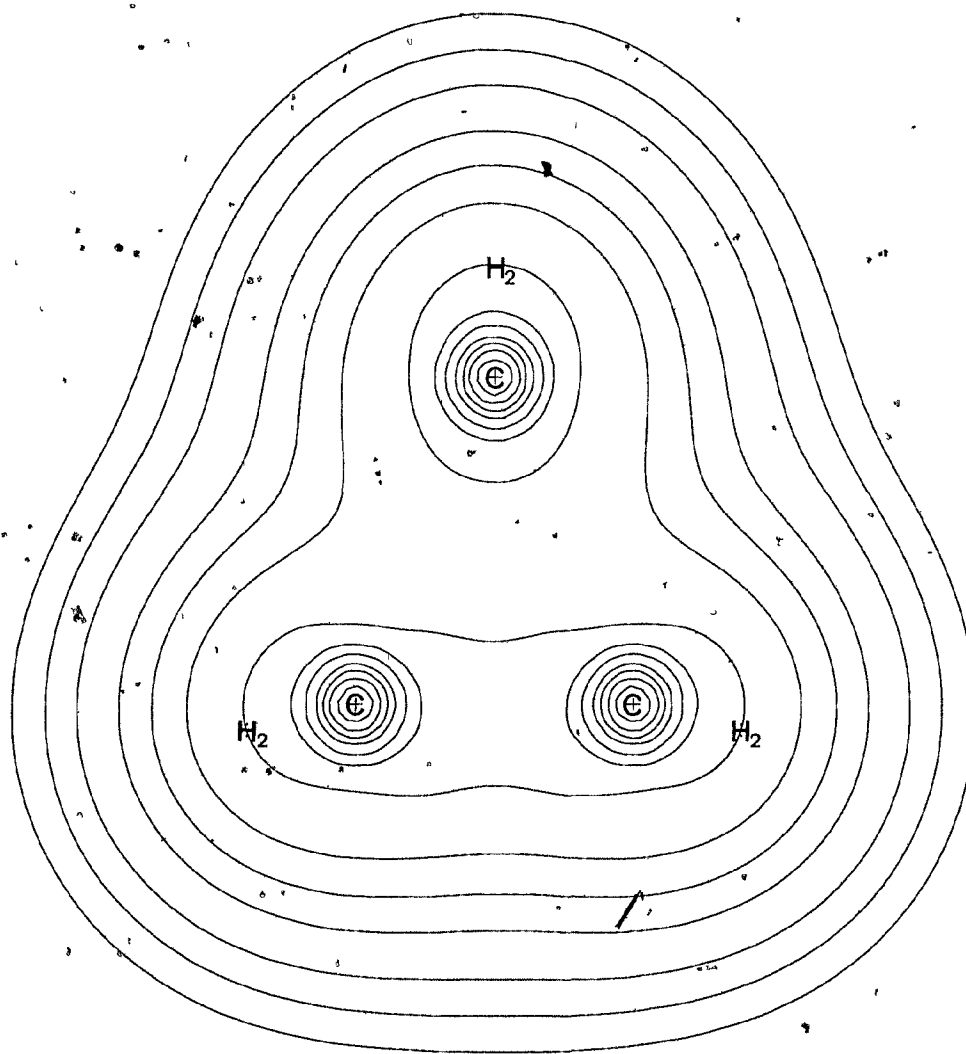
Figure 23. Electron density distribution in 22^+ (90,90 conformer, $^2B_2$ state).

127

possibilities. In the first, the spin is localized on C_2. This may be described as an "ethyl cation-methyl radical" pair. In the other case the charge is localized on C_2; this would be an "ethyl radical-methyl cation" pair. Since the ionization potential of the methyl radical is greater than the ionization potential of the ethyl radical (95) the former case would be expected to be energetically favourable. The alternate lengthening of the C_2C_3 bond and shortening of the C_1C_3 bond may be a result of the charge polarization. The redistribution of the electron density in order to stabilize the positive charge leads to an increased negative charge on C_3 at the expense of removing electron density from between C_2 and C_3. The weakened C_2C_3 bond is reflected by the increased length.

In the 0,0 conformer of **22$^+$**, 85% of the charge is on the C_1 and C_2 methylenes and only 15% of the charge is on the C_3 methylene. The large negative charge on C_3 is likely a result of polarization of electron density similar to that found for the 90,0 conformer. As expected, most of the spin density is shared between C_1 and C_2. It is found, however, that while C_3 has an excess of α spin density, the hydrogens bonded to C_3 do **not** have, as expected, an excess of β spin density. Instead, these hydrogens also have an excess of α spin density. The reason for this unusual behaviour is not understood.

2.3.2 Isomerization of 22$^{\pm}$

The surface for cis-trans isomerization and racemization of 22 has been studied experimentally (85) and by molecular orbital methods (93, 95). The theoretical calculations predict that the barrier to racemization is less than the barrier to isomerization. This effect has been rationalized in terms of orbital symmetry allowed opening of the cyclopropane ring. At the transition state (the 0,0 conformer) there is "pseudo-conjugation" through the central methylene, leading to the "allowed" conrotatory closure to give 22. The energy difference between the barriers for isomerization and racemization has been estimated to be approximately 2.5 kcal mol^{-1} (95).

There has been interest, recently, in the applicability of orbital symmetry rules to the electrocyclic reactions of odd-electron species (96). It is interesting to compare the results obtained for the isomerization and racemization of 22$^+$ to those results for 22. At the outset, it should be noted that the work of Collins and Gallup (81a) predicted the energy of the $^2A_1$ conformer to be 6.6 kcal mol^{-1} higher than that of the $^2B_2$ structure. The results obtained from this study show that at all levels of theory used, the $^2A_1$ structure is lowest in energy (Table 14). Furthermore, recent experimental results have comfirmed that the unpaired electron occupies the 6a$_1$ orbital (97).

The calculated barrier to cis-trans isomerization of 22 using a minimal basis set and configuration interaction of

129

the ground state and all single and double substitutions is 52.6 kcal mol^{-1} (93). This is an underestimate of the experimental value (65 kcal mol^{-1}, 85) since CI was performed only on the 90,0 comformer. There should be a large negative correction to the energy of **22** when CI is included. Since, for **22**$^{+}$ ($^{2}A_1$), the electron has been removed from an orbital which is predominantly bonding between C_1 and C_2, the strength of the resulting one-electron, two-centre bond should be no more than half of the experimental bond strength in **22**. The calculated strength of the one-electron, two-centre bond depends on the basis set used (Table 14). However, even at the MP2/4-31G* level, the bond strength is still less than half of the experimental value. It is clear that as the basis set becomes more sophisticated, the calculated bond strength increases and, that inclusion of polarization functions has as great an effect as electron correlation.

The calculated activation energy associated with racemization (Table 14) is greater than the activation energy for isomerization when electron correlation is not included. However, the effect of electron correlation is to reduce the calculated barrier to racemization (in contrast to the effect of electron correlation on isomerization which is to increase the barrier). The result is that the calculated barrier to racemization is much less than the calculated barrier to isomerization when electron correlation is included. This energy difference is as much

130

Table 14. Relative energies of conformers of **22**[+] (kcal mol^{-1}).

Conformer	4-31G //4-31G	4-31G* //4-31G	MP2/4-31G //4-31G	MP3/4-31G //4-31G	MP2/4-31G* //4-31G
90,90 ($^2A_1$)	0.00[a]	0.00[b]	0.00[c]	0.00[d]	0.00[e]
90,90 ($^2B_2$)	6.16	4.10	2.64	3.21	1.16
90,0 ($^2A''$)	17.54	22.17	24.13	24.24	30.09
0,0 (^2A)	20.72	26.24	16.22	16.60	20.58

[a] Total energy is -116.5735881 hartrees.

[b] Total energy is -116.6324484 hartrees.

[c] Total energy is -116.8123945 hartrees.

[d] Total energy is -116.8406159 hartrees.

[e] Total energy is -116.9798358 hartrees.

as 10 kcal mol^{-1}; far greater than the analogous energy difference calculated for racemization versus isomerization in **22**.

The conrotatory closure of the 0,0 conformer of **22**[+] is an allowed process by orbital symmetry. Since this conformer has a ^2A ground state, the singly occupied MO is symmetric with respect to rotation about the C_2 axis. Examination of the molecular orbital coefficients reveals that there is no contribution from the atomic orbitals on the C_3 methylene. This should be expected since the 0,0

conformer is structurally related to the allyl radical (a protonated allyl radical). The singly occupied MO of the 0,0 conformer is, in fact, very similar to the singly occupied MO of the allyl radical (Figure 24).
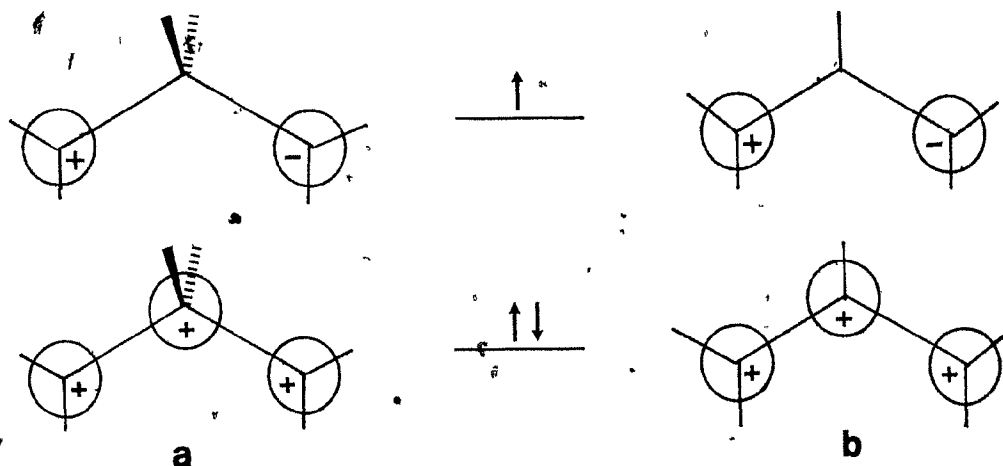
Figure 24. Representation of the occupied MO's of (a) the 0,0 conformer of 22^+ and (b) the allyl radical.

The partial surface for twisting of one methylene from the $^2A_1$ state of 22^+ to the 90,0 conformer has been obtained. The fully optimized geometries of 22^+ in the 90,0; 90,10; 90,20; 90,30; 90,60;and 90,90 conformers reveals several interesting trends. The energy profile for twisting is shown in Figure 25. It is clear that near the transition state, the tortional surface is very "soft"; i.e. since there is little bonding between C_1 and C_2, rotation of C_2 has only a small effect on the relative energy. Near the $^2A_1$ structure, however, small changes in θ_2 result in larger changes in the relative energy. This is expected since the one-electron, two-centre bond is being broken by
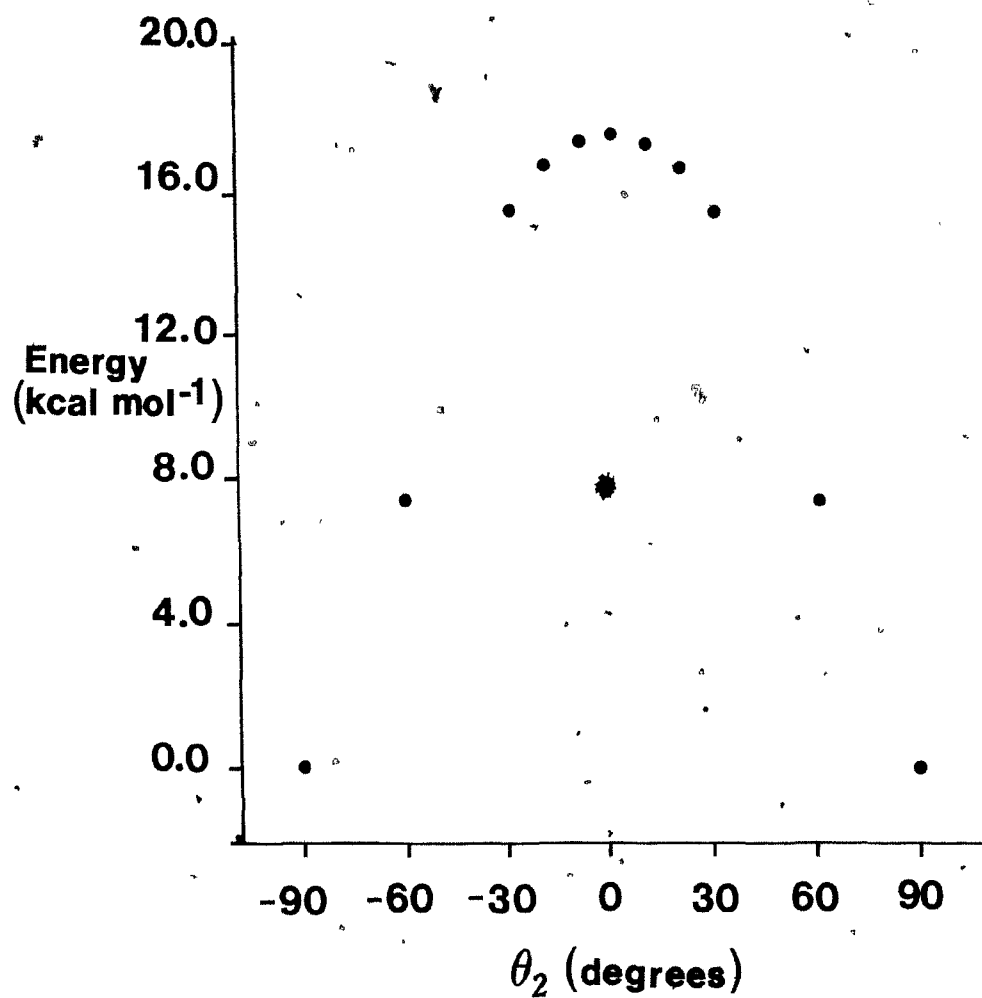
Figure 25. Energy versus tortional angle (θ_2) for the twisting of the C_2 methylene in the 90,90 ($^2A_2$) conformer to the 90,0 conformer of 22^+.

twisting. This can be compared to twisting in the ethylene radical cation (98) where the tortional potential is much softer. At a tortional angle of 30 degrees, the energy change is only 1.6 kcal mol^{-1} at this level of theory (compared to over 7 kcal mol^{-1} in 22^+).

The geometric changes associated with twisting are also of interest. As the tortional angle is decreased from 90 to 0 degrees, there is a progressive increase in the value of $\angle C_1 C_3 C_2$. This is expected as the extent of bonding between C_1 and C_2 decreases (Figure 26a).

The associated wagging of the methylenes (C_1 and C_2) is particularly intriguing. Salem and his coworkers, in their study of the isomerization of 22, found that large pyramidal distortions were associated with the trimethylene structures (99a). For the 90,0 conformer (of 22) this distortion from planarity was 14 degrees for the carbon which had twisted (93). At the STO-3G level, a pyramidal distortion of the C_2 methylene (in the 90,0 conformer of 22^+) of 28 degrees is observed. However, at the 4-31G level, this distortion completely disappears. Salem was using a minimal basis set of STO's in his work and, the possibility that the distortions is a basis set related problem must be considered.

The wagging motion of the C_1 methylene of 22^+ as the tortional angle is decreased from 90 to 0 degrees reveals that initially there is a small pyramidal distortion away from the central methylene (Figure 26b). This distortion
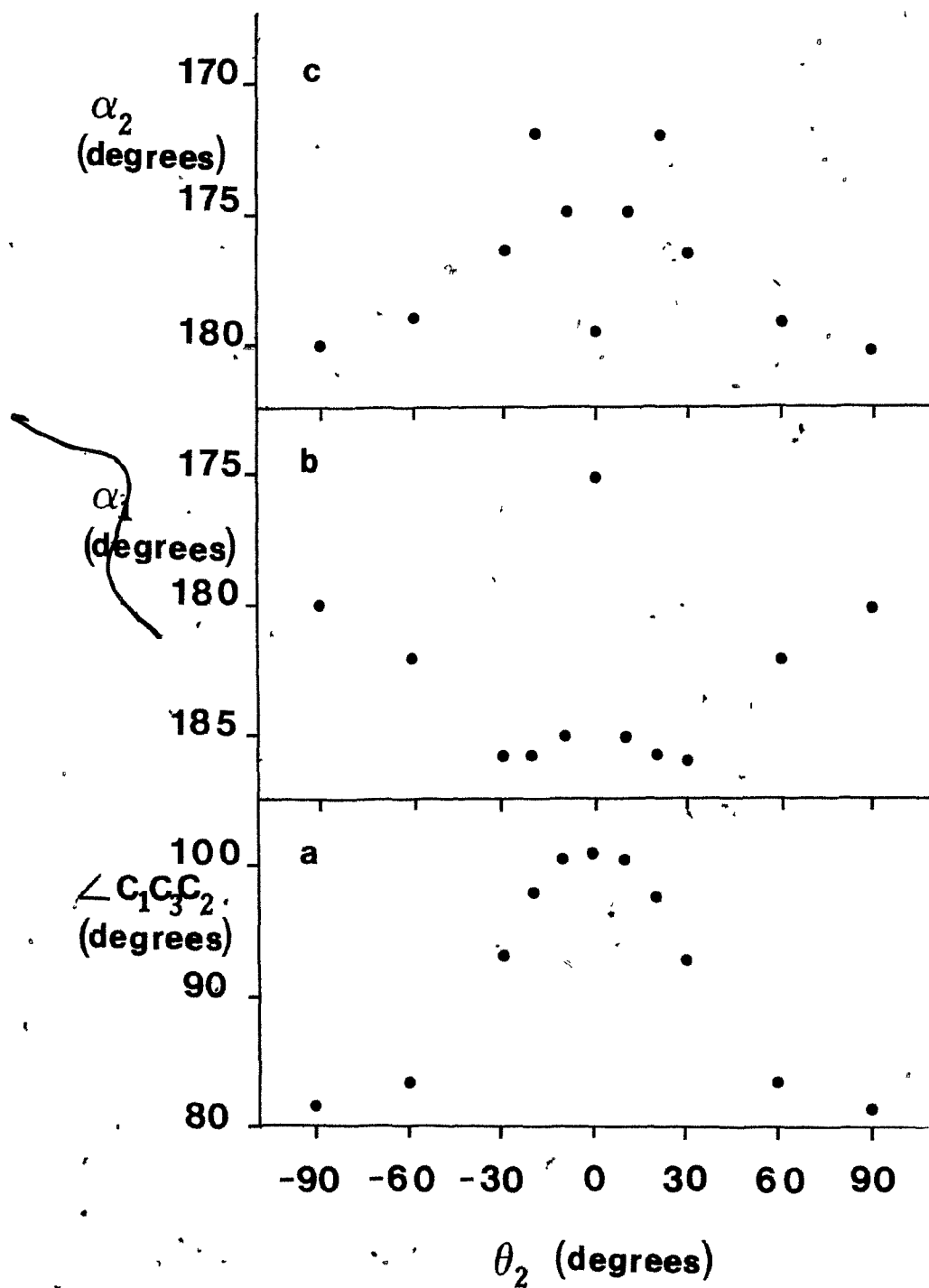
Figure 26. (a) $\angle C_1C_3C_2$ versus tortional angle (θ_2), (b) wagging angle of the C_1 methylene (α_1) versus tortional angle (θ_2) and (c) wagging angle of the C_2 methylene (α_2) versus tortional angle (θ_2) for twisting of the C_2 methylene.

135

reaches a minimum near $\theta_2 = 30$ degrees and, near the transition state undergoes an inversion such that at the transition state, the C_1 methylene is pyramidally-distorted towards the central methylene. The inversion near the transition state is best rationalized as a result of the steric repulsion between the hydrogens of the C_1 methylene and the hydrogen of the C_2 methylene. The initial pyramidalization away from the central methylene can lead to increased hyperconjugative interaction between C_3 and the hydrogens bonded to C_3. This explanation would account for the trend observed, however, the 90,0 conformer is a $^2A''$ state and is antisymmetric with respect to reflection (i.e. any bonding overlap with one hydrogen would be cancelled by an antibonding overlap with the other).

The C_2 methylene slowly pyramidalizes away from the C_1 methylene as the tortional angle decreases (Figure 26c) and reaches a maximum near $\theta_2 = 15$ degrees. At the transition state, there is no pyramidal distortion at the C_2 methylene. This motion may be a response to increased steric interaction with the C_1 methylene which moves towards one of the hydrogens bonded to C_2. The observation that the distortion of the C_2 methylene continues even after the distortion of the C_1 methylene has reached a maximum is consistent with this idea. At (or near) a tortional angle of 15 degrees, further pyramidalization of the C_2 methylene becomes less favourable energetically than depyramidalization of the C_1 methylene. So, while the

wagging motion of the C_2 methylene can be rationalized as a a motion coupled to the motion of C_1, it is not immediately clear why pyramidalization of C_1 should be favourable. Goddard and his coworkers (99b) suggested that the pyramidal distortions in trimethylene were favourable since this conformation avoided eclipsing of more than two bonds. This explanation is feasible in the trimethylene system where the distortions are large. For 22^+, where the distortions are much smaller, this suggestion seems less likely. However, this represents a non-dynamic path between the 90,90 $(^2A_1)$ comformer and the 90,0 $(^2A'')$ conformer since the conformation of the C_1 methylene is fixed.

It is interesting to note that the experimentally determined π-bond strength in ethylene (86) is approximately the same as the σ-bond strength in cyclopropane (85). The difference in the calculated activation energies (at the 4-31G level) of 22^+ (17.5 kcal mol^{-1}) and $C_2H_4^+$ (27.2 kcal mol^{-1}, 98) should therefore be dicussed. The one-electron oxidation of ethylene leads to a species which has little internal strain. It is tempting, therefore, to attribute the difference between the activation energies for cis-trans isomerization of 22^+ and $C_2H_4^+$ to the ring strain in the cyclopropane radical cation. We must use caution, however, since the difference between the calculated activation barrier for isomerization in C_3H_6 and C_2H_4 using the same basis set is not available. If the calculated activation barrier for C_2H_4 is significantly

higher than that for C_3H_6, the difference in the radical cations may be meaningless. (One calculation using a double-zeta basis set with polarization and diffuse functions estimates the activation barrier for ethylene to be 62.5 kcal mol^{-1} (100)). It should be noted that the experimentally determined torsional angle at the energy minimum in $C_2H_4^+$ is 25 degrees; apparently a compromise between π-overlap and hyperconjugation (101). The ab initio calculations failed to predict this conformational preference. The planar structure, however, is only 0.67 kcal mol^{-1} higher in energy than the twisted minimum.

2.3.3 The 1,2-Divinylcyclopropane Radical Cation (23$^+$)

Several interesting features of 23$^+$ are evident. In structures 23a$^+$, 23b$^+$ and 23c$^+$ (Figure 20) the values of $\angle C_1 C_3 C_2$ are similar to the bond angle in the unsubstituted radical cation (Table 15). This is significant since using the geometry of the allyl cation maximizes the π-overlap between the vinyl groups and the respective cyclopropane carbons. This should have the result of lengthening the $C_1 C_2$ bond since it may be expected that the more effectively the electron density is delocalized, the weaker the $C_1 C_2$ bond should become. The value of $\angle C_1 C_3 C_2$ in the 90,0 conformation is larger than that in the unsubstituted radical cation. This may be a consequence of the increased steric interactions with the allyl system at C_1. The steric repulsions in structure 23d$^+$ are predominant. Because of

Table 15. Relative energies of conformers of 23^{+a}.

Conformer	Energy (kcal mol^{-1})	$\angle C_1C_3C_2$ (degrees)[b]
$23a^+$	0.00	77.4
$23b^+$	4.25	81.7
$23c^+$	13.43	77.9
$23d^+$	>100	>125
$90,0^c$	16.00	112.8
$90,0^d$	14.23	113.0
$90,0^e$	14.56	109.1

[a]STO-3G energies relative to $23a^+$ for which the STO-3G total energy is -267.34486 hartrees.

[b]The value of $\angle C_1C_3C_2$ for the 90,90 ($^2A_1$) conformer of 22^+ is 75.8 degrees at the STO-3G level. For the 90,0 conformer, this angle is 102.1 degrees. The energy difference between the 90,90 and the 90,0 conformers is 23.2 kcal mol^{-1}.

[c]The C_2 vinyl group has rotated in the direction of the C_3 methylene. The C_2 vinyl group has the geometry of the allyl cation.

[d]The C_2 vinyl has rotated in the direction of the C_3 methylene. The C_2 vinyl group has the geometry of the allyl radical.

[e]The C_2 vinyl group has rotated in the direction of the C_1 methylene. The C_2 vinyl group has the geometry of the allyl radical.

CPU time restrictions it was not feasible to optimize the dihedral angles about the methylenes. However, it seems likely that the radical cation in this conformation should undergo a facile Cope rearrangement since the activation energy for the analogous rearrangement of cis-23 is only 20 kcal mol^{-1} (102).

The charge and spin distributions in 23a$^+$ (the lowest energy 90,90 conformer) and in the 90,0 conformation are shown in Figures 27 and 28 respectively. Only the $^2A_1$ structure was considered for the cyclopropane system. The experimental evidence obtained from CIDNP studies (23) is best interpreted in terms of a structure of this type. Furthermore, involvement of the $^2B_2$ structure would render two substituents in spacially non-equivalent environments. The loss of the symmetry would complicate the choice of model geometries for each vinyl group. Finally, it seems likely that a structure similar to the $^2A_1$ geometry would be involved in cis-trans isomerization.

The geometry of the vinyl groups was based on the STO-3G geometry of the allyl cation. Since almost all of the spin density appears on C_2 in the 90,0 conformation, the geometry of the allyl radical was used for the C_2 vinyl group in this case. The difference in energy using the allyl cation geometry at C_2 and that using the allyl radical geometry was only 1.8 kcal mol^{-1}.
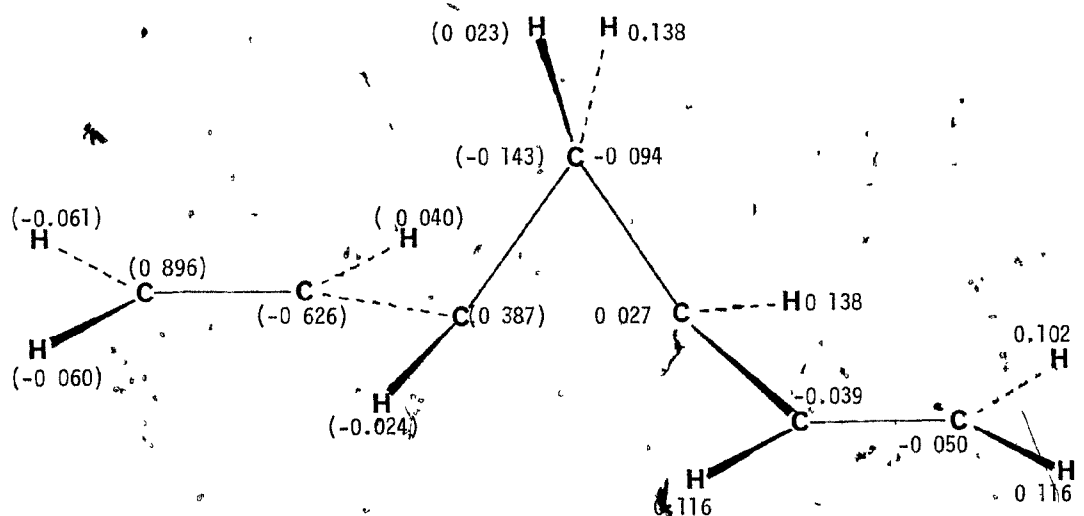
Figure 27. Charge and spin distributions in **23a**[+]. The spin
densities are in parentheses.

141

0 123
(0 033) H

0 119
H(0.034)

0 136
(0 003)

H

0 156
(-0,006)
H

0 076
(0 093)

-0 145
C (-0.110)

0 104
H(-0 071)

C

-0 088
(-0 042)

C

C 0 175
(-0 046)

C -0 020
(1 080)

H

0 170
(-0.006)

0.154
(0 003)

-0 063
C (-0.872)

0.081
H (-0 071)

H

0 039
(0 056)

C -0 099
(1 071)

0 082
H (-0.072)
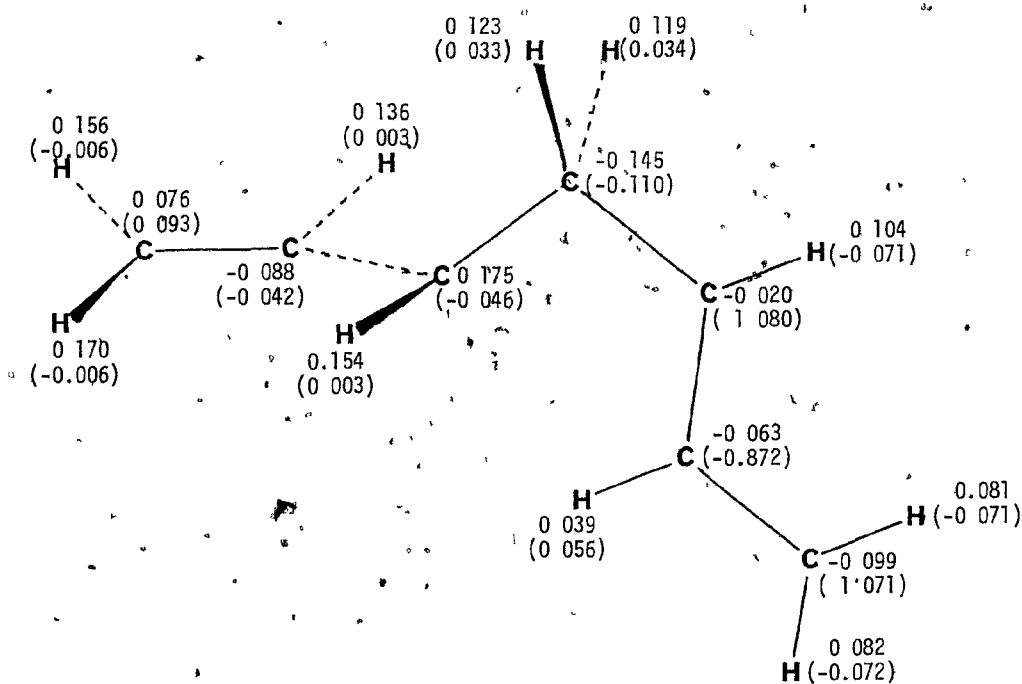
Figure 28.   Charge and spin distributions in the 90.0
               conformer of **23**⁺.   The spin densities are in
               parentheses.

142

In the 90,90 conformation, both charge and spin are delocalized into the vinyl groups. The C_3 methylene still has 18% of the charge (compared to approximately 20% in the unsubstituted case). Similarly, in the 90,0 conformation, only 10% of the charge is delocalized to the C_3 methylene and 12% to the C_2 vinyl system (compared to 8% and 21% respectively in the unsubstituted radical cation). Essentially all of the spin density remains at the C_2 vinyl system in this conformation.

2.3.4 Isomerization of 23[+]

An estimate of the activation barrier for isomerization of the 1,2-diphenylcyclopropane radical cation, which is known not to isomerize rapidly, may be obtained by comparing the energies of the 90,90 and 90,0 conformations of 23[+]. This is a reasonable model considering the benzylic and allylic C-H bond dissociation energies of toluene and propene are approximately equal (42a). The calculated energies of 23[+] relative to structure 23a[+] are shown in Table 16.

The relative energies of 23a[+], 23b[+] and 23c[+] are consistent with the results of recent calculations on vinylcyclopropane (103); s-trans being more stable. Structures 23a[+] and 23b[+] are geometric isomers having the same conformation of the vinyl groups (s-trans). The energy difference between 23a[+] and 23b[+] (4.25 kcal mol^{-1}) is similar to the energy difference observed from the thermal

isomerization of 1,2-diphenylcyclopropane (about 2.3 kcal mol^{-1}) (104).

The energy difference between **23a**$^+$ and the radical cation in the 90,0 conformation represents the activation barrier for isomerization of the radical cation. The value of 14.23 kcal mol^{-1} indicates a bond weakening of approximately 9 kcal mol^{-1} relative to the unsubstituted radical cation (Table 15). This may be compared to the difference in σ-bond strength observed experimentally between cyclopropane and 1,2-diphenylcyclopropane; about 30 kcal mol^{-1} (104). The effect of the substituents on the stability of the transition state relative to the ground state in the neutral molecule is expected to be far greater than in the radical cation; there is charge and spin delocalization in both the ground and transition state in the radical cation.

In the photochemical generation of the radical ions, this activation barrier would prevent cis-trans isomerization of the radical cation. If a preexponential factor of 10^{14} is assumed for the isomerization (105), the rate constant for cis-trans isomerization of the radical cation would be only 4.3 x 10^3 s^{-1} at 300 K.

2.4 CONCLUSIONS

The activation barrier to cis-trans isomerization and racemization of **22**$^+$ may be comparable to the activation barriers to other reactions such as the rearrangement to

144

propene radical cation (106). Only when electron correlation is included does the calculated barrier to isomerization become greater than the calculated barrier to racemization. Electron correlation increases the relative energy of the 90,0 conformer but decreases the relative energy of the 0,0 conformer.

The π-overlap with vinyl groups does not substantially weaken the one-electron two-centre bond of 23^+ relative to 22^+. This has important experimental implications. The cis-trans isomerization of the 1,2-diphenylcyclopropane radical cation is not observed on the CIDNP time scale. However, it will be interesting to look at the temperature effect on this isomerization. Furthermore, if the optically active compound is prepared, the relative rates of isomerization and racemization may be obtained. This will be interesting since the rate of racemization is slightly faster in the case of 1,2-diphenylcyclopropane (104).

PART III. SUBSTITUENT EFFECTS ON BENZYL RADICAL HYPERFINE
COUPLING CONSTANTS.

3.1   INTRODUCTION

3.1.1 Linear Free Energy Relationships (LFER)

One of the most successful empirical models for the
study of the relationship between structure and reactivity
that has been developed is the linear free-energy
relationships (LFER). The best known LFER is the Hammett
equation (Equation 37) which is based on the dissociation
constants for a series of substituted benzoic acids (107).

$$\log(K/K_0) = \rho \log(K'/K'_0) = \rho \sigma \qquad [37]$$

In this equation, the term $\log(K'/K'_0)$ is defined as the
substituent constant, σ, which is assumed to be an intrinsic
property of each substituent, and, ρ is the reactivity
parameter which is a measure of the sensitivity of the
equilibrium constant to the nature of the substituent. This
empirical relationship is an LFER inasmuch as the
equilibrium constants are related to the change in the
Gibb's free-energy (Equation 38).

$$\Delta G^0 = -RT \ln K \qquad [38]$$

146

The logical extension of the LFER is the correlation of the substituent effects, not with changes in equilibrium constants, but with changes in rate constants. In this approach, the LFER is a correlation of the changes in activation free-energies with a substituent parameter. The use of relationships of this kind has played an important role in the elucidation of reaction mechanisms in organic chemistry.

Specific deviations from the Hammett relationship have led to the development of a plethora of substituent parameters which are used to account for anomalous resonance and/or inductive interactions. The most important of these substituent parameters are σ^+(108), σ^-(109), σ_I (110) and σ_R^o (111). While the use of these substituent parameters has extended the range of applicability of the Hammett relationship, the selection of an appropriate substituent parameter scale has become much more subjective (112a). Furthermore, multiparameter extensions of the Hammett relationship have made the evaluation of substituent effects more complicated. The use of extended Hammett correlations has invoked much criticism since deviations from the single parameter treatment invariably depend on a subjective choice of substituents and usually a limited range of substituents (112b).

3.1.2 Substituent Effects on Free Radical Reactions

The effect of substituents on the rates of free radical

reactions is not well understood. The rates of many free

radical reactions, in fact, correlate very well with

substituent parameters derived for ionic reactions (113).

This effect has been rationalized in terms of a polar effect

at the transition state (114, Figure 29). This polar effect

$$\left[\overset{+}{R}\cdots\overset{\bullet}{H}\cdots\overset{-}{X} \leftrightarrow \overset{\bullet}{R}\cdots\overset{\bullet}{H}\cdots\overset{\bullet}{X} \leftrightarrow \overset{-}{R}\cdots\overset{\bullet}{H}\cdots\overset{+}{X} \right]^{\ddagger}$$
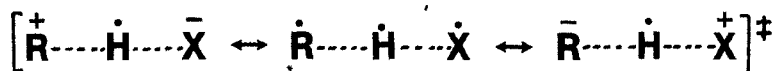
Figure 29.   Charge separated valence bond structures leading
to a polar transition state in a hydrogen atom
abstraction reaction.

encountered in free radical kinetics has complicated the

evaluation of the effect of substituents on an isolated free

radical. There have been many attempts to derive a

substituent parameter which reflects the effect of the

substituent on free radicals (115). In all of these cases,

the sigma dot ($\sigma^{\bullet}$) scales were based on kinetic data; the

substituent effect on the free radical could be estimated

only after some assumption of the polar effect on the

relative rates was made. It is, therefore, not surprising

that of the various free radical substituent parameters,

many fail to agree even in sign, let alone magnitude.

Recently, Dust and Arnold (116) developed a new

substituent parameter, sigma dot alpha ($\sigma_\alpha^\bullet$) based on the

α -H hyperfine coupling constants (hfc) of a series of

para- and meta- substituted benzyl radicals (Table 16,

Equation 39). This approach is based on the premise that

the extent of spin delocalization is inversely proportional

to the α -H hfc. The α -H hfc should be a measure of

the spin density in the benzylic carbon 2p orbital (117).

$$\sigma_\alpha^\bullet = 1 - \frac{hfc_X}{hfc_H}$$

[39]

This electron spin resonance (esr) approach has been

criticized by Jackson (118) who argued that the variation in

hfc over the range of substituents is too small to be

significant. However, while the variation in hfc over the

range of substituents is is only 10 percent, the magnitude

of the hfc can be determined to an accuracy of approximately

0.2 percent.

The $\sigma_\alpha^\bullet$ scale has several other advantages over other

kinetically derived free radical subtituent parameters: (1)

the measured effects are free from polar factors (other than

intrinsic polar effects); (2) since the radical is being

observed directly, any effects observed can be unambiguously

assigned to effects on the radical; (3) the radicals are

generated in an unambiguous manner and (4) the esr

parameters can be accurately determined.

The usefulness of the $\sigma_\alpha^\bullet$ scale depends upon the

Table 16. $\sigma_\alpha^\bullet$ values calculated from the α-H hyperfine coupling constants in substituted benzyl radicals[a].

Substituent	$\sigma_\alpha^\bullet$	Substituent	$\sigma_\alpha^\bullet$
4-SMe	0.063	4-Cl	0.011
4-COMe	0.060	4-i-Pr	0.009
4-SPh	0.058	4-t-Bu	0.008
4-COPh	0.055	4-S(O)$_2$Me	0.005
4-COOMe	0.043	3-Me	0.002
4-CN	0.040	4-OCOPh	0.000
4-SCOMe	0.029	H	0.000
4-OMe	0.018	3-OMe	-0.001
4-OPh	0.018	3-OPh	-0.002
4-S(O)Me	0.018	4-OCOMe	-0.005
4-S(O)$_2$Ph	0.018	3-Cl	-0.007
4-Si(Me)$_3$	0.017	3-F	-0.009
4-S(O)OMe	0.016	4-CF$_3$	-0.009
4-Me	0.015	4-F	-0.011
4-S(O)$_2$OMe	0.013	3-COOMe	-0.014
4-Et	0.012	3-CF$_3$	-0.017
		3-CN	-0.026

[a]Calculated from Equation 39.

reaction under study. Reactions with very large polar effects (e.g. the NBS bromination of substituted toluenes (119)) correlate very well with ionic substituent parameters. In these cases, the correlation with $\sigma_\alpha^\bullet$ is poor and, the extended Hammett treatment (including both ionic substituent parameters and $\sigma_\alpha^\bullet$) leads to no improvement of the correlation coefficient (r) compared to the simple treatment with ionic parameters alone.

Reactions with very small polar effects, on the other hand, (e.g. the rearrangement of substituted 2-aryl-3,3-dimethylmethylenecyclopropanes (119)) correlate very well

with $\sigma_\alpha^\cdot$. Correlation with ionic parameters is poor and, extended Hammett treatment leads to no improvement over the correlation with $\sigma_\alpha^\cdot$ alone.

More typically, however, there are reactions in which the polar effects and the intrinsic free radical effects are comparable and, in these cases (e.g. the NBS bromination of 4-substituted-3-cyanotoluenes (115e)) the best correlation is obtained with the extended Hammett treatment. In these systems, the relative ratios of $\rho^\cdot$ to ρ (where $\rho^\cdot$ is proportional to the senstivity of the activation free-energy to free radical effects and ρ is the sensitivity to ionic effects) reflects changes on the relative contributitions of free radical and ionic factors.

In the final analysis, the usefulness of the $\sigma_\alpha^\cdot$ scale will be decided only after it has been applied to many more reactions. However, the available esr data presents an opportunity to study the interactions of a substituent with a free radical. The purpose of this section is to assess the interactions of the para and meta substituents in the benzyl radical series. All of the esr spectra from the previous study (116) have been remeasured and fourteen new benzyl radicals have been added.

While the interactions of the substituents are important in general, there are two classes of substituents which are particularly interesting and these have been studied as Part III of this thesis. The alkyl substituents can delocalize spin density by hyperconjugation. The

151

assessment of hyperconjugation in radicals compared to hyperconjugation in cations is of fundemental interest. The sulphur containing substituents are also interesting since the role of the 3d orbitals on sulphur in the interaction with radicals is not clear.

Besides the measured esr parameters, molecular orbital methods are used to investigate the interactions of the substituents with the benzyl radicals. The adequacy of molecular orbital theory to interpret substituent effects on the measured hfc's of the benzyl radicals is determined and, some general concepts which are important to the interaction of substituents in these radicals are pointed out.

3.2 RESULTS

The benzyl radicals were generated in the esr cavity by hydrogen atom abstraction from the corresponding toluenes or by bromine atom abstraction from the benzyl bromides. The spectra were recorded using a signal averager and plotted with an X-Y recorder via a 12 bit D/A converter. The benzyl radical hyperfine coupling constants (hfc) are shown in Table 17. The hfc's were determined by initial measurement of the line positions from the signal averager and refined by computer simulation (120). The coupling constants are assigned to various positions on the basis of calculated spin densities and comparison to other spectra. For the meta substituted radicals the assignment of the aryl hydrogen hfc's are considered tentative since the three hfc's are typically within 1 G of each other. The uncertainty in the measured hfc's is believed to be ±0.03 G. For the meta substituted radicals the uncertainty in the aryl hydrogen hfc's is somewhat larger (±0.06 G), however, the uncertainty in the α-H hfc is still ±0.03 G.

Table 17. Benzyl Radical Hyperfine Coupling Constants[a].

X	a_1	a_2	a_3	a_4	a_5	a_6
4-SMe	15.23	5.08	1.73	0.90[b]	1.73	5.08
4-COMe	15.28	5.00	1.75	0.50[b]	1.75	5.00
4-SPh	15.30	5.03	1.85	–	1.85	5.03
4-COPh	15.35	4.98	1.76	–	1.76	4.98
4-COOMe	15.55	5.05	1.75	0.37[b]	1.75	5.05
4-CN	15.60	5.00	1.78	0.96[c]	1.78	5.00
4-SCOMe	15.77	5.03	1.81	–	1.81	5.03
4-S(O)Ph	15.83	5.10	1.80	–	1.80	5.10
4-OMe	15.95	5.02	1.60	0.75[b]	1.60	5.02
4-OPh	15.95	5.11	1.70	–	1.70	5.11
4-S(O)Me	15.95	5.03	1.75	0.35[b]	1.75	5.03
4-S(O$_2$)Ph	15.95	5.05	1.80	–	1.80	5.05
4-SiMe$_3$	15.97	5.03	1.71	–	1.71	5.03
4-S(O)OMe	15.99	5.07	1.73	–	1.73	5.07
4-Me	16.00	5.05	1.60	6.50[b]	1.60	5.05
4-S(O$_2$)OMe	16.04	5.03	1.71	–	1.71	5.03
4-Et	16.05	5.00	1.85	3.25[d]	1.85	5.00
4-Cl	16.07	5.24	1.75	0.50[e] 0.60[e]	1.75	5.24
4-i-Pr	16.10	5.10	1.80	2.85[f]	1.80	5.10
4-t-Bu	16.12	5.10	1.75	–	1.75	5.10
4-S(O$_2$)Me	16.17	5.09	1.78	1.05[b]	1.78	5.09
3,5-di-Me	16.19	5.20	3.35	6.08	3.35	5.20
3-Me	16.22	5.15	3.38[b]	6.15	1.75	5.00
4-OCOPh	16.25	5.22	1.80	–	1.80	5.22
H	16.25	5.10	1.70	6.13	1.70	5.10
3-OMe	16.27	5.30	–	6.30	1.65	4.50
3-OPh	16.29	5.15	–	6.15	1.75	5.00
4-OCOMe	16.33	5.27	1.80	–	1.80	5.27
3-Cl	16.37	5.15	–	6.33	1.83	5.05
3-F	16.39	5.15	4.72[g]	6.19	1.80	4.95
4-CF$_3$	16.39	5.19	1.76	6.88[h]	1.76	5.19
4-F	16.42	5.30	1.75	14.43[g]	1.75	5.30
3-COOMe	16.48	5.22	–	6.15	1.75	4.98
3-CF$_3$	16.53	5.18	3.30[h]	6.13	1.80	4.38
3-CN	16.68	5.25	0.30[c]	6.18	1.80	4.95

[a] Positions given in diagram below. X is the substituent. Values are believed to be accurate ±0.03 G.
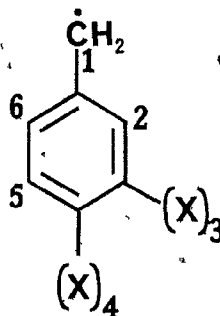[b] Hydrogen of CH_3.
[c] Nitrogen of CN.
[d] Hydrogen of ethyl.
[e] Cl.
[f] Hydrogen of isopropyl.
[g] F.
[h] Fluorine of CF_3.

3.3   DISCUSSION

3.3.1   Interaction of Substituents with a Free Radical

There are some general features of the $\sigma_\alpha^\bullet$ scale which can be pointed out. Most of the para substituents delocalize unpaired electron density more effectively compared with the unsubstituted radical. On the other hand, most of the meta substituents delocalize unpaired electron density less effectively than the unsubstituted radical. The effect of meta and para substitution can give valuable insight into the interaction of substituents with benzylic radicals.

Substituents in the para position can interact directly with the unpaired electron (Figure 30a). The substituents fall into two classes. Those with non-bonded lone pairs can interact with the unpaired electron by donating an electron (Figure 30b). In this case the substituent is a β-spin
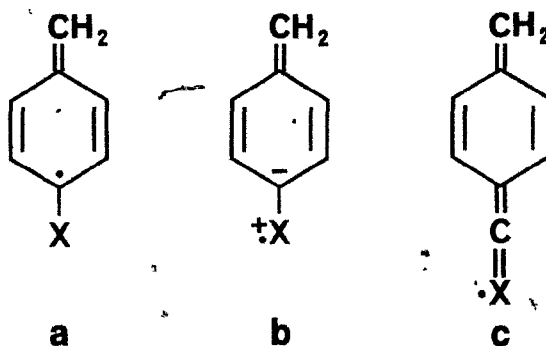

Figure 30.   Important valence bond contributors to the delocalization of spin. (a) delocalization to the para position, (b) β-spin donating substituent, (c) α-spin accepting substituent.

donor. Unsaturated substituents can interact with the unpaired electron by accepting an electron (Figure 30c). In this case the substituent is an α-spin acceptor. The orbital interactions can be represented using simple perturbation molecular orbital (PMO) theory (121). For the β-spin donating substituents, the orbital interactions are two-orbital three-electron interactions (122) and lead to a net one electron stabilization (Figure 31a). On the other hand, for the α-spin accepting substituents, the orbital interactions are three-electron three-orbital interactions and lead to a net two electron stabilization (122, Figure 31b).

From this simple treatment, some qualitative predictions can be made. For the β-spin donors, the stabilization energy will depend on the energy of the lone pair. As the energy separation between the interacting orbitals increases, the stabilization energy decreases (123). It is expected that the energy separation will increase as the ionization potential of the lone pair increases. This effect is equivalent to a decreasing contribution of the valence bond structure shown in Figure 30b. This rational leads to the correct prediction that the order of increasing delocalization of unpaired electron density in the benzyl radical series is -F < -Cl < -OR < -SR (Table 18).

Similarly, as the energy of the π orbitals of the α-spin acceptors decreases, spin delocalization in the
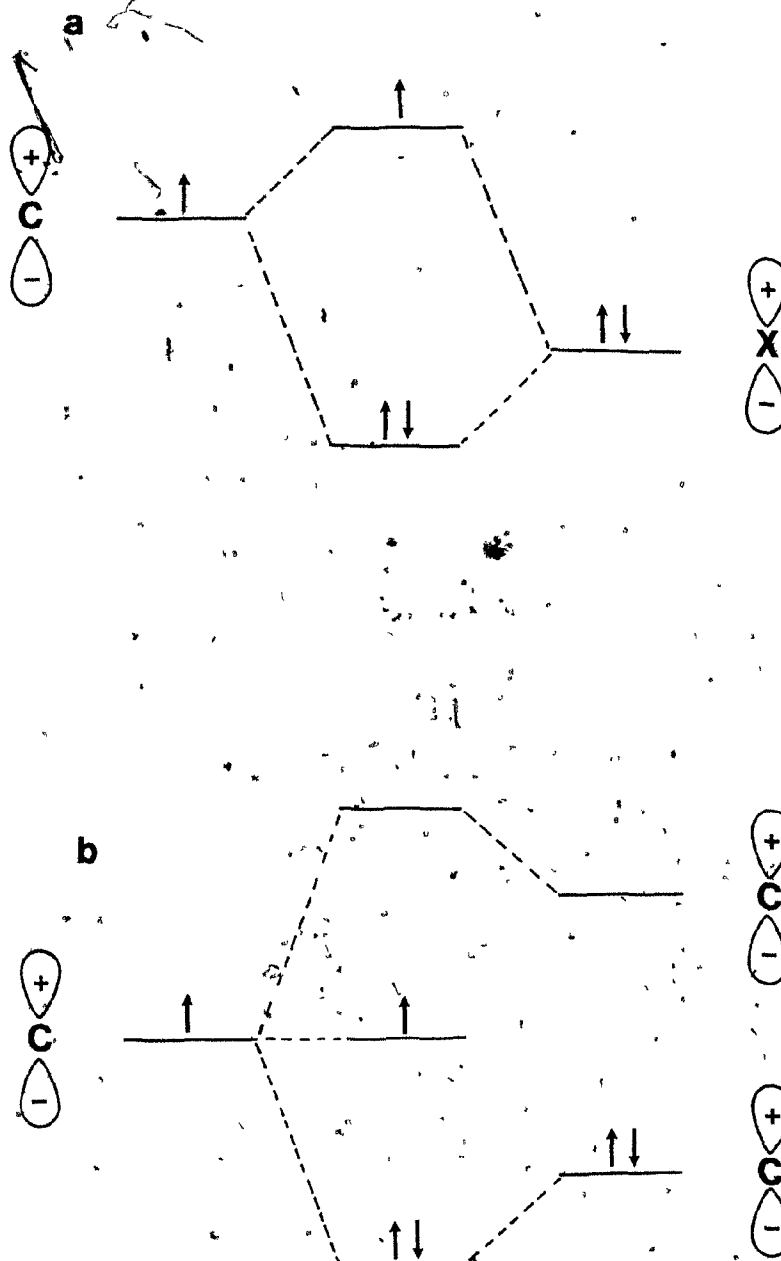
Figure 31. Molecular orbital interactions of a substituent with a radical: (a) β-spin donor and (b) α-spin acceptor.

Table 18. Ionization potentials of first-row and second-row hydrides[a].

Molecule	Ionization Potential (eV)
HF	15.77
HCl	12.80
H_2O	12.61
H_2S	10.48

[a]From reference 122.

benzyl radical also should decrease. This leads to the correct qualitative prediction that, for these substituents, unpaired electron density delocalization increases in the order, $-CF_3$ < CH_3 < $-CN$ < COR. The $4-CF_3$ and the $4-CH_3$ substituents can be α-spin acceptors by considering conjugation with a filled σ-orbital of the group as shown in Figure 32. In this case, the stabilizing effect will be much smaller since the energy separation between the interacting orbitals is expected to be much greater (124).
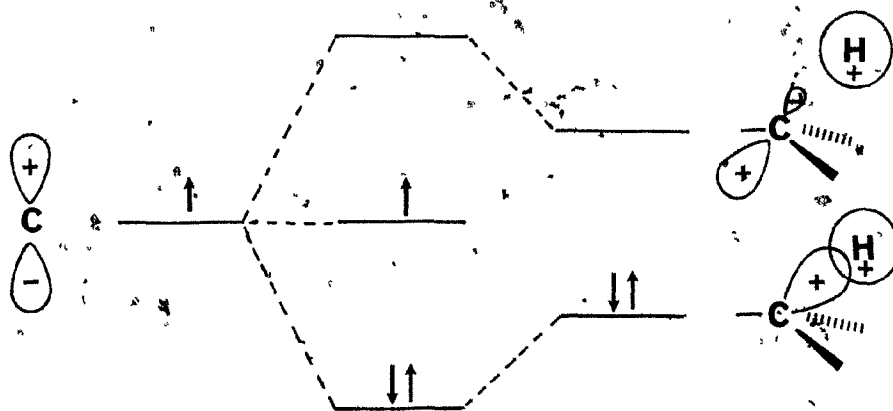

Figure 32. The interaction of a methyl group with a radical.

This approach assumes that hydrogen as a substituent has no stabilizing effect. As a result, the relative stabilization of the benzyl radical of a _para_ substituent can be predicted but, it is impossible to predict _a priori_ where hydrogen will fit in the series. Furthermore, it is not possible to rank the relative effect of the α-spin acceptors against the β-spin donors. The key omission in this approach is that only effects on the π-framework are considered; effects on unpaired electron delocalization through the σ-framework are ignored. Furthermore, since electron correlation effects are important for the transmission of spin from the π-framework to the σ-framework, it is not possible to predict what this effect will be . Since the _meta_ substituents do not interact appreciably with the π-system, these substituted radicals can be used to assess the effect of substitution on delocalization in the σ-framework.

The interaction of _meta_ substituents in the benzyl radical series may be straightforward. Correlation of the α-H hfc's with σ_m, in fact, gives a slope of 0.6 and a correlation coeffient (r) of 0.927 with the ten points (Figure 33). The correlation of _meta_ substituted derivatives with also was noted by Creary (119b) from his study of the 2-aryl-3,3-dimethylmethylenecyclopropanes and was related to the electrophilic nature of the radical. The decreased delocalization by inductive withdrawl of electrons will not be unique to the _meta_ substituents. The three _para_
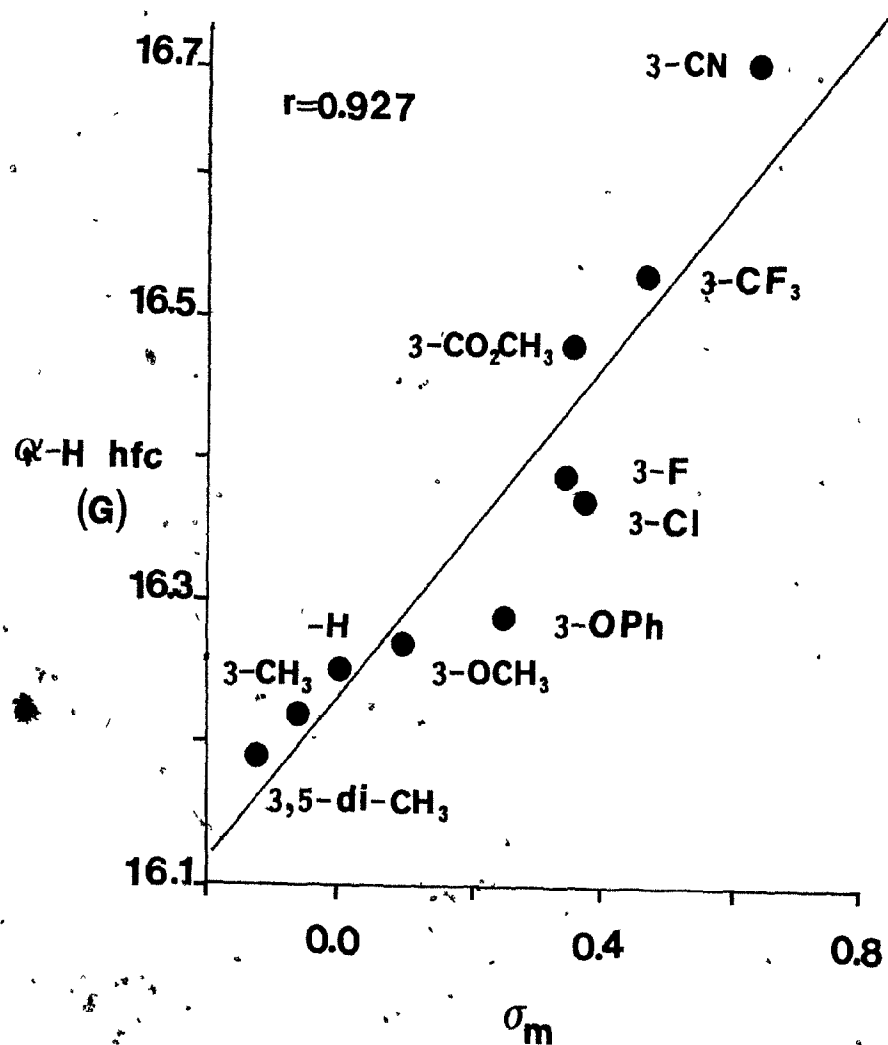
Figure 33. α-H hfc versus σ_m for the meta-substituted benzyl radicals.

substituents which lead to decreased delocalization
(relative to the unsubstituted radical) are inductively
withdrawing substituents (the σ_p values for 4-CF$_3$, 4-F and
4-OCOMe are 0.53, 0.15, and 0.31 respectively (111)).
Certainly in the case of 4-F and 4-CF$_3$ delocalization from
the π-framework is expected to be small (125) so, in these
cases, it appears that decreased delocalization of the
unpaired electron density may also be related to the
inductive withdrawl of electrons. The decrease in
delocalization of unpaired electron density as the
substituent becomes more electron withdrawing in nature
should not come as a complete surprise. The electrophilic
nature of many radicals is well known (126) and, while this
has often been considered to be a transition state polar
effect (127), it is not unreasonable that the benzyl radical
can be intrinsically electrophilic. If, according to the
McConnell equation (117), the α-H hfc is proportional to
the spin density in the benzyl 2p orbital, then the
inductive withdrawl of electrons in this system must lead to
a net withdrawl of β-charge density from the π-system.

The effect of perturbation of the σ-framework on the
π-spin distribution in benzyl radicals cannot be predicted.
The decreased delocalization by _meta_ substituents is
predicted by HMO and INDO calculations (_vide infra_) but even
ab initio calculations fail to predict the decreased
delocalization in the 4-fluorobenzyl radical (128).

3.3.2 Molecular Orbital Considerations

Two levels of theory have been used to investigate the effects of substitution on delocalization in benzyl radicals. Huckel molecular orbital (HMO) theory (129) uses a simple π-basis set and, therefore, gives very qualitative information about the effects on bonding in the π-system. The most useful parameter from these calculations is the free valence index which is a measure of bond order (130). A useful approximation is that the free valence index is proportional to spin delocalization in the π-system; i.e. as the free valence index decreases, the bond order increases and, it is expected that the higher bond order will reflect greater delocalization. A plot of the free valence index versus the α-H hfc's of the benzyl radicals (Figure 34) gives a reasonable correlation; certainly, the trend is clear (the correlation coefficient, r, is 0.937 for the 14 points). The important features of the results are: (1) the α-spin acceptors in the para position have the smallest free valence index, (2) the β-spin donors in the para position have a free valence index smaller than the unsubstituted radical, and (3) none of the meta substituted radicals have a free valence index less than that of the unsubstituted radical. The magnitude of the meta effect is greatly underestimated by this method, however, it is encouraging that the effect is in the right direction.

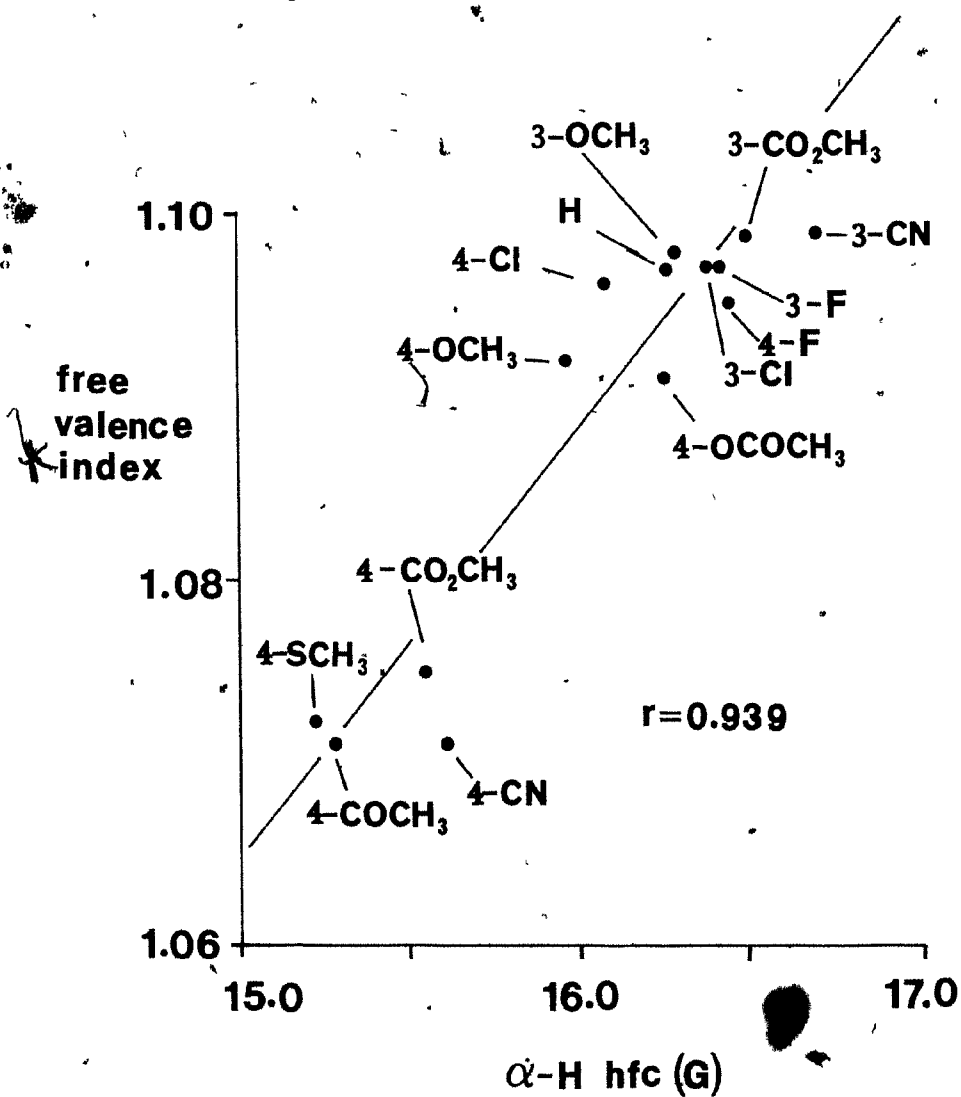Semi-empirical methods may be more useful since in

Figure 34. Free valence index at the benzylic position
versus the a-H hfc.

163

these calculations all of the valence electrons on each
nucleus are considered. The intermediate neglect of
differential overlap (INDO) method is an SCF procedure but,
it avoids the evaluation of many of the difficult two-
electron integrals. Instead, some experimental results are
used to normalize (or parameterize) the calculated
observable properties. This method is useful for
interpreting correlations in experimental data (74a).

The calculated hfc's for several meta and para
substituted benzyl radicals are shown in Table 19. The
ratio of the experimental hfc to the calculated hfc is
approximately constant for most of the radicals. It is
clear, however, that the spin distribution in the benzyl
radical is not adequately reproduced for quantitative
evaluation of the effects. As in the HMO calculations, the
general trends are reproduced. Again, the meta effect is
underestimated and the decreased delocalization in the 4-
fluorobenzyl radical is not predicted. With this semi-
empirical method it is not necessary to have a p orbital on
the substituent in order to increase delocalization. The
para alkyl substituents, however, all have the same -H
hfc. It may still be possible, however, to assess the
importance of hyperconjugation (131) in these radicals from
the INDO calculations (vide infra).

Other semi-empirical calculations on substituted benzyl
radicals have been reported (132). The results of all of
the semi-empirical methods, in general, do not agree with

164

Table 19. Calculated (INDO) hyperfine coupling constants for some substituted benzyl radicals[a].

Substituent	a_1	a_2	a_3	a_4	a_5	a_6
4-CN	-16.73 (0.932)	-6.52 (0.767)	3.98 (0.447)	1.22 (0.786)	3.98 (0.447)	-6.52 (0.767)
4-Me	-16.86 (0.949)	-6.43 (0.790)	3.67 (0.436)	7.18 (0.905)	3.67 (0.436)	-6.43 (0.790)
4-Et	-16.86 (0.952)	-6.38 (0.783)	3.66 (0.505)	b	3.66 (0.505)	-6.38 (0.783)
4-i-Pr	-16.86 (0.954)	-6.39 (0.798)	3.70 (0.486)	b	3.70 (0.486)	-6.39 (0.798)
4-t-Bu	-16.86 (0.956)	-6.38 (0.799)	3.72 (0.470)	b	3.72 (0.470)	-6.38 (0.799)
4-F	-16.92 (0.970)	-6.51 (0.814)	3.63 (0.482)	13.43 (1.074)	3.63 (0.482)	-6.51 (0.814)
3-Me	-17.00 (0.954)	-6.55 (0.786)	-3.74 (0.904)	-5.75 (1.070)	3.64 (0.481)	-6.51 (0.768)
H	-17.01 (0.955)	-6.43 (0.793)	3.61 (0.471)	-5.63 (1.089)	3.61 (0.471)	-6.43 (0.793)
3-F	-17.03 (0.962)	-6.45 (0.767)	-7.70 (0.613)	-5.56 (1.113)	3.69 (0.488)	-6.51 (0.791)
3-CN	-17.05 (0.978)	-6.84 (0.767)	-1.72 (0.417)	-5.94 (1.040)	3.78 (0.476)	-6.65 (0.744)

[a]The ratio of the experimental hfc to the calculated hfc is in parentheses.

[b]These hfc'c depends on the preferred conformation of the C-H bond with respect to the aryl ring.

experimental results. The relative changes upon substitution show a general trend, but, these methods will be of limited value for the development of a microscopic theory to describe all of the observed effects. The fact that HMO theory gives the same qualitative results as INDO MO theory suggest that (as expected) the π-effects are the dominant interactions which determine the extent of delocalization of the unpaired electron. The interactions between the σ- and the π- systems are too complicated for most levels of molecular orbital theory, and determining the equilibrium geometries, even at the INDO MO level, would not be feasible on most computing systems. However, these factors must play an important role in determining the spin distributions in the benzyl radicals.

3.3.3 Hyperconjugative Effects

The variation in carbocation stability as a function of the degree of branching of an adjacent alkyl group has received much attention (133) over a period extending back more than fifty years, to the original proposal of hyperconjugation involving an adjacent C-H bond (134). Unambiguous evidence for hyperconjugation has been difficult to obtain. The problem is assessing the relative contributions of steric and electronic (both inductive and hyperconjugative) factors from relative rate data (135). In addition, the adjacent C-C bond can participate in hyperconjugative interactions. Brown and his coworkers

166

addressed this problem in their study of the rates of solvolysis of alkyl substituted cumylchlorides (136). In this work the relative contribution of inductive donation by the alkyl group was estimated from the rate of solvolysis of the _meta_ substituted compounds. On this basis it·was found that hyperconjugation to each C-C bond is approximately 80 percent of the effect to C-H bonds.

Although there is good evidence that hyperconjugative effects contribute to the delocalization of free radicals (137), essentially nothing is known about the effect of variation of alkyl branching on the hyperconjugative interactions in these species. .This void of fundamental knowledge may be a result of the justifiable realization that the effect of adjacent alkyl branching on the rate of most radical reactions will be small; too small perhaps to be accurately measured by kinetic methods and, probably complicated by steric or transtion state polar effects. For example, in the 2-aryl-3,3-dimethylmethylenecyclopropane rearrangements (for which the polar effect will be small) the rates of reaction of the 4-methyl and the 4-_tert_-butyl derivatives are within 5 percent of each other (119b). Nevertheless, there is a need to define and understand the effect of branching on the delocalization of an unpaired electron.

The study of the alkyl substituted benzyl radicals offers an opportunity to evaluate this effect in a system free from steric and polar effects. All of these radicals

have α-H hfc's less than that of the unsubstituted benzyl radical. This is indicative of the ability of a para-alkyl group to delocalize spin density from the aryl ring. The 4-methyl substituent, which has the greatest effect of the alkyl substituents, decreases the α-H hfc to an extent almost as large as that of a 4-methoxy substituent Table 17).

Of course, this delocalization includes both inductive and hyperconjugative effects. The inductive effect can be estimated from the α-H hfc of the 3-methylbenzyl radical. In this case the effect is small, but inductive donation by a methyl group appears to increase delocalization. Although the esr spectrum of the 3-tert-butylbenzyl radical has not been measured, the effect of the meta-methyl substituent is so small that the α-H hfc for the 3-tert-butylbenzyl radical is expected to be close (within experimental error) to that value for the 3-methylbenzyl radical. Since inductive effects are very similar in the meta and para positions (138), an inductive delocalization amounting to 0.03 G is estimated for all of the alkyl substituted benzyl radicals. Therefore, the extra delocalization by methyl, which is attributed to hyperconjugation, amounts to 0.22 G and, for the tert-butyl group 0.10 G (both with an error limit of 0.04 G). This means that hyperconjugation to a C-C bond in a radical is approximately 55 percent of hyperconjugation to a C-H bond. .

While the variation between the individual members of

the series (Table 17) is not large, the overall difference between the 4-methylbenzyl and the 4-tert-butylbenzyl radical is significantly greater than the experimental error. When the spectra are directly compared, the order of increasing α-H hfc is -Me < -Et < -i-Pr ≤ -t-Bu. However, since the differences are so small, the error in the estimate of the contribution of the C-C and the C-H bonds to hyperconjugation is quite large (±20 percent).

The extent of hyperconjugation involving the C-H bond is indicated by additional coupling to the substituent. While the barrier to rotation of the alkyl groups is undoubtedly low, there will be preferred conformations which minimize the steric repulsions between the β-methyl groups and the meta hydrogens on the aryl ring (139). Maximum hyperconjugation requires the C-H bond to be parallel to the aryl carbon 2p orbital. The conformational dependence on hyperconjugation of the C-H bond with respect to the plane of the aryl ring follows a $\sin^2\theta$ relationship (140, Equation 40) where θ is the dihedral angle between the C-H bond and the plane of the ring.

$$\beta\text{-hfc} = B_0 + B_1\sin^2(\theta)\qquad\qquad [40]$$

From the INDO calculations, the values of B_0 and B_1 are constant for all of the alkyl substituents, with values of 0.5±0.1 and 13.5±0.2 respectively. It has been found that

for an ethylaryl system, the low energy conformer has the methyl group perpendicular to the plane of the ring ($\theta = 30$ degrees) and the high energy conformer has the methyl in the plane of the ring ($\theta = 60$ degrees). Conversely, for an isopropylaryl system, the low energy and high energy conformers occur at $\theta = 0$ degrees and $\theta = 90$ degrees respectively (139). Since the barriers to rotation are low (< 2 kcal mol^{-1}), the alkyl groups do not adopt exclusively one conformation; however, the Boltzmann distribution of conformers is affected.

The rotational barriers of alkyl groups in free radicals can be calculated from the measured α-H hfc and the $\sin^2\theta$ relationship (139). For the nitroethane and the 2-nitropropane radical anions, rotational barriers of approximately 1.4 kcal mol^{-1} have been determined in this way (141). The hfc associated with the alkyl substituent in the benzyl radical series shows qualitatively similar results.

.It is possible to assess the relative importance of C–C and C–H hyperconjugation in the benzyl radicals from the INDO calculations since this effect is due to interactions with the π-system. The calculated spin densities on the carbon atoms of the tert-butyl group of 4-tert-butylbenzyl radical and on the hydrogens of the methyl group of the 4-methylbenzyl radical are shown in Table 20. The contribution from the spin polarization mechanism for transmission of spin (137,74a) is estimated from the spin

density on the atom at $\theta = 0$ since there is no contribution from hyperconjugation in this conformation. Subtraction of this value from the calculated spin density at each β-atom will give an indication of the degree of hyperconjugative interaction of the alkyl group. It is found that for the 4-methybenzyl radical the contribution of hyperconjugation is about 96 percent of the total spin delocalization while for the 4-tert-butylbenzyl radical the contribution of hyperconjugation is 93 percent. These results can be compared to those for the ethyl radical (INDO) where it is found that 93 percent of spin delocalization is

Table 20. Hyperconjugative interactions of C-H and C-C bonds.

| | Spin Density on the β-Atom | | |
(degrees)	H^a	C^b	ratio[c]
0.0	0.0011	0.0011	–
30.0	0.0072	0.0052	0.67
60.0	0.0193	0.0127	0.64
90.0	0.0255	0.0163	0.62

[a]Hydrogens of the methyl group in 4-methylbenzyl radical.

[b]Carbons of the tert-butyl group in 4-tert-butylbenzyl radical.

[c]Calculated by subtracting the spin density from the spin polarization mechanism ($\theta = 0$) from the spin density on the atom. The ratio of the difference is an estimate of the relative contribution of hyperconjugation.

171

hyperconjugative (74a). The results in Table 20 also show that C-C hyperconjugation is about 65 percent of C-H hyperconjugation. This result compares favourably with the results determined experimentally from the esr spectra.

3.3.4 The Effect of Sulphur Substituents

In general, it is found that the order of delocalization of spin density by the sulphur containing substituents is: -SR > -S(O)R > -S(O$_2$)R (142,143). The effect of R depends on the oxidation state of the sulphur.

In the case of the sulphide, the 4-methylthio substituent delocalizes spin more effectively than the 4-tolylthio group (144). This order is reversed for the corresponding sulphinyl and sulphonyl groups. Furthermore, the difference in α-H hfc for the 4-methylthio- and the 4-tolylthiobenzyl, the 4-methylsulphinyl- and 4-tolylsulphinylbenzyl and the 4-methylsulphonyl- and 4-tolylsulphonylbenzyl radicals increases as the oxidation state increases (these differences are -0.07 G, 0.12 G and 0.22 G respectively, Table 17). Any explanation of the interaction of the sulphur containing substituents with the benzyl radical must rationalize both the direction and magnitude of these trends.

It is useful to review briefly the effects of sulphur containing substituents in ionic reactions. The Hammett σ values for some sulphur containing substituents (145,142a) are shown in Table 21. The electron-withdrawing ability of

Table 21. Hammett σ constants for several sulphur containing substituents.

Substituent	σ	Reference
4-SMe	-0.047	145a
4-SPh	0.075	145a
4-S(O)Me	0.48	145b
4-S(O)Ph	0.47	145a
4-S(O$_2$)Me	0.72	145a
4-S(O$_2$)Ph	0.70	145a

the substituent increases as the oxidation state increases.

Sulphide may act as an electron-donating group (146) or an electron-withdrawing group (147) depending on the electron demand of the aryl or alkyl group to which it is bound. The electron-donating ability of the 4-methylthio substituent is indicated by the σ^+ value (146) ($\sigma^+ = -0.60$). The ability of sulphide to act as both an acceptor or a donor has been explained by molecular orbital theory (148). Bernardi, Wolfe and their coworkers have suggested that, relative to oxygen, sulphur forms a stronger π-bond to an adjacent cationic centre (148d). The ability of sulphur to stabilize an adjacent carbanion has been rationalized in terms of polarizability (148c) and hyperconjugation (148a).

Sulphinyl and sulphonyl groups are electron-withdrawing groups. The degree to which 3d orbitals are involved in the

173

stabilization of adjacent carbanions has been a subject of controversy (142c); however, there is convincing evidence that 3d-orbitals can interact in the sulphone. Ramasamy and coworkers (149) found, from a study of angular correlation of positron annihilation radiation, that a well-marked increase in the region of d-orbital radial momentum is observed for arylalkyl sulphones. Such an increase was not found for sulphides. Work by Wolfe and coworkers (150) also has suggested that the role of d-orbitals in α-sulphinyl and α-sulphonyl carbanions may be more important than previously believed.

The trends observed from the esr parameters of the substituted benzyl radicals are similar to those observed for the analogous methyl radicals (Tables 17 and 22).

Table 22. Hyperfine coupling constants for some substituted methyl radicals $(XCH_2 \cdot)$.[a]

X	α-H hfc (G)	γ-H hfc (G)
-SMe	16.5	3.6
-S(O)Me	20.0	—
-S(O_2)Me	22.3	2.1
-H	22.9	—

[a]Reference 143.

174

Delocalization by -SR

The delocalization of a free radical by an adjacent
sulphide group has been studied by esr spectroscopy
(143,151) and molecular orbital theory (122). The observed
rotational barriers for XCH_2 radicals (where X=OMe,SMe)
suggest that the π-bond formed for X=SMe is stronger than
that for X=OMe. This result has been rationalized by
Bernardi, Epiotis, Wolfe and their coworkers (122) who
suggest that the two orbital three electron interaction
(Figure 35b) is more important than the 3d orbital effects.
This greater stabilization by sulphur is thought to be a
consequence of the lower lone pair ionization potential
(Table 18) and, hence, the greater polarizability, of the
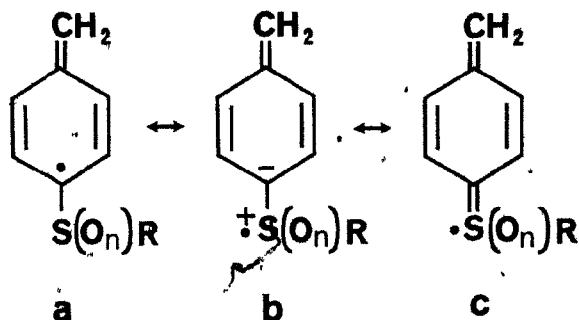sulphur relative to oxygen.

Figure 35. The delocalization of a radical by an adjacent
sulphur substituent; (a) localized spin in aryl
ring, (b) sulphur as a β-spin donor and, (c)
sulphur as an α-spin acceptor.

The 4-tolylthiobenzyl radical has a larger α-H hfc than that value for the 4-methylthiobenzyl radical. Hudson and coworkers (151a), on the other hand, found that in the analogous methyl radicals the α-H hfc for the phenylthiomethyl radical was smaller than that for the methylthiomethyl radical. In the case of the benzyl radicals the observed effect may be due to cross-conjugation in the 4-tolylthio derivative. If it is assumed that delocalization by sulphide groups are a result of sulphur acting as a β-spin donor (Figure 35b), then, cross-conjugation by an aryl ring would in effect reduce the electron density available to stabilize the radical centre (i.e. increase the ionization potential). Further support for this reasoning may be found. The α-H hfc is larger in the 4-thiolacetylbenzyl radical than that in the 4-tolylthiobenzyl radical. This is consistent with the above explanation. The lone pair on sulphur will be conjugated more effectively to acetyl than to tolyl. Clearly, if the sulphide group participated predominantly as an α-spin acceptor (Figure 35c) (i.e. if conjugation through the sulphur were possible) the effect would be in the opposite direction (152). Similarly, it is found that the α-H hfc for 4-methoxybenzyl radical is the same as that for 4-phenoxybenzyl radical. On the other hand, the 4-acetoxybenzyl radical actually is less delocalizing relative to the unsubstituted radical. This, again, may be rationalized in terms of cross-conjugation. The decrease in

the contribution of the two-electron two-orbital interaction allows the effect of inductive withdrawl to be observed (vide supra). The inability of 4-phenoxy to effectively participate in cross-conjugation is consistent with the small effect found for the sulphide as well as the decreased polarizability of the oxygen.

Delocalization by -S(O)R

It is evident from the α-H hfc's that the 4-methylsulphinyl group is less delocalizing than the 4-methylthio group (Table 17). This trend was also observed in the methyl radical series (143) (Table 22). The sulphinyl group is still able to participate in the two-orbital three- electron delocalization (Figure 35b) since it has one lone pair of electrons. The delocalizing effect is less than it is for the corresponding sulphide since the electronegative ligand will contract the orbital containing the lone pair (149). There is some spectroscopic evidence that the methylsulphinyl group can be a net resonance donor; however, if the methylsulphinyl group is para to a strong donating group, it can become a resonance acceptor (153).

In the delocalization of a benzyl radical by a sulphinyl group, does the sulphinyl group act as a net donor or a net acceptor? The the hyperfine coupling constant assigned to the substituent methyl group is much less for the 4-methylsulphinylbenzyl radical than those values for

177

either the 4-methylthiobenzyl radical or the 4-methylsulphonylbenzyl radical. It has been suggested that the coupling to the methyl group in the methylthiomethyl radical is a result of hyperconjugative interactions with the spin on sulphur, while coupling in the methylsulphonylmethyl radical is a result of spin polarization (143). The hyperconjugative mechanism results in positive spin density while spin polarization leads to negative spin density in the methyl group. In the case of the methylsulphinylmethyl radical, the smaller value for a_x reflects contributions from both of these mechanisms. This trend is also observed in the analogous benzyl radicals so a similar explanation may be offered. However, since only the magnitude of the hyperfine coupling constant is known and not the sign, it is still impossible to determine from this evidence if the sulphinyl group is a net β-spin donor or a net α-spin acceptor.

Replacement of the substituent methyl group with tolyl leads to a decrease in the α-H hfc. It is tempting to conclude from this evidence that the sulphinyl group is a net α-spin acceptor since the cross-conjugative effect found in the sulphide derivative is not observed. However, the delocalization offered by the sulphur accepting spin density is far less than that observed in the 4-methylsulphinylbenzyl radical (vide infra). Replacement of the methyl group by tolyl can have two opposing effects. The first, which causes a decrease in delocalization of spin

178

density, is cross-conjugation which has already been discussed. The second effect, which leads to an increase in delocalization of spin density may be a result of further stabilization of the MO which is accepting the spin. It is possible that the 3d orbitals on sulphur, which contract in the presence of the highly electronegative oxygen, contribute. Since cross-conjugation will be less effective than in the sulphide (the lone pair is also contracted) it is not surprising that the stabilization of the MO which is accepting spin is comparatively more important. Hence, the sulphinyl group is a net spin donor.

Delocalization by $-S(O_2)R$

Since the sulphur in the 4-methylsulphonylbenzyl radical has no lone pairs, delocalization of a free radical is only possible with sulphur as an α-spin acceptor. Even though the 3d orbitals are contracted to a greater extent than those in the 4-methylsulphinylbenzyl radical very little delocalization results (the α-H hfc is only 16.17 G). Under the most favourable conditions for 3d orbital interaction, extra delocalization, compared to the unsubstituted radical, only amounts to an effect of 0.08 G (compared to 1.02 G for the corresponding sulphide where lone pair interactions dominate). The conclusion that the 4-methylsulphinyl group is a net β-spin donor, therefore, seems reasonable. The extra delocalization gained when the methyl group is replaced by tolyl (or phenyl) is almost

twice as large as that found in the sulphinyl derivative.
This serves to reinforce the idea that the tolyl group
interacts to further stabilize the MO which is accepting the
spin density since the interaction with the more highly
contracted 3d orbitals should be more effective.

Delocalization by -S(O)OMe and -S(O_2)OMe

While it is found that the 4-methylsulphinate group is
less delocalizing than the 4-methylsulphinyl group, the
corresponding 4-methylsulphonate group is more delocalizing
than the 4-methylsulphonyl group. Again, these trends may
be rationalized using the simple concepts outlined above.
The 4-methylsulphinate group will be more delocalizing than
the isomeric 4-methylsulphonyl group since the former has a
lone pair of electrons on the sulphur. Since the 4-
methylsulphinyl group is a net β-spin donor, the
replacement of methyl with methoxy will further contract the
lone pair. This less polarizable lone pair leads to the
effect observed.

The 4-methylsulphonate group is somewhat different.
Since the sulphur has no lone pairs, the effect of the third
oxygen is to further contract the 3d orbitals. Rather than
becoming a less effective β-spin donor (as in the 4-
methylsulphinate group), the 4-methylsulphonate group
becomes a more effective α-spin acceptor.

It is more difficult to interpret the effects of the substituents on the observed esr parameters for the methyl radicals since the substituents may induce changes in conformation at the radical centre. In addition, the possibility of through space interactions cannot be precluded. One of the advantages of studying the esr parameters of the benzyl radicals is that the substituent, undoubtedly, will have a negligible effect on the conformation of the benzylic carbon. Therefore, the α-H hfc's of the benzyl radicals should not correlate with the α-H hfc's of the methyl radicals. However, there is a trend at least, for the four substituents in Table 22. There are also obvious differences.

The strong carbon-sulphur π-bond in the methylthiomethyl radical leads to restricted internal rotation at temperatures as high as -20 C (151a). There is no evidence for restricted internal rotation in the 4-methylthiobenzyl radical at -30 C (the two _meta_ hydrogens still appear to be equivalent).

3.4 CONCLUSIONS

Substituents in the _pará_ position of a benzylic radical will generally increase delocalization of the unpaired electron density relative to the unsubstituted radical. The two important interactions of substituents with the radical are two-orbital, three-electron interactions (for substituents with a non-bonding lone pair of electrons) and

three-orbital, three-electron interactions (for substituents which are unsaturated). The three-orbital, three-electron interactions are normally more effective than the two-orbital, three-electron interactions since the former lead to a net two-electron stabilization while the latter leads to only a net one-electron stabilization.

The meta substituted benzylic radicals will generally decrease the delocalization of unpaired electron density. This effect is interpreted as an inductive effect, primarily on the σ-framework and is related to an intrinsic electrophilicity of the benzyl radical system. The decrease in spin delocalization relative to the unsubstituted radical by inductive withdrawl of electrons is observed with para substituents which do not interact effectively with the π-system.

The alkyl substituents can increase delocalization by hyperconjugative interactions. The α-H hfc's for these substituent indicate that hyperconjugation to a C-C bond of the alkyl group is approximately 55 percent as effective as hyperconjugation to a C-H bond. INDO calculations agree with this result.

The delocalizing effects of sulphur containing substituents on benzyl radicals are easily rationalized. A group such as 4-SR is a net β-spin donor. If R is an electronegative group or a conjugating group then delocalization of spin density relative to 4-SMe is decreased as a result of decreased polarizability of the

182

lone pairs or cross-conjugation.

A group such as 4-S(O)R may be a β-spin donor and an α-spin acceptor. When R is an electronegative group delocalization of spin density relative to 4-S(O)Me decreases as a result of the decreased polarizability of the lone pair. On the other hand, when R is a conjugating group delocalization relative to 4-S(O)Me increases as a result of enhanced stabilization of the MO accepting the spin density.

A group such as $4-S(O_2)R$ is a net α-spin acceptor. If R is an electronegative group or a conjugating group then delocalization of spin density relative to $4-S(O_2)Me$ increases as a result of 3d orbital contraction or enhanced stabilization of the accepting MO.

The interpretation of the substituent effects on spin delocalization by MO theory met with only limited success. While the general trends are reproduced, more quantitative agreement is not obtained. One problem with this approach is that model geometries must be used since it is not feasible to optimize each structure. Furthermore, the effects of electron correlation on the spin distribution in these systems is another important factor which is not considered in these calculations.

3.5 EXPERIMENTAL

3.5.1 General Information

Esr spectra were recorded on a Varian Associates E109B electron paramagnetic resonance spectrometer equipped with a liquid nitrogen variable temperature accessory. All spectra were recorded with the aid of the Nicolet 1170 signal averager. Typically 16 spectra were averaged (2 minutes per spectrum). Coupling constants were measured directly from the oscilloscope and refined by computer simulation (120) using the IBM-PC. All spectra were reproducible within the experimental error. The estimated uncertainty of 0.03 G is the limit of resolution of the recording device used to plot the experimental spectra and the simulations. [1]Hmr spectra were recorded on a Varian T-60 spectrometer and are reported in parts per million downfield from TMS. Infra red spectra were recorded on a Pye Unicam SP1000 infra red spectrometer and are reported in wavenumbers. Melting points were recorded on a Sybron Corporation Thermodyne hotstage (uncorrected).

3.5.2 Materials

Di-tert-butyl peroxide (DTBP) and triethylsilane were obtained from Pfaltz and Bauer Inc. and were used without further purification. Hexamethylditin was obtained from Alpha Products and used without further purification. 4-

184

Methoxyacetophenone (PMA) was obtained from Aldrich Chemical Company Inc. and was recrystallized twice from 95% ethanol prior to use. Chlorobenzene (J. T. Baker Chemicals Inc.) was stirred over concentrated sulphuric acid, washed successively with water, saturated sodium bicarbonate and water, dried over anhydrous magnesium sulphate and distilled through a Vigreux column.

3.5.3 Prepartion of Benzyl Bromides

The method of Grice and Owen (155) was used for the conversion of substituted benzyl alcohols to the bromides. Typically, the benzyl alcohol (0.02 mol) was dissolved in benzene (100 mL). Hydrogen bromide gas was passed through the solution, for 1 hour or until the solution was saturated. The reactants were heated to reflux and the water which formed was removed via a Dean-Stark trap. The solution was then dried over anhydrous magnesium sulphate, filtered and the solvent removed at reduced pressure. The bromide was then purified by sublimation.

4-Ethylbenzylbromide

4-Ethybenzyl alcohol (2.0g, 0.015 mole, Aldrich) was dissolved in benzene (100 mL). The solution was then saturated with anhydrous hydrogen bromide (1 hour) and the resulting solution was refluxed for 1 hour with a Dean-Stark trap. The solution was dried over anhydrous magnesium sulphate, filtered and the solvent was removed under reduced

pressure. The product was purified by vacuum distillation (88 C at 1 torr) to give 2 g (70 percent) of the bromide (156). ^{1}Hmr (CDCl$_3$): 7.18 (m, 4H), 3.80 (s, 2H), 2.65 (q, 2H), 1.23 (t, 3H).

4-(2-Propyl)benzylbromide

The 4-(2-Propyl)benzyl alcohol (3.0g, 0.020 mole, Aldrich) was dissolved in benzene (100 mL). The solution was then saturated with anhydrous·hydrogen bromide (1 hour) and refluxed for 1 hour with a Dean-Stark trap. The solution was dried over anhydrous magnesium sulphate, filtered, and the solvent was removed under reduced pressure. The product was purified by vacuum distillation (62 C at 0.02 torr) to give 3.1 g (73 percent) of the bromide (157). ^{1}Hmr (CDCl$_3$): 7.17 (m, 4H), 4.38 (s, 2H), 2.87 (m, 1H), 1.22 (d, 6H).

4-(Methylthio)benzylbromide

The benzyl alcohol (3.0 g, 0.02 mol, Aldrich) was dissolved in benzene (100 mL). This solution was then saturated with anhydrous hydrogen bromide (1 hour) and the resulting solution refluxed for 1 hour with a Dean-Stark trap. The solution was then dried over anhydrous magnesium sulphate, filtered and the solvent was removed at reduced pressure. The bromide was purified by vacuum sublimation (40 C, 0.1 Torr) to give colourless crystals. The yield was 2.8 g, 65%. (mp 43-44 C, lit. 44 C) (155). ^{1}Hmr (CDCl$_3$):

186

7.21 (s,4H), 4.43 (s,2H), 2.45 (s,3H).

4-(Bromomethyl)phenyl methylsulphone

4-(Methylthio)benzylalcohol (3.0 g, 0.02 mol) was dissolved in dichloromethane (100 mL). To this solution, at 0 C, 3-chloroperbenzoic acid (8.0 g, 0.045 mol) in dichloromethane (50 mL) was added dropwise over 30 minutes. The mixture was stirred for 18 hours, filtered, washed successively with 5% sodium hydroxide and water then dried over anhydrous magnesium sulphate. Evapouration of the solvent at reduced pressure gave 2.4 g of the benzyl alcohol (67%).

The benzyl alcohol (2.4 g, 0.013 mol) was dissolved in benzene (100 mL) and the solution was saturated with anhydrous hydrogen bromide. The resulting solution was refluxed under a Dean-Stark trap (2 hours), dried with anhydrous magnesium sulphate and the solvent evapourated at reduced pressure. The crude bromide was purified by sublimation (120 C, 0.1 Torr) to give colourless crystals. The yield was 2.0 g, 62%. (mp 94-96 C; lit. 95-95.8 C) (158). ir (CHCL$_3$) cm 1155(s), 1322(s); ^{1}Hmr (CDCl$_3$): 7.82 (m,4H), 4.53 (s,2H), 3.07 (s,3H).

3.5.4 Preparation of Substituted Toluenes

Most of the toluenes are available commercially (Aldrich). The preparation of some of the toluenes have been described previously (116).

4,4'-Dimethyldiphenylsulphide

4,4'-Dimethyldiphenylsulphoxide (5.0 g, 0.022 mol) was added to a stirred solution of cobalt(III) chloride hexahydrate (9.6 g, 0.040 mol) in ethanol (300 mL). The solution was cooled to 0 C. Sodium borohydride (7.6 g, 0.2 mol) was added over a 1 hour period. The reduction proceeded as outlined by Chasar (159). Water was added, the mixture stirred for a further 1 hour and, then, the mixture was poured into water (500 mL). The solution was washed with diethyl ether (three 100 mL portions). The ethereal extracts were dried and the ether removed at reduced pressure leaving an ethanolic solution from which the product crystallized. The yield was 4.0 g, 85%. (mp 55-57 C; lit. 57.5 C (160)). ^{1}Hmr (CDCl$_3$): 7.17 (m,8H), 2.30 (s,6H).

4,4'-Dimethyldiphenylsulphone

4,4'-Dimethyldiphenylsulphoxide (5.0 g,0.022 mol) in dichloromethane (100 mL) was allowed to stir at 0 C. 3-Chloroperbenzoic acid (4.2 g, 0.024 mol) was added over 1 hour. The reaction mixture stirred for 18 hours. Workup consisted of washing the dichloromethane solution with water, 10% sodium bicarbonate solution and finally with water. The dichloromethane was dried over anhydrous magnesium sulphate, filtered and solvent removed at reduced pressure. The product was recrystallized twice from

chlorobenzene to give colourless platelets. The yield was 4.4 g, 81%. (mp 157-158 C; lit. 158.1 C (161)). ^{1}Hmr (CDCl$_3$): 7.50 (m,8H), 2.33 (s,6H).

4-Methyldiphenylsulphone

4-Tolylsulphonylchloride (5.0 g, 0.03 mol) in benzene (50 mL) was added dropwise to a stirred solution of aluminum chloride (4.0 g, 0.03 mol) in benzene (100 mL) over 20 minutes. After the addition was complete, the mixture was slowly warmed to 60 C and stirred at that temperature until the evolution of hydrogen chloride had subsided (about 30 minutes). The mixture was then refluxed for an additional 1 hour period after which it was carefully poured onto 200 g of crushed ice. This mixture was heated to break up the complex, the layers were separated and and the organic layer washed successively with 5% sodium bicarbonate and water. The solution was then dried over anhydrous magnesium sulphate and the solvent evapourated at reduced pressure. Recrystallization of the crude product from ethanol afforded colourless crystals. The yield was 4.8 g, 69%. (mp 128-129 C; lit. 129 C (162)). Ir (CHCl$_3$) cm^{-1}: 1161(s), 1320(s); ^{1}Hmr (CDCl$_3$): 7.55 (m,9H), 2.33 (s,3H).

Methyl(4-tolylsulphinate)

The sulphinic ester was prepared by the method of Field and Locke (163). To a refluxing solution of ditolyldisulphide (3 g, 0.012 mol, Aldrich Chemical Company

189

Inc.) chloroform (25 mL) and methanol (25 mL) in a 250 mL three neck flask, lead tetraacetate (25 g) in chloroform (100 mL) was added dropwise over a 1 hour period. The solution was allowed to reflux for an additional 24 hours. Most of the solvent (100 mL) was distilled from the reaction flask, and, water (20 mL) was added. The mixture was cooled, filtered through Celite and washed with water until all traces of lead were removed (163). The solvent was dried and the solvent was removed at reduced pressure. The yield was 3.8 g, 93%. Ir (NaCl disk) cm^{-1}: 1080(s); ^{1}Hmr (CDCl$_3$): 7.42 (m,4H); 3.40 (s,3H), 2.37 (s,3H).

4-Tolylthiolacetate

Acetylchloride (4.7 g, 0.06 mol) in benzene (50 mL) was added dropwise to a solution of 4-thiocresol (7.5 g, 0.06 mol) in benzene (100 mL) over 15 minutes. The solution was warmed to reflux for 1 hour. The reaction mixture was cooled then washed three times with 10% sodium hydroxide and twice with water, then, dried over anhydrous magnesium sulphate. The solvent was removed at reduced pressure. The product was purified by distillation (85 C, 0.1 Torr (152)). Ir (NaCl disk) cm^{-1}: 1712(s); ^{1}Hmr (CDCL$_3$): 7.22 (br s,4H), 2.33 (s,6H).

4-Methyldiphenylether

This ether was prepared by the method of Bacon and Stewart (164). A mixture of 4-cresol (10.8 g, 0.1 mol),

bromobenzene (7.85 g, 0.05 mol), cuprous oxide (7.15 g, 0.05
mol) in 2,4,6-trimethylpyridine (25 mL) was refluxed for 48
hours. The mixture was poured into 6M HCl (200 mL) and
extracted with ether (2 x 200 mL). The ether layer was then
washed with 5% sodium hydroxide solution and water, then
dried over anhydrous magnesium sulphate. The solvent was
removed at reduced pressure and the product purified by
distillation (104 C, 0.1 Torr). The yield was 5.0 g, 55%.
^{1}Hmr (CDCl$_3$) : 7.00 (m,9H), 2.30 (s,3H).

3.4.5 Esr Experiments

Toluenes. A static solution of DTBP (0.5 mL) and the
toluene (100mg) with PMA (45 mg) was irradiated in the esr
spectrometer cavity using a filtered (methanol in a quartz
tube) 1 kW Xe-Hg high pressure lamp. Temperatures ranged
from 20 C to -60 C (depending on the solubility), with the
majority of the samples examined at -20 C. All samples were
purged with nitrogen for 5 minutes prior to irradiation.

Benzylbromides. Two methods were used to generate the
benzyl radicals. In method 1, a static solution of DTBP
(0.2 mL), triethylsilane (0.2 mL) and the bromide (50-100
mg) diluted if necessary with chlorobenzene was purged with
nitrogen and irradiated as described above in the esr
spectrometer cavity. In method 2, a solution of the bromide
(50-100 mg) in tert-butylbenzene or chlorobenzene was

continuously purged while hexamethylditin (0.1 mL) was injected via the nitrogen purge tube. It was necessary to have a glass wool plug in the purge tube to filter the hexamethylditin. This solution was irradiated as described above. The use of chlorobenzene allowed cooling of the sample to temperatures as low as -20 C without precipitation of the hexamethylditin.

3.4.6 Control Experiments

The linearity of the field was checked against the line of $[Cr(NH_3)_5Cl]Cl_2$ doped with 2% $[Co(NH_3)_5Cl]Cl_2$ (165). The accuracy of the field was checked against the coupling constants for Wursters blue perchlorate in ethanol. The esr spectra of the benzyl radical, the 3-cyanobenzyl radical, and the 4-fluorobenzyl radical all have been shown to be independent of solvent (up to 50% v/v chlorobenzene or carbontetrachloride) and temperature (20 C to -60 C) (116). Similarly, the esr spectra of the 4-tolylthiobenzyl radical shows no solvent effect (up to 50% v/v chlorobenzene) or temperature effect (20 C to -60 C). The spectra of the 4-methylthiobenzyl radical and the 4-methylsulphonylbenzyl radical show no temperature dependence between 0 C and -60 C. The insolubility of the bromides in DTBP precluded checking the esr spectra in the absence of solvent. However, for each of the bromides, similar spectra were obtained using either chlorobenzene or dimethoxyethane as solvent.

REFERENCES

1. For example see (a) D. J. Cowley and D. C. Nonhebel. "Organic Reaction Mechanisms 1980", A. C. Knipe and W. E. Watts (editors), John Wiley and Sons, 1980, pp 87-192.

    (b) D. J. Cowley and D. C. Nonhebel. "Organic Reaction Mechanisms 1979", A. C. Knipe and W. E. Watts (editors), John Wiley and Sons, 1979, pp 75-172.

2. (a) S. L. Mattes and S. Farid. "Organic Photochemistry" A. Padwa (editor), Marcel Dekker Inc., New York, 1983, V. 6, pp231-326.

    (b) A. K. Chibisov. Russ. Chem. Rev., **50**, 1169 (1981)

    (c) A. J. Bard, A. Ledwith and H. J. Shine. Adv. Phys. Org. Chem., **13**, 155 (1976).

3. (a) Y. Yokosowa and I. Miyashita. J. Chem. Phys., 25, 796 (1956).

    (b) S. I. Weissman, E. deBoer and J. J. Conradi. J. Chem. Phys., **26**, 963 (1957).

    (c) A. Carrington, F. Dravnieks and M. C. R. Symons. J. Chem. Soc., 947 (1959)

4. F. Kehermann and L. Deseracs. Ber., **48**, 318 (1950).

5. R. S. Mulliken. J. Am. Chem. Soc., **72**, 610 (1950).

6. R. S. Mulliken. J. Am. Chem. Soc., **74**, 811 (1952).

7. M. W. Hanna and J. L. Lippert. "Molecular Complexes", R. Foster (editor), Paul Elek Ltd., London, 1973, V. 1.

8. D. Rehm and A. Weller. Isreal J. Chem., **8**, 259 (1970).

9. A. W. Adamson. "A Textbook of Physical Chemistry", Academic Press, New York, 1973.

10. (a) R. A. Marcus. J. Chem. Phys., **24**, 966 (1956).

    (b) R. A. Marcus. Ann. Rev. Phys. Chem., **15**, 155 (1964).

11. (a) "The Exciplex", M. Gordon and W. R. Ware (editors), Academic Press, New York, 1975.

    (b) S. L. Mattes and S. Farid. Acc. Chem. Res., **15**, 80 (1982).

12. H. Beens and A. Weller. Acta Phys. Polon., **34**, 593 (1968).

13. N. Mataga, T. Okada and N. Yamamoto. Chem. Phys. Lett., **1**, 119 (1967).

14. H. Knibbe, K. Rollig, F. P. Schaefer and A. Weller. J. Chem. Phys., **47**, 1184 (1967).

15. H. Masuhara and N. Mataga. Acc. Chem. Res., **14**, 312 (1981).

16. (a) S. L. Mattes and L. Farid. J. Chem. Soc. Chem. Commun., 126 (1980).

    (b) K. Schulten, H. Staeck, A. Weller, H. J. Werner and B. Nickel. Z. Phys. Chem. N. F., **101**, 371 (1976).

17. R. N. Adams. "Electrochemistry at Solid Electrodes", Marcel Dekker Inc., New York, 1969.

18. (a) R. S. Nicholson and I. Shain. Anal. Chem., **36**, 706 (1964).

    (b) V. D. Parker. Pure and Appl. Chem., **51**, 1021 (1979).

    (c) P. Delahay. "Double Layer Electrode Kinetics", John Wiley and Sons, Inc., New York, 1965.

    (d) V. D. Parker. Adv. Phys. Org. Chem., **19**, (1983).

19. A. J. Fry. "Synthetic Organic Electrochemistry", Harper and Row, Publishers, New York, 1972.

20. M. M. Baizer. "Organic Electrochemistry", Marcel Dekker Inc., New York, 1973.

21. J. R. Brenet and K Traore. "Transfer Coefficients in Electrochemical Kinetics", Academic Press, New York, 1971.

22. Numerous examples of 1,2-radical ions can be found. See, for example, reference 2, 11, 20 and:

    (a) G. Burgbacher and H Schafer. J. Am. Chem. Soc., **101**, 7590 (1979).

    (b) R. A. Neunteufel and D. R. Arnold. J. Am. Chem. Soc., **95**, 4080 (1973).

    (c) D. R. Arnold and A. J. Maroulis, J. Am. Chem. Soc.,

99, 7355 (1977).

23. (a) P. C. Wong and D. R. Arnold. Tetrahedron Lett., 2101 (1979).

    (b) H. D. Roth and M. L. M. Schilling. J. Am. Chem. Soc., **102**, 7956 (1980).

24. (a) H. D. Roth and M. L. M. Schilling. J. Am. Chem. Soc., **103**, 7210 (1981).

    (b) H. D. Roth, M. L. M. Schilling and G. Jones II. J. Am. Chem. Soc., **103**, 1246 (1981).

25. V. R. Rao and S. S. Hixson. J. Am. Chem. Soc., **101**, 6458 (1979).

26. B. Juan, J. Schwarz and R. Breslow. J. Am. Chem. Soc., **102**, 5741 (1980).

27. R. Borg and D. R. Arnold. Can. J. Chem., in press.

28. (a) Y. Shigemitsu and D. R. Arnold. J. Chem. Soc. Chem Commun., 407 (1975).

    (b) D. R. Arnold and A. J. Maroulis. J. Am. Chem. Soc., **98**, 5931 (1976).

29. R. S. Davidson. Adv. Phys. Org. Chem., **19**, 1 (1983).

30. A. M. deP. Nicholas and D. R. Arnold. Can. J. Chem., **60**, 2165 (1982).

31. D. R. Arnold and R. W. R. Humphreys. J. Am. Chem. Soc., **101**, 2743 (1979).

32. A. R. Ubbelohde and J. A. Burgess. J. Chem. Soc. B., 1106 (1970).

33. (a) F. Wilkinson. J. Phys. Chem., **66**, 2569 (1962).

    (b) A. A. Lamola and G. S. Hammond. J. Chem. Phys., **43**, 2129 (1965).

34. D. R. Arnold. unpublished results.

35. A. M. deP. Nicholas and D. R. Arnold. Can. J. Chem., **60**, 2165 (1982).

36. B. G. Cox, G. R. Hedwig, A. J. Parker and G. W. Watts. Aust. J. Chem., **27**, 477 (1974).

37. A. M. deP. Nicholas and D. R. Arnold. Can. J. Chem., **60**, 3011 (1982).

38. S. P. McManus and C. U. Pittman, Jr. "Organic Reactive Intermediates", S. P. McManus (editor), Academic Press, New York, 1973, pp 193-335.

39. M. H. Abraham. J. Am. Chem. Soc., **101**, 5477 (1979).

40. D. R. Arnold and A. Okamoto. Unpublished results.

41. CODATA Bulletin No. 28, ICSU CODATA, Paris 1978. J. Chem. Thermodynamics, **10**, 903 (1978).

42. (a) D. F. McMillen and D. M. Golden. Ann. Rev. Phys. Chem., **33**, 493 (1982).

    (b) G. LeRoy. Int. J. Quantum Chem., **23**, 271 (1983).

43. R. Dietz, M. E. Peover and R. Wilson. J. Chem. Soc. B. 75 (1968).

44. J. L. Marshall. "Carbon-carbon and carbon-hydrogen NMR couplings", Verlag Chemie Int., New York, 1983.

45. W. G. Miller and C. U. Pittman, Jr. J. Org. Chem., **39**, 1955 (1974).

46. S. Farid. Private communication.

47. (a) F. D. Lewis, T. I. Ho and J. T. Simpson. J. Am. Chem. Soc., **104**, 1924 (1982).

    (b) F. D. Lewis and T. I. Ho. J. Am. Chem. Soc., **102**, 1751 (1980).

    (c) P. J. Wagner and A. E. Puchalski. J. Am. Chem. Soc., **102**, 6177 (1980).

    (d) P. J. Wagner and A. E. Puchalski. J. Am. Chem. Soc., **100**, 5948 (1978).

48. J. Q. Chambers. "The Chemistry of the Quinonoid Compounds", S. Patai (editor), John Wiley and Sons, New York, 1974, Chapter 14.

49. (a) V. D. Parker. J. Chem. Soc. Chem. Commun., 716 (1969).

    (b) B. R. Eggins and J. Q. Chambers. J. Electrochem. Soc., **117**, 186 (1970).

50. E. Laviron. J. Electoanal. Chem., **164**, 213 (1984).

51. C. J. Schesener, C. Amatore and J. K. Kochi. J. Am. Chem. Soc., in press.

52. M. M. Davis. "Acid-Base Behaviour in Aprotic Organic Solvents", NBS Monograph No. 105, 1968.

53. C. U. Pittman, Jr. and W. G. Miller. J. Am. Chem. Soc., 95, 2947 (1973).

54. A. J. Bard and J. Phelps. J. Electroanal. Chem., 25, App. 2 (1970).

55. "CRC Handbook of Chemistry and Physics". R. C. Weast, (Editor), CRC Publishing Co., 1971.

56. J. D. Stuart and W. E. Ohnsorge. J. Am. Chem. Soc., 93, 4531 (1971).

57. T. Skono and Y. Matsumura. J. Org. Chem., 35, 4157 (1970).

58. A. Streitweiser, Jr. "Molecular Orbital Theory for Organic Chemists". John Wiley and Sons, Inc. New York (1961).

59. "Comprehensive Chemical Kinetics". C. H. Bramford and C. F. H. Tipper (editors), Elsevier Publishing Co., Amsterdam, 1972, V. 13, pp. 139-163.

60. T. H. Lowry and K. S. Richardson. "Mechanism and Theory in Organic Chemistry", Harper and Row, Publishers, New York, second edition, 1981.

61. S. W. Benson. "Thermochemical Kinetics", John Wiley and Sons, Inc., New York, 1968.

62. V. D. Parker., Colloq. Int. CNRS 278, 217 (1977). CA 91 148269.

63. For example: (a) E. M. Kosower and M. Ito. Proc. Chem. Soc., 25, 1962.

    (b) A. C. Goodman and R. H. Eastman. J. Am. Chem. Soc., 86, 908 (1964).

    (c) I. Prins, J. W. Verhoefen, Th. J. deBoer and C. Worrell. Tetrahedron, 33, 127 (1977).

64. L. Heiss, E. F. Paulus and H. Rehling. Liebigs Ann. Chem., 1583 (1980).

65. C. S. Marvel and W. S. Sperry. Org. Syn. Coll., 1, 95.

66. J. E. Hodgkins and M. P. Hughes. J. Org. Chem., 27, 4187 (1962).

67. L. L. Miller and R. F. Boyer. J. Am. Chem. Soc., **93**, 650 (1971).

68. W. J. Middleton, R. W. Heckert, E. L. Little and C. G. Krespun. J. Am. Chem. Soc. **80**, 7283 (1958).

69. (a) R. W. R. Humphreys and D. R. Arnold. Can. J. Chem., **55**, 2286 (1977).

    (b) R. W. R. Humphreys and D. R. Arnold. Can. J. Chem., **57**, 2652 (1979).

70. C. R. H. Allen and S. Converse. Org. Syn. **6**. 226 (1941), or by the addition of methyl magnesium bromide to the substituted benzophenone forllowed by dehydration.

71. D. R. Arnold, D. D. M. Wayner and M. Yoshida. Can. J. Chem., **60**, 2313 (1982).

72. T. Shida, E. Haselbach and T. Bally. Accts. Chem. Res., **17**, 180 (1984).

73. "Chemically Induced Dynamic Nuclear Polarization", L. T. Muus, P. W. Atkins, K. A. Mclauchlan and J. B. Pederson (editors), D. Reidel Publishing Co., Boston, 1977.

74. (a) J. A. Pople and D. L. Beveridge. "Approximate Molecular Orbital Theory". McGraw-Hill Book Company, New York, 1970.

    (b) A. Szabo and N. S. Ostlund. "Modern Quantum Chemistry: Introduction to Advanced Electronic Structure Theory". MacMillan Publishing Company, New York, 1982.

    (c) R. S. Mulliken and W. C. Ermler. "Polyatomic Molecules: Results of *ab initio* Calculations"., Academic Press, New York, 1981.

    (d) I. N. Levine. "Quantum Chemistry"., Allyn and Bacon, Inc., Boston, Ma., 1974.

75. A. de Meijere. Angew. Chem. Int. Ed., **18**, 809 (1979).

76. A. D. Walsh. Trans. Faraday Soc., **45**, 1979 (1949).

77. C. A. Coulson. "Valence"., Oxford University Press, London, 1953.

78. W. A. Bennett. J. Chem. Ed., **44**, 17 (1967).

79. (a) H. H. Jaffe and M. Orchin. "Theory and Applications of Ultraviolet Spectroscopy". John Wiley and Sons, Inc., New York, 1962.

    (b) S. Winstein and R. Baird. J. Am. Chem. Soc., **79**, 756 (1957).

80. C. F. Wilcox, L. M. Loew and R. Hoffman. J. Am. Chem. Soc., **95**, 8192 (1973).

81. (a) J. R. Collins and G. A. Gallup; J. Am. Chem. Soc., **104**, 1530 (1982).

    (b) J. A. Tossell, J. H. Moore and M. A. Coplan; Chem. Phys. Lett., **57**, 356 (1979).

    (c) C. G. Rowland; Chem. Phys. Lett., **9**, 169 (1971).

    (d) E. Haselbach; Chem. Phys. Lett., **7**, 428 (1970).

82. W. J. Bouma, D. Poppinger and L. Radom. Israel J. Chem., **23**, 21 (1983).

83. H. D. Roth and M. L. M. Schilling. Can. J. Chem., **61**, 1027 (1983).

84. S. Beran and R. Zahradnik. Coll. Czech. Commun., **41**, 2303 (1976).

85. J. A. Berson. Ann. Rev. Phys. Chem., **28**, 111 (1971) and references cited therein.

86. J. E. Douglas, B. S. Rabinovich and F. S. Looney. J. Chem. Phys., **23**, 315 (1955).

87. L. Salem. "Photochemistry IV: Plenary Lectures"., Butterworth and Company, Ltd., Toronto, 1973.

88. J. S. Binkley, R. S. Whiteside, R. Krishnan, R. Seeger, D. J. deFrees, B. Schegel, S. Topiol, L. R. Kahn and J. A. Pople. QCPE, **13**, 406 (1981).

89. J. S. Binkley, R. S. Whiteside, P. Hariharan, R. Seeger and J. A. Pople. QCPE, **11**, 368 (1978).

90. C. Moller and M. S. Plessett. Chem. Phys. Rev., **46**, 618 (1934).

91. J. A. Pople and R. K. Nesbet. J. Chem. Phys., **22**, 571 (1954).

92. R. A. Whiteside, M. J. Frisch, J. S. Binkley, D. J. Defrees, H. B. Schlegel, K. Raghavacgari and J. A. Pople. "Carnegie-Mellon Quantum Chemistry Archive", 2nd

edition, 1981.

93. J. A. Horsely, Y. Jean, C. Moser, L. Salem, R. M. Stevens and J. S. Wright. J. Am. Chem. Soc., **94**, 279 (1972).

94. J. E. Wertz and J. R. Bolton. "Electron Spin Resonance", McGraw-Hill Book Company, New York, 1972.

95. R. G. Bergman. "Free Radicals", J. K. Kochi (editor), John Wiley and Sons, New York, 1973; and references cited therein.

96. (a) N. L. Bauld, D. J. Belleville, R. Pabon, R. Chelsky, and G. Green. J. Am. Chem. Soc., **105**, 2378 (1983).

    (b) E. Haselbach, T. Bally and Z. Lanyiova. Helv. Chem. Acta, **62**, 577 (1979).

97. M. Iwasaki, K. Toriyama and K. Numone. J. Chem. Soc. Chem. Commun., 202 (1983).

98. D. J. Belleville and N. L. Bauld. J. Am. Chem. Soc., **104**, 294 (1982).

99. (a) Y. Jean and L. Salem. J. Chem. Soc. Chem. Commun., 382 (1971).

    (b) P. J. Hay, W. J. Hunt and W. A. Goddard, III. J. Am. Chem. Soc., **94**, 638 (1972).

100. R. J. Beunker and S. D. Peyerimhoff. Chem. Phys., **9**, 75 (1976).

101. H. Koppel, W. Domke, L. S. Cederbaum and W. J. von Neissen. J. Chem. Phys., **69**, 4252 (1978).

102. J. M. Brown, B. T. Golding and J. J. Stafko, Jr. J. Chem. Soc. Chem. Commun., 319 (1973).

103. G. R. deMare and M. R. Peterson. J. Mol. Struct. (Theochem), **89**, 213 (1982).

104. R. J. Crawford and T. R. Lynch. Can. J. Chem., **46**, 1457 (1968).

105. D. R. Arnold, D. D. M. Wayner and M. Yoshida. Can. J. Chem., **60**, 2313 (1982).

106. F. W. McLafferty, M. P. Barbalas and F. Turecek. J. Am. Chem. Soc., **105**, 1 (1983).

107. L. P. Hammett. J. Am. Chem. Soc., **59**, 96 (1937).

108. H. C. Brown and Y. Okamoto, J. Am. Chem. Soc., **80**, 4979 (1958).

109. A. Fischer, G. J. Leary, R. D. Topson and J. Vaughan. J. Chem, Soc. B., 782 (1966).

110. S. Ehrensen, R. T. C. Brownlee and R. W. Taft. Prog. Phys. Org. Chem., **10**, 1 (1973).

111. R. W. Taft, E. Price, I. R. Fox, I. C. Lewis, K. K. Anderson and G. T. Davis. J. Am. Chem. Soc., **85**, 709, 3146 (1963).

112. (a) N. B. Chapman and J. Shorter. "Correlation Analysis in Chemistry", Plenum Press, New York, 1978.

    (b) O. Exner. "Advances in Linear Free Energy Relationships", N. B. Chapman and J. Shorter (editors), Plenum Press, London, 1972.

113. (a) W. H. Davis and W. A. Pryor. J. Am. Chem. Soc., **99**, 6305 (1977).

    (b) R. W. Henderson. J. Am. Chem. Soc., **97**, 213 (1975).

    (c) E. V. Blackburn and D. D. Tanner. J. Am. Chem. Soc., **102**, 692 (1980).

114. W. A. Pryor, T. H. Lin, J. P. Stanley and R. W. Henderson. J. Am. Chem. Soc., **95**, 6993 (1973).

115. (a) A. P. G. Kieboom. Tetrahedron, **28**, 1325 (1972).

    (b) R. Ito, t. Migita, N. Morikawa and O. Simamura. Tetrahedron, **21**, 955 (1965).

    (c) Y. Yamamoto and T. Otsu. Chem. Ind. (London), 787 (1967).

    (d) H. Sakurai, S. Hayishi and A. Hosomi. Bull. Chem. Soc. Jpn., **44**, 1945 (1971).

    (e) T. H. Fisher and A. W. Meierhoefer. J. Org. Chem., **43**, 224 (1978).

    (f) W. J. Leigh, D. R. Arnold, R. W. R. Humphreys and P. C. Wong. Can. J. Chem., **58**, 2537 (1980).

    (g) S. Dincturk, R. A. Jackson, H. Townson. H Agirbas, N. C. Billingham and B. March. J. Chem. Soc., Perkin Trans. II, 1121 (1981).

116. (a) J. M. Dust and D. R. Arnold. J. Am. Chem. Soc., **105**, 1211 (1983).

(b) J. M. Dust and D. R. Arnold. J. Am. Chem. Soc., 105, 6531 (1983).

117. (a) H. M. McConnell. J. Chem. Phys., 24, 1066 (1956).

(b) H. S. Jarrett. J. Chem. Phys., 26, 1289 (1958).

118. S. Dincturk and R. A. Jackson. J. Chem. Soc. Perkin. Trans. II, 1127 (1981).

119. (a) X. Creary. J. Org. Chem., 43, 1777 (1978).

(b) X. Creary. J. Org. Chem., 45, 280 (1980).

120. U. M. Oehler and E. G. Janzen. Can. J. Chem., 60, 1542 (1982).

121. T. H. Lowry and K. S. Richardson. "Mechanism and Theory in Organic Chemistry", Harper and Row, Publishers, New York, 1976.

122. F. Bernardi, N. D. Epiotis, W. Cherry, H. B. Schlegel, M. H. Whangbo and S. Wolfe. J. Am. Chem. Soc., 98, 469 (1976).

123. R. Hoffmann. Acc. Chem. Res., 4, 1 (1971).

124. A. Pross and L. Radom. Prog. Phys. Org. Chem., 13, 1 (1981).

125. L. M. Stock and M. R. Wasielewski. Prog. Phys. Org. Chem., 13, 253 (1981).

126. W. H. Davis Jr. and W. A. Pryor. J. Am Chem. Soc., 99, 6365 (1977) and references therein.

127. W. A. Pryor, D. F. Church, F. Tang and R. Tang. "Frontiers of Free Radical Chemistry", W. A. Pryor (editor), Academic Press, New York, 1980, pp 355-79.

128. A. M. deP. Nicholas and D. R. Arnold. unpublished results.

129. E. Huckel. Z. Phys., 70, 204 (1931).

130. K. Yates. "Huckel Molecular Orbital Theory", Academic Press, New York, 1978.

131. M. C. R. Symons. Tetrahedron Lett., 793 (1975) and references therein.

132. (a) E. Gey and N. E. Kruglyak. Z. Phys. Chem. (Leipzig), 255, 915 (1974).

(b) E. Gey and N. E. Kruglyak. Z. Phys. Chem. (Leipzig), **256**, 737 (1975).

,(c) E. Gey and T. Tino. Croat. Chem. Acta, **51**, 11 (1978).

133. J. W. Baker. "Hyperconjugation", Oxford Press, London, 1952.

134. (a) R. S. Mulliken. J. Chem. Phys., **7**, 339 (1939).

(b) R. S. Mulliken, C. A. Reike and W. G. Brown. J. Am. Chem. Soc., **63**, 41 (1941).

135. M. J. S. Dewar. "Hyperconjugation", Ronald Press Co., New York, 1962 and references therein.

136. H. C. Brown, J. D. Brady, M. Grayson, and W. H. Bonner. J. Am. Chem. Soc., **79**, 1897 (1957).

137. D. H. Geske. Prog. Phys. Org. Chem., **4**, 125 (1966).

138. P. B. Ayscough. "Electron Spin resonance in Chemistry", Methuen and Co., London, 1967.

139. W. J. E. Parr and T. Schaeffer. Acc. Chem. Res., **13**, 400 (1980).

140. C. Heller and H. M. McConnell. J. Chem. Phys., **32**, 1535 (1960).

141. E. W. Stone and A. H. Maki. J. Chem. Phys., **37**, 1326 (1962).

142. (a) S. Oae. "Organic Chemistry of Sulphur", Plenum Press, New York, 1977.

(b) E. Block. "Reactions of Organosulphur Compounds", Academic Press, New York, 1978.

(c) H. Kwart and K. King. "d-Orbital in the chemistry of Silicon, Phosphorous and Sulphur", Springer-Verlag, New York, 1977.

143. P. M. Carton, B. C. Gilbert, H. A. H. Laue, R. O. C. Norman and R. C. Sealy. J. Chem. Soc. Perkin Trans. II, 1246 (1975).

144. The 4-tolyl derivatives are often more readily available than the phenyl derivatives. In the case of the 4-phenysulphonylbenzyl radical, where the difference between the methyl and the phenyl derivatives is large, the difference between the phenyl and the 4-tolyl

derivatives is insignificant.

145. (a) H. H. Smantz and G. Suld. J. Am. Chem. Soc., 78, 3400 (1956).

    (b) F. G. Bordwell and P. J. Boutan. J. Am. Chem. Soc., 79, 717 (1957).

    (c) F. G. Bordwell and P. J. Boutan. J. Am. Chem. Soc., 78, 854 (1956).

    (d) F. G. Bordwell and G. D. Cooper. J. Am. Chem. Soc., 74, 1058 (1952).

146. H. C. Brown and Y. Okamoto. J. Am. Chem. Soc., 80, 4979 (1958).

147. S. Oae, M. Yoshihara and W. Tagaki. Bull. Chem. Soc. Jpn., 40, 951 (1967).

148. (a) N. D. Epiotis, R. L. Yates, S. Bernardi and S. Wolfe. J. Am. Chem. Soc., 94, 5435 (1976).

    (b) S. Wolfe, A. Rauk, L. M. Tel and I. G. Csizmadia. J. Chem. Soc. Chem. Commun., 96 (1970).

    (c) J. M. Lehn and G. Wipff. J. Am. Chem. Soc., 98, 7498 (1976).

    (d) F. Bernardi, I. G. Csizmadia, H. B. Schlegel and S. Wolfe. Can. J. Chem., 53, 1144 (1974).

149. S. Ramasamy, V. M. Kanagasabapathy and T. Nagarajan. Phys. Lett., 73A, 166 (1979).

150. D. J. Mitchell, S. Wolfe and H. B. Schlegel. Can. J. Chem., 59, 3280 (1981).

151. (a) I. Biddles, A. Hudson and J. T. Wippen. Tetrahedron, 28, 867 (1972).

    (b) J. Q. Adams. J. Am. Chem. Soc., 92, 4535 (1970).

    (c) P. J. Krusic and J. K. Kochi. J. Am. Chem. Soc., 93, 846 (1971).

152. V. Baliah and K. Ganapathy. Trans. Faraday Soc., 59, 1784 (1963).

153. N. C. Cutress, T. B. Grindley, A. R. Katritsky, M. Shome and R. D. Topsom. J. Chem. Soc. Perkin Trans. II, 268 (1974).

154. (a) R. W. Fessenden and R. H. Schuler. J. Chem. Phys.,

43, 2704 (1965).

(b) D. E. Wood and R. F. Sprecher. Mol. Phys., **26**, 1311 (1973).

(c) P. J. Krusic and P. Meakin. J. Am. Chem. Soc., **98**, 228 (1976).

155. R. Grice and L. N. Owen. J. Chem Soc., 1947 (1963).

156. V. I. Rozenberg, R. I. Gorbachiva, V. A. Nikanorov, Yu. G. Bundel and O. A. Reutov. Zh. Org. Chim., 2222 (1975).

157. J. I. Crowley and H. Rapoport. J. Org. Chem., **45**, 3215 (1980).

158. "Beilsteins Handbuch der Organischen Chemie", Springer-Verlag, New York, 1982, Volume 6, Supplement 4, p 2210.

159. D. W. Chasar. J. Org. Chem., **36**, 613 (1971).

160. H. Rheinboldt and E. Giessbrecht. J. Am. Chem. Soc., **69**, 2310 (1947).

161. H. Rheinboldt and E. Giessbrecht. J. Am. Chem. Soc., **68**, 973 (1946).

162. H. R. Henze and N. E. Artman. J. Org. Chem., **22**, 1410 (1957).

163. H. E. Baumgarten. "Organic Synthesis: Collective Volume V", Wiley and Sons, New York, 1973.

164. R. G. R. Bacon and O. J. Stewart. J. Chem. Soc., 4953 (1965).

165. W. T. M. Andriessen. J. Magn. Reson., **23**, 339 (1976).